

A NEW ROLE FOR TISSUE-TYPE PLASMINOGEN ACTIVATOR IN LIVER INJURY

by

Liang-I Kang

B.S. in Biological Sciences, University of Delaware, 2006

Submitted to the Graduate Faculty of
School of Medicine in partial fulfillment
of the requirements for the degree of
Doctor of Philosophy

University of Pittsburgh

2013

UNIVERSITY OF PITTSBURGH

SCHOOL OF MEDICINE

This dissertation was presented

by

Liang-I Kang

It was defended on

March 6, 2013

and approved by

James L. Funderburgh, Ph.D., Professor, Departments of Ophthalmology and Cell Biology

Youhua Liu, Ph.D., Professor, Department of Pathology

George K. Michalopoulos, M.D., Ph.D., Professor and Chairman, Department of Pathology

Donna Beer Stolz, Ph.D., Associate Professor, Department of Cell Biology and Physiology

Committee Chair: Charleen T. Chu, M.D., Ph.D., Professor, Department of Pathology

Dissertation Advisor: Wendy M. Mars, Ph.D., Associate Professor, Department of Pathology

Copyright © by Liang-I Kang

2013

A NEW ROLE FOR TISSUE-TYPE PLASMINOGEN ACTIVATOR IN LIVER INJURY

Liang-I Kang, Ph.D.

University of Pittsburgh, 2013

Chronic liver disease is increasing in prevalence worldwide; however, few medical therapies are available to treat liver cirrhosis and failure. Hepatic stellate cell (HSC) activation and trans-differentiation into myofibroblast-like (MFB-like) cells is a key process in liver injury and fibrogenesis. Greater understanding of the role of matrix regulating proteases, such as the plasminogen activators, in HSC activation could provide new therapeutic targets for treating chronic liver disease. Mice lacking plasminogen activators exhibit delay in liver repair; however, their exact functions after liver injury remain unclear. Recent studies in kidney demonstrate that low density lipoprotein receptor-related protein 1 (LRP1)-dependent signaling by tissue-type plasminogen activator (t-PA) is an essential regulator of the myofibroblast phenotype after injury. This study investigated the role of t-PA and LRP1 in HSC activation and *in vivo* liver injury. We find that, in contrast to kidney fibroblasts, exogenous t-PA antagonizes activation of primary and immortalized HSCs *in vitro*. Similar to kidney, these effects are independent of the proteolytic function of t-PA and require phosphorylation of LRP1. Antagonism of LRP1 or PI3K/Akt signaling pathways is able to prevent t-PA-mediated decreases in α -SMA. During recovery following acute liver injury, mice lacking t-PA (globally) or LRP1 (conditionally on HSCs) retain higher densities of the α -SMA⁺ MFB-like cell population compared to control mice. These differences are seen at time points that correspond to the appearance of co-

localization between p-LRP1 and α -SMA, as well as t-PA immunolocalization at sites of α -SMA-positive cells. Additionally, t-PA may regulate macrophage phenotype and drug metabolism, as t-PA null mice exhibit increased macrophage accumulation and lack of normal compensatory down-regulation of a key metabolic enzyme after acute injury. Finally, more collagen I deposition remains in the livers of t-PA null mice up to two weeks after cessation of chronic liver injury, suggesting a decreased rate of matrix turnover. These data reveal that t-PA has multiple functions in liver repair and is able to affect the phenotype of several cell types, in addition to its classical plasminogen activating role. Further preclinical studies are needed to evaluate the clinical potential of using t-PA as a treatment for chronic liver injury and fibrosis.

TABLE OF CONTENTS

PREFACE.....	XIII
1.0 GENERAL INTRODUCTION.....	1
1.1 THE LIVER AND ITS REGENERATION AFTER INJURY.....	1
1.1.1 Cell types of the liver	2
1.1.2 Regeneration models	5
1.1.3 Cellular sources for repopulation in liver regeneration.....	7
1.1.3.1 Resident liver cells.....	7
1.1.3.2 Bone marrow derived cells.....	10
1.1.3.3 Oval/Progenitor cells and trans-differentiation	10
1.2 LIVER INJURY AND FIBROSIS	12
1.2.1 Hepatic fibrogenesis	12
1.2.2 Challenges to treating hepatic cirrhosis	15
1.3 PLASMINOGEN ACTIVATORS	16
1.3.1 Structure, function, and clearance of plasminogen activators	16
1.3.2 Plasminogen activators in liver homeostasis	19
1.3.3 Plasminogen activators in liver injury and fibrosis.....	20
1.4 LOW DENSITY LIPOPROTEIN RECEPTOR-RELATED PROTEIN 1 (LRP1)	22

1.4.1	General structure and function	22
1.4.2	t-PA and LRP1 in kidney fibrosis	24
1.4.3	Role of LRP1 in smooth muscle cells	25
2.0	TISSUE-TYPE PLASMINOGEN ACTIVATOR DOWN-REGULATES HEPATIC STELLATE CELL ACTIVATION THROUGH LDLR-RELATED PROTEIN 1 IN RATS AND MICE	27
2.1	INTRODUCTION	27
2.2	EXPERIMENTAL PROCEDURES	29
2.2.1	Reagents and Antibodies.....	29
2.2.2	Rat hepatic stellate cell isolation and cell culture	29
2.2.3	MTT and [³ H]Thymidine Incorporation Assays	30
2.2.4	SDS-PAGE and Western Blot	31
2.2.5	Immunoprecipitation.....	32
2.2.6	Reverse Transcription and Polymerase Chain Reaction	32
2.2.7	Gene Array Analysis	33
2.2.8	Carbon tetrachloride acute injury and resolution experiments.....	34
2.2.9	Immunohistochemical staining and fluorescent labeling.....	34
2.2.10	Image Capture and Analysis	35
2.2.11	Statistical Analysis.....	36
2.2.12	Animal use approval	36
2.3	RESULTS	37
2.3.1	Exogenous t-PA decreases markers of HSC activation in primary and transformed cells	37

2.3.2	Global gene expression changes after t-PA treatment of HSC-T6 cells ...	39
2.3.3	The effects of t-PA on HSC activation are dependent on LRP1-mediated signaling	39
2.3.4	p-LRP1 and t-PA co-localization with α -SMA precedes resolution of injury in WT mice	43
2.3.5	t-PA- and LRP1-deficient mice retain more α -SMA-positive cells after injury	46
2.4	DISCUSSION.....	50
3.0	FURTHER INSIGHTS INTO TISSUE-TYPE PLASMINOGEN ACTIVATOR FUNCTION IN LIVER AND LIVER INJURY.....	54
3.1	INTRODUCTION	54
3.2	EXPERIMENTAL PROCEDURES	55
3.2.1	Carbon tetrachloride chronic injury and resolution.....	55
3.2.2	SDS-PAGE and western blot from liver tissue	56
3.2.3	Immunohistochemical staining and image capture.....	57
3.3	RESULTS	58
3.3.1	Increased macrophage populations in t-PA null mice after injury.....	58
3.3.2	Cytochrome P450 2E1 expression in WT and t-PA knockout mice.....	60
3.3.3	Chronic injury studies in WT and t-PA deficient mice.....	64
3.4	DISCUSSION.....	66
4.0	GENERAL REMARKS	68
4.1	SUMMARY	68
4.2	DISCUSSION AND FUTURE DIRECTIONS	69

4.2.1	Dissection of t-PA and LRP1 signaling partners in HSCs	69
4.2.2	t-PA and LRP1 kinetics and distribution after injury	72
4.2.3	Evaluation of observed differences in t-PA null mice	74
4.2.4	Follow-up studies in LRP1 conditional null mice	76
4.2.5	Evaluation the efficacy of t-PA treatment in chronic liver injury	77
APPENDIX A		79
APPENDIX B		97
BIBLIOGRAPHY		98

LIST OF TABLES

Table 1. Fold changes in selected genes in HSC-T6 cells after treatment with t-PA.	79
Table 2. Absolute changes in selected genes in HSC-T6 cells after treatment with t-PA.	84

LIST OF FIGURES

Figure 1. Architecture of the liver.....	4
Figure 2. Signals and cells contributing to cell repopulation during liver regeneration.....	9
Figure 3. Progression from liver injury to fibrosis.	14
Figure 4. Relationships and effects of plasmin in fibrinolysis and in hepatic homeostasis.....	17
Figure 5. Schematic illustrating the different functional domains of t-PA.....	18
Figure 6. The plasminogen activators promote liver homeostasis.....	20
Figure 7. Schematic of LRP1 and ligand-binding regions.....	24
Figure 8. Exogenous t-PA suppresses HSC activation <i>in vitro</i>	38
Figure 9. t-PA effects are protease-independent.....	41
Figure 10. Transient activation of ERK by t-PA in HSC-T6 cells.	43
Figure 11. LRP1 is activated on HSCs during resolution of acute hepatic injury <i>in vivo</i>	45
Figure 12. t-PA contributes to resolution of acute hepatic injury in mice.....	47
Figure 13. HSC LRP1 contributes to resolution of acute hepatic injury in mice.	49
Figure 14. Schematic of chronic CCl ₄ administration in mice.	55
Figure 15. Increased macrophage numbers in t-PA null mice after injury.....	59
Figure 16. Phenobarbital pre-treatment equalizes CYP2E1 protein expression, CCl ₄ -induced necrosis and HSC activation between wildtype and t-PA null mice.	61

Figure 17. Baseline and post-phenobarbital protein expression of CYP2E1 in wildtype and t-PA null mice..... 63

Figure 18. Increased collagen I deposition in t-PA null mice 14 days after cessation of chronic injury regimen..... 65

Figure 19. Effects of proteolytically-active t-PA in antagonism to TGF- β 1..... 72

Figure 20. Immunohistochemical evaluation of t-PA expression during injury resolution in wildtype mice..... 73

PREFACE

Some people go to graduate school because they're not sure what they want to do in life and hope graduate school will give them time and shelter while they decide. To those who have already traveled the road, this may be a laughable strategy as the trials and tribulations you encounter in graduate school are not for the faint of heart. You encounter the high of highs (I have publishable data!), the low of lows (hypothesis proved wrong...again), frustrations (the pre-conference or pre-committee meeting data jinx), anxieties (constant fear of getting scooped), resignations (I won't be graduating this year...), and exhilaration (grant got funded!!), amongst other emotions. It's enough to make you wonder if you're emotionally unstable.

Despite the roller-coaster of emotions, somewhere along the way, I did a lot of "growing up." Although I am lucky to be able to say that I came to graduate school purposefully, not as a backup or last resort or means to an end, I was still not mentally prepared for the maturation process that occurs. The process is partly due to the age at which I pursued my graduate studies (mid-late 20s), but also partly due to the life events that ran concurrent to and had to be juggled with graduate school: getting married, family sickness and crises, adopting pets, overcoming personal fears. I ran my first half-marathon in 2011, with an encore in 2012. The challenge of tackling and meeting this fitness goal is an achievement I hold dear and, in many ways, I see as a parallel to attaining my degree. The training I received in my graduate studies has been a slow

but steady escalation of responsibility and competence to ready me for race day: the embarking of my career. Although I do not know what the weather conditions will be like during the “race,” I am confident that the lessons I learned and the scars I bear will see me through to the end. I will know to keep hydrated (i.e. have a balanced life to keep my energy and motivation up), to pace myself (i.e. not take on too much too early), to keep looking for the next mile marker (i.e. set goals and milestones to work towards), that finding dependable running buddies makes the road easier (i.e. collaborate often and with trustworthy people), that having cheerleaders on the sideline helps keep spirits up (i.e. keep family and friends and mentors close), and finally, that beyond the achievement of finishing the race, I am a better and fitter person for the training that I did to reach my goal.

I have so many people to thank for the growth as a person and as a scientist that this body of work represents. First and foremost, I want to thank my thesis advisor, **Dr. Wendy Mars**. Without you, this project would not have been possible in either conception or completion, and I could not have asked for a better or more compatible mentor. You and I have weathered many problems, joys, crises, and achievements together, and I want to thank you for always holding me as an equal, both in expectation and in regard. For the record, I refuse to take responsibility for starting your latte addiction (although I concede that I enable its continuation). Second, I would like to thank **Dr. George Michalopoulos** for being an equally important research mentor to me over the last several years. I have learned so much by being a member of the greater Michalopoulos lab community, as well as from your generous spirit, practicality, and pure curiosity of mind. Next, I’d like to thank the rest of my thesis committee members, **Drs. Charleen Chu, Jim Funderburgh, Donna Stolz, and Youhua Liu**. As an entire committee, you all challenged me and asked me hard questions when I needed them, were encouraging and

approving when I was ready, and have individually each been a source of great help and encouragement. I could not have asked for a better committee. Of course I need to thank my trusty and dynamic labmates, past and present: **Bill Bowen, Anne Orr, Kelly Koral, Vishakha Bhave, Shashi Donthamsetty, Michael Ding, Shirish Paranjpe, John Stoops, Aaron Bell, Meagan Haynes, Hena Bukhari, Rachel Stewart, Jennifer Hurd, Callie Norris, Yu Yang, Bowen Liu, Chih-Wen Lin, Akhil Venkatesan, Paul Siebert, Josiah Radder, and Diane Hsu.** Thank you for enduring my sometimes incessant ranting and raving, my obsessive-compulsive tendency to rearrange things in the lab, and my futile attempts to fatten you up with my baking. I would also like to thank my collaborators, **Drs. A. Jake Demetris, Kumiko Isse, Selen Muratoglu, and Dudley Strickland.** You all helped me take my project from just interesting to truly publishable. I appreciate so much your generosity of time and resources. Last but not least, I want to fully acknowledge my family and close friends. To my husband and my much better half, **Michael Sung:** I want to thank you for your love, support, sacrifices, laughter, and hope for the future. I am so lucky to have found someone awesome to share every step of the road ahead. To **my parents:** thank you for your sacrifices and care throughout my life, for your high expectations, and your continual encouragement and support. I love you both and hope to keep making you proud. To my little sister, **Lena:** despite our inherent differences, I hope we can continue to foster a close and supportive relationship. My goal has always been and will continue to be to encourage you to achieve your potential. You have so much talent and energy! To my college roommate and good friend **Jessica Keister:** we have traveled and eaten the world together! I am glad that time and distance has not lessened our friendship in the least, and I look forward to a lifetime shared over cats and pastries and bibimbap. To my good friend and running buddy, **Shannon Svilar:** I am so glad to have found you as a friend at this time period in my life.

I know we'll be friends for life, no matter what the distance between us. And finally, to my MSTP brothers-in-arms, **Vineet Agrawal, David Svilar, Samuel Shin, Pavle Milutinovic, Ben Mantell, Amin Afrazi, Vivek Patel, Mark Doyal, Jeff Koenitzer, and David Wheeler**: I may have been the only female in our class but you always made me feel like "one of the guys" and included me as an equal in every way. I am so proud of all of you and to be amongst you, and I hope we'll always keep in touch and collaborate.

There are so many more people to thank and acknowledge, but for brevity, they are listed below:

- My grandparents, aunts, uncles, and family in Taiwan
- My parents-in-law, Peter and Leah Sung, and brother-in-law, Paul Sung
- My Uncle Yangming and Aunt Tracy Chen
- The Lin family
- My friend and college roommate, Dara Missan
- Tim and Kathy Keister
- My friend, Susan Specht
- Floormates: the Monga lab, the Strom lab, the Liu lab, and the Zarnegar lab, most especially Dr. Emily Wickline, Dr. Prince Awuah, Evan Delgado, Dr. Kari Nejak-Bowen, Dee Seneviratne, Dr. Yingjian Li, Lin Lin, and Dr. Marc Hansel
- Collaborators Dr. Gina Coudriet and Dr. Jon Piganelli
- My MSTP Career Advisor, Dr. Bruce Pitt
- MSTP Director Emeritus Dr. Clayton Wiley, current MSTP Director Dr. Richard Steinman, Co-director Dr. Nathan Urban, Dr. Manjit Singh, and Justin Markuss

- Pathology Medical Student Interest Group faculty advisors, past and present, Drs. Trevor Macpherson, Larry Nichols, and Marie DeFrances
- My endocrinology LCC preceptor, Dr. Maja Stefanovic-Racic
- My research administration mentor, Dr. Jennifer Woodward
- My undergraduate research advisor, Dr. Melinda Duncan
- The SOM Office of Graduate Studies, especially Carol Williams, Clare Gauss, and Jennifer Walker
- CMP Administrative Coordinator Shari Tipton
- The University of Pittsburgh DLAR and IACUC, especially Nicole Scales, Lindsay Bihler, Paula Chalmers, and the staff at the PLUM facility
- The University of Pittsburgh CTSI Pre-doctoral fellowship program (funding 2009-2011)
- NIDDK, F30 DK091959 (2011-2014)

1.0 GENERAL INTRODUCTION

1.1 THE LIVER AND ITS REGENERATION AFTER INJURY

Liver is a multi-functional organ that controls key physiological processes. These include nutrient processing following intestinal absorption, waste processing and excretion (urea cycle and bile synthesis), detoxification of xenobiotics, energy and nutrient storage and regulation, production of serum proteins (coagulation factors, oncotic proteins, carrier proteins) and hormones (thrombopoietin (1), IGF1), and other functions.

The ability of the liver to carry out these normal duties is so essential that liver mass is maintained within a very narrow range in relation to the overall body mass. If there is loss or gain of liver mass, such as through liver injury or pregnancy, respectively, compensatory proliferation or apoptosis of cells allows restoration of original liver/body mass ratio once the stimulus is removed. The term “hepatostat” has been coined to describe this unique homeostatic relationship (2). When the hepatostat is derailed and loss of liver function due to parenchymal injury falls below a critical point (build-up of toxic metabolites, inability to maintain glucose levels and blood pressure, and coagulopathy), multi-organ failure and death follows.

The robust programmed proliferative response to loss of parenchymal function is widely known as “liver regeneration.” A more accurate description may be “compensatory hyperplasia and hypertrophy,” as resection of the liver does not induce spatial replacement of the part of the

organ that was lost. Instead, the cells in the remaining portion proliferate and/or increase in size to restore the original liver mass (3). Repopulation of the liver can be achieved via one of two mechanisms: 1) self-replication of individual cell types, or 2) trans-differentiation from facultative stem cells, or liver progenitor cells.

As management of chronic liver injury and its sequelae are growing health care burdens worldwide (4), knowledge of the principles and cellular compartments governing successful restoration of liver function after insult is the key to discovering therapeutic strategies applicable to human hepatic disease.

1.1.1 Cell types of the liver

The main unique cell types of the liver are hepatocytes, cholangiocytes (or biliary epithelial cells), Kupffer cells, hepatic stellate cells, and sinusoidal endothelial cells. Hepatocytes are organized into cords that line an intricate, specialized capillary bed lined with fenestrated endothelial cells (Figure 1A). The vascular network is organized into a system that allows for unidirectional flow from branches of the inflow vascular supply, the portal vein and the hepatic artery, through the sinusoids to the central veins, which coalesce into the hepatic vein and connects to the inferior vena cava. The portal vein and hepatic artery are found in cluster along with a collecting bile duct, collectively referred to as the “portal triad,” and spaced out at the corners of a roughly hexagonal unit (“the hepatic lobule,” Figure 1B) that is repeated throughout the liver tissue. Blood flows away from the portal triads through the sinusoid capillaries, while bile flows in the opposite direction through the bile canaliculi, which coalesce into bile ducts (shown in Figure 1). In addition, lymphatic vessels are found in portal regions and drain lymph that originates from the hepatic sinusoids. As macromolecules pass through the sinusoidal

endothelial fenestrae, excess fluid collects in the Space of Disse, the area between the endothelial cells and the hepatocytes, and drains towards the portal regions (5). The lobule can be divided into three general zones: periportal (zone 1), pericentral (zone 3), and transitional (zone 2). The hepatocytes in Zone 1 to Zone 3 are exposed to increasing concentrations of processed xenobiotics/toxins and decreasing concentrations of oxygen (Figure 1B).

The hepatocyte is the parenchymal cell of the liver, performing all the essential functions of the organ described in the section above. In addition, the hepatocytes produce bile, secreted from the apical membrane into the bile canaliculi that run between hepatocytes and merge to form bile ducts, which are lined with cholangiocytes. Cholangiocytes and hepatocytes share a common precursor cell, the hepatoblast, in development. This common lineage is attributed because of the ability of cholangiocytes and hepatocytes to transdifferentiate in the setting of injury where one or the other cannot replicate sufficiently to replace its own cell compartment and the other then compensates. The “non-parenchymal cell” population includes sinusoidal endothelial cells, Kupffer cells, and hepatic stellate cells. Sinusoidal endothelial cells are fenestrated to allow passage of macromolecules and lipoproteins in and out of the hepatocytes. Kupffer cells are resident liver macrophages, which along with other liver-associated immune cells play important roles in immune tolerance of the liver (6). The hepatic stellate cell is a multifunctional cell of mesenchymal origin found to have roles in immune function, vitamin storage, matrix turnover, growth factor secretion, vascular tone, and perhaps progenitor cell niche. During injury, hepatic stellate cells become “activated” and transform into myofibroblast-like cells, depositing extracellular matrix and becoming contractile (7).

During liver regeneration, whether following surgical resection or parenchymal injury and loss, all of the cell types of the liver can proliferate to replace their own cell population.

When unable to do so, however, there are internal or external (e.g. hematopoietic) sources of progenitor cells that are able to differentiate into the various cells of the liver to restore cell compartments.

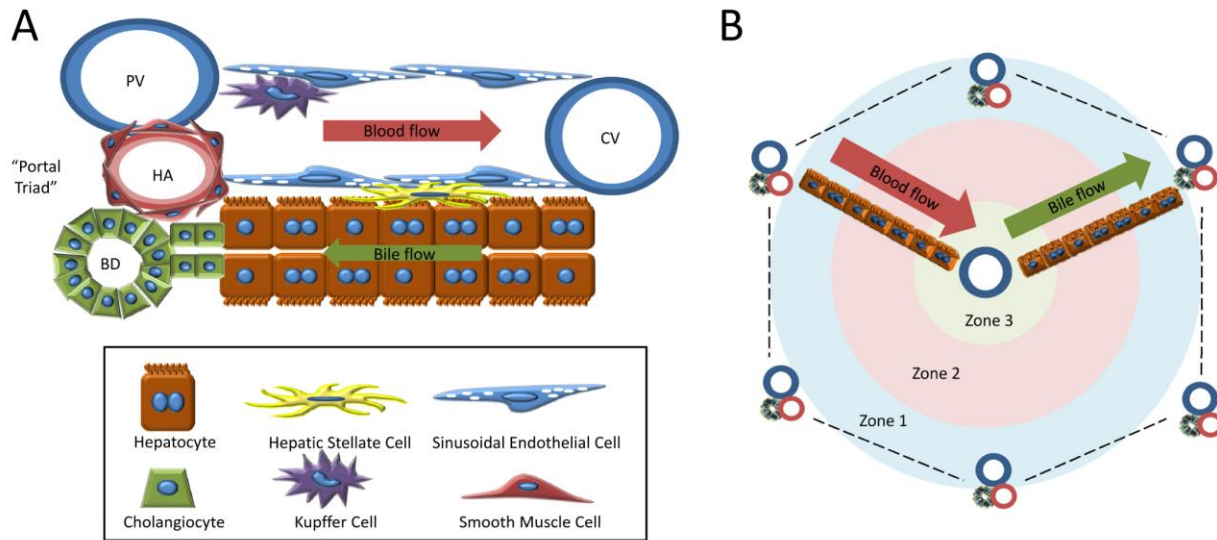


Figure 1. Architecture of the liver. (A) Schematic depicting the architecture and cell type composition of the hepatic sinusoid. Blood enters the lobule from branches of the portal vein (PV) and hepatic artery (HA) and progresses through the sinusoidal capillaries, collecting at the central veins (CV). Bile flows in the opposite direction towards the portal triad and exits through the bile ducts (BD). Hepatocytes are lined up along the sinusoids in “plates” 1-2 hepatocytes thick. Hepatic stellate cells reside in between the sinusoidal endothelial cells and hepatocytes in the “space of Disse.” (B) Diagram illustrating the organization of the hepatic lobule, including vascular structures and relative zonality of the lobule. This unit is repeated throughout the liver. Representative plates of hepatocytes are shown for orientation; these rows of hepatocytes would fill the entire lobule and be lined with sinusoids. Adapted from (8).

1.1.2 Regeneration models

The two-thirds partial hepatectomy (PHx) model was first described in 1931 (9) and remains one of the most widely used models of liver regeneration. The rodent liver is multi-lobular, the two largest of which approximates 70% parenchymal mass. When these two lobes are excised via a straightforward surgical procedure (10), the cells of the remaining lobes restore liver mass over the course of 1-2 weeks. There are two key advantages to this approach: 1) the model is easily scalable, allowing investigators to study phenomena associated with minor (~30% PHx) to severe (~90% PHx) parenchymal loss simply by removing one less or one more lobe of the liver, and 2) because there is no overt injury to the remaining hepatocytes, PHx provides a “clean” model in which to study the timing and extent of contribution of different variables, which is less optimally studied in injury models using hepatotoxins that are associated with necrosis/inflammation. However, the main drawback to this approach is the limited applicability of the PHx model for interpreting dynamics of regeneration in human disease, which often involves components of hepatocyte death and inflammation. Even in the clinical situations which hepatic resection is used, such as for early stage hepatocellular carcinoma or cancer metastases from other organs, the process of regeneration may be altered from the ideal due to several reasons: 1) prior or concurrent chemotherapeutic treatment, 2) background fibrosis that is commonly found with hepatocellular carcinoma, and 3) superimposed ischemia-reperfusion injury as a complication of surgery. In addition, PHx alone does not require liver progenitor cells for successful regeneration, and thus is not a useful model to study progenitor cell-mediated regeneration.

In comparison, several chemical injury models also exist. These cause hepatocyte injury and death, which activates an inflammatory response in addition to a regenerative response. One

commonly used class of agents causes hepatocyte injury and death selectively in the pericentral zone (Zone 3); these include carbon tetrachloride (11, 12) and acetaminophen (13-15). They require metabolic activation by drug-specific cytochrome P450 (CYP) enzymes, a process which often generates hepatotoxic free radicals. The CYP-expressing hepatocytes die first, creating a centrilobular distribution of injury and death. Allyl alcohol administration has been used to induce acute periportal injury (16). There are two main advantages in using a hepatotoxin model to study regenerative response after parenchymal injury: 1) it more closely approximates the regenerative response that occurs in common human hepatic diseases, including the damage and inflammatory infiltrate, and 2) unlike PHx (17), there are few surgical complications with repeated administrations, so it is easy to extend the acute injury model to chronic injury and cirrhosis. An emerging concept from the hepatic toxicology field is the “progression of injury”: primary injured/necrotic hepatocytes release phospholipases (18, 19) and proteases (20) into the extracellular space, which then injure neighboring hepatocytes and delay/inhibit their ability to undergo normal regeneration. It is likely these processes occur in a variety of acute and chronic human liver diseases and intoxications, where there is also *in situ* hepatocyte injury and death. Therefore, despite the relative lack of clarity about cellular origins of signals occurring as a result of chemical injury models, the importance of synthesizing our understanding of ideal liver regeneration from PHx with data from chemical injury models cannot be understated. It may be the key to future understanding of the limitations of current interventions and finding more suitable therapeutic targets for human disease and acute intoxication (21, 22).

A final model of liver growth is augmentative hepatomegaly (also known as “direct hyperplasia”), in which liver is stimulated to grow to a supraphysiological mass by growth factors, hormones (23-26), or xenobiotics. There are two classes of xenobiotics commonly used

in this experimental model: peroxisome proliferator-activated receptor (PPAR) family agonists (27) and *constitutive androstane receptor* (CAR) agonists (28). Continuous administration of these chemicals induces liver growth until a new equilibrium is reached, which is different for each chemical. Upon removal of the hormone or xenobiotic treatment, however, the liver shrinks back to the original mass through hepatocyte apoptosis (29-31). These phenomena suggest that the innate hepatostat is disrupted or readjusted in response to these xenobiotics, returning to normal when the chemical is removed, although it is not clear which pathways are relevant for this purpose. Due to the dependence on specific nuclear receptor pathways, there are some key differences between augmentative hepatomegaly and normal liver regeneration (compensatory hyperplasia) (32). However, it has been shown that the same genetic alterations that enhance (33) or suppress (34) compensatory hyperplasia can also enhance (35, 36) or suppress (37) augmentative hepatomegaly, so lessons learned from the augmentative hepatomegaly model may bear relevance to enhancing compensatory liver regeneration. There are scenarios where augmentative hepatomegaly is clinically relevant: 1) elevated estrogens during pregnancy are thought to increase liver weight to meet increased metabolic needs, 2) several prescribed drugs, such as phenobarbital (38), phenytoin, and diazepam, can bind to CAR and sensitize the patient to acetaminophen toxicity.

1.1.3 Cellular sources for repopulation in liver regeneration

1.1.3.1 Resident liver cells

After PHx, a well-orchestrated set of cell replications occurs amongst the resident cells of the liver in order to replace the lost liver mass and function. First and foremost, the hepatocytes undergo cell proliferation, with the peak of proliferation being at approximately 24 hours in the

rat (39) and approximately 36-42 hours in the mouse (10). Cholangiocytes respond to the same mitogenic signals and start proliferating almost as early as hepatocytes, while non-parenchymal cells initiate DNA synthesis at a slower pace, with Kupffer cells and stellate cells peaking at 48-72 hours and sinusoidal endothelial cells at 96 hours (39-41).

Most hepatocytes participate in cell proliferation during regeneration to restore liver mass. In the two-thirds PHx model in younger rats, over 95% of hepatocytes undergo DNA synthesis, and this only decreases to about 75%, even in older rats (42-44). Exogenous infusion of mitogens can improve the proliferative response in older animals, indicating that age-related decreases in hepatocyte proliferation are not due to inherent inability to proliferate (senescence) but perhaps changes in the ability to respond to extracellular environment and signals (24, 45). The remarkable capacity of hepatocytes to undergo innumerable proliferation cycles is demonstrated by successful regeneration after serial PHx (up to 12 documented (46)) and serial repopulation of small numbers of isolated hepatocytes into host animal livers with impaired native cells (calculated 69 doublings of each cell over six repopulations (47)). Indeed, during regeneration hepatocytes express markers of stem cells, or reprogramming factors, such as Oct4, Nanog, and KLF4 (48), lending even more credence to their self-renewal capabilities.

During the regenerative process, hepatocytes can secrete many growth factors to which non-parenchymal cells are responsive. These include transforming growth factor- α (TGF- α) (49), fibroblast growth factors (FGFs) (50), vascular endothelial growth factor (VEGF) (51), and platelet-derived growth factor A (PDGF-A) (52). In turn, the non-parenchymal cells provide hepatocytes with many growth factors. New hepatocyte growth factor (HGF) is synthesized by stellate cells and endothelial cells (51, 53, 54). Epidermal growth factor (EGF) production increases from Brunner's glands in the duodenum, and heparin-binding epidermal growth factor

(HB-EGF) is available from endothelial cells and macrophages (55). Macrophages provide interleukin-6 (IL-6) and tumor necrosis factor- α (TNF- α). The secretion of growth factors by the different cell types to regulate hepatocyte proliferation during regeneration is summarized in Figure 2A.

Revascularization of the hepatic plates after proliferation occurs through a signaling “conversation” between hepatocytes and endothelial cells. Increases in expression of growth factor receptors on endothelial cells during regeneration, such as VEGF receptors Flk-1/KDR and Flt-1, allow them to be responsive to hepatocyte-derived VEGF (56). The endothelial cells that surround avascular clumps of newly-replicated hepatocytes also selectively express the Angiopoietin receptor Tie-1 (56). Activation of these VEGF and Angiopoietin receptors induces the endothelial cells to proliferate and invade in between the hepatocytes to form new sinusoids (40, 57, 58).

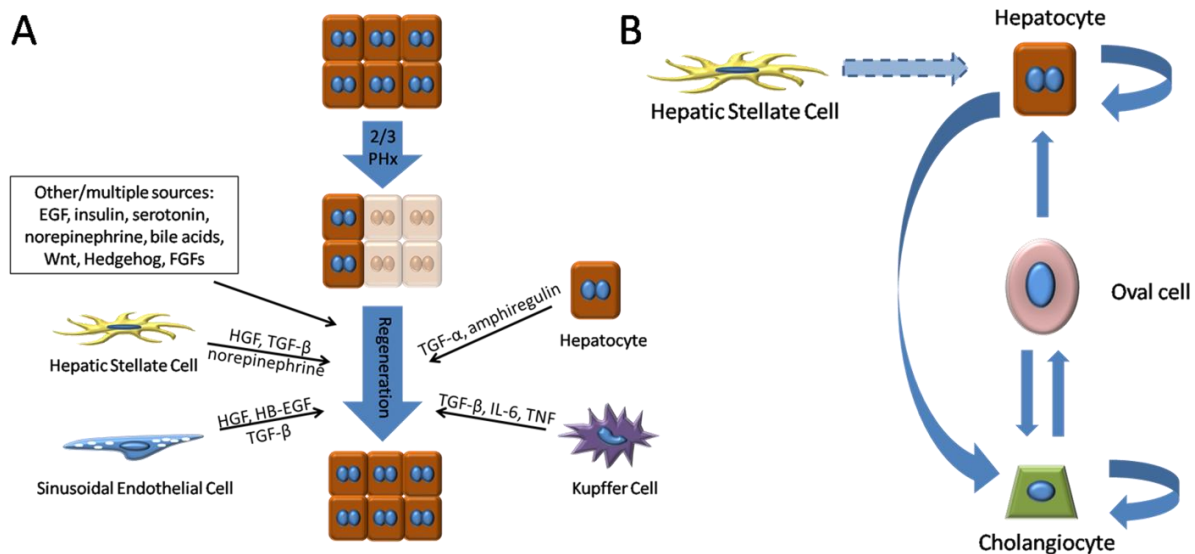


Figure 2. Signals and cells contributing to cell repopulation during liver regeneration. (A) Upon loss of two-thirds of the liver mass after PHx, molecular signals from several cell types contribute to hepatocyte repopulation during regeneration. (B) Both hepatocytes and cholangiocytes undergo self-renewal in normal

regeneration; however, trans-differentiation can occur via the relationships indicated. Dotted arrows indicate relationships based on newly emerging literature. Adapted from (8).

1.1.3.2 Bone marrow derived cells

Mobilization of bone marrow has been reported after PHx in rodents (59) and also in humans (60). Circulating bone marrow-derived mesenchymal stem cells contribute to new sinusoidal endothelial cell repopulation and are a major source of newly synthesized HGF after PHx (61, 62). It has been a topic of discussion whether circulating bone marrow cells contribute to hepatocyte repopulation during regeneration. In experimental models in which hepatocyte proliferation was inhibited, hematopoietic lineage cells were able to repopulate a portion of the hepatocytes (63, 64). However, more recent studies have suggested that the observations made from those experiments were perhaps due to cell fusion events between the bone marrow hematopoietic stem cells and hepatocytes (65, 66).

1.1.3.3 Oval/Progenitor cells and trans-differentiation

While there is still an ongoing search for conclusive proof of a resident liver stem cell population, a variety of studies have established that several liver cell types can act as facultative stem cells and trans-differentiate to replace the epithelial cell compartments during regeneration (67, 68).

One of the best-described examples is the emergence of “oval cells” in experimental models (e.g. administration of the chemical AAF prior to PHx) and diseases where hepatocytes cannot proliferate (69-71). Oval cells are named based on the shape of their nuclei, and they express cell markers of both hepatocytes and biliary cells as well as stem cell markers (72); they

can be induced to differentiate into either cell type (Figure 2B). They appear in the periportal areas, and pulse-chase labeling of these cells with tritiated thymidine in the AAF + PHx model indicate that over the course of regeneration, they acquire hepatocyte-associated markers and phenotypic characteristics (69). Many of the growth factors discussed earlier in this review have been implicated in oval cell differentiation into hepatocytes, such as TGF- α , HGF, transforming growth factor- β (TGF- β), and Notch (73-76), although some oval-cell specific signaling pathways have been identified (77, 78). Some disagreement exists about the origins of oval cells; however, it is likely that they derive from the biliary cell compartment for the following reasons: 1) most “oval cell markers” are shared markers with biliary cells (cholangiocytes), 2) in situations where they appear, such as massive hepatocyte necrosis of the human liver, they emanate from and cluster around the portal tract (79), 3) early in oval cell-inducing experimental protocols, hepatocyte markers (e.g. hepatocyte nuclear factor 4) appear in the nuclei of biliary cells of intact bile ducts prior to the appearance of oval cells, which also express these hepatocyte markers (80), and 4) toxin-mediated damage to the bile ducts prior to the AAF + PHx protocol can completely prevent the appearance of oval cells (81). As a proliferative biliary response, termed “ductular reaction,” is seen in many human liver disease conditions in which there is attrition of hepatocytes, it is likely that oval cell-mediated regeneration is relevant to human liver regeneration (82).

Hepatocytes have also been noted to possess trans-differentiation capabilities under certain conditions, particularly hepatocytes immediately proximal to the portal tract (67). In experiments where hepatocytes positive for the DPPIV marker were injected into DPPIV-negative rats that had been subjected to PHx and retrorsine intoxication, the regenerated chimeric liver possessed no DPPIV-positive bile ducts *unless* a biliary proliferative stimulus (e.g. bile duct

ligation) also accompanied the procedure. In the combined hepatocyte injury and biliary proliferation scenario, approximately 1.5% of the bile ducts became DPPIV-positive. If the ability of the native cholangiocytes to proliferate was inhibited by the biliary-specific toxin methylene dianiline (DAPM), the number of DPPIV-positive bile ducts increased to nearly 50% after bile duct ligation + PHx/retrorsine (83), demonstrating the capacity of DPPIV-positive hepatocytes to participate in repopulation of the biliary cell compartment.

Emerging evidence points to a stem cell niche in the hepatic stellate cells of the liver (84). One lineage tracing study used GFP to label cells that expressed glial fibrillary acidic protein (GFAP), a stellate cell marker, before subjecting mice to a diet-based model of liver injury and oval cell activation. After the injury, GFP-positive cells lost stellate cell markers and acquired stem/oval cell markers. These transitional cells disappeared as GFP-positive hepatocytes emerged (85).

1.2 LIVER INJURY AND FIBROSIS

1.2.1 Hepatic fibrogenesis

Hepatic cirrhosis is characterized by extensive scar tissue (fibrosis) that surrounds regenerative nodules and initiates extensive vascular changes, altering the liver's hemodynamic flow. Fibrogenesis begins with chronic injury to the liver's parenchymal cells, the hepatocytes, which then recruit an inflammatory milieu that further promotes extracellular matrix remodeling (86). Hepatic stellate cells (HSCs) become activated in response to signals such as pro-inflammatory

cytokines, growth factors, and reactive oxygen species from both the injured hepatocytes and the infiltrating immune cells. Consequently, the HSCs acquire a myofibroblast-like phenotype, secreting matrix proteins such as collagen types I and III (87). Other sources of myofibroblasts in liver fibrosis may include hepatic portal fibroblasts (88), bone marrow progenitor cells (89), or epithelial-to-mesenchymal transition (90, 91). Pro-fibrotic cytokines such as transforming growth factor- β 1 (TGF- β 1) (92) and connective tissue growth factor (CTGF) (93) promote sustained synthesis of extracellular matrix components by myofibroblasts. Paradoxically, HSCs are also key regulators of matrix breakdown in the liver, secreting metalloproteinase (MMP)-1, -2, -3, and -9 and their activators in early liver repair (94, 95). As injury becomes chronic, however, they start producing the tissue inhibitors of metalloproteinases (TIMPs), resulting in net extracellular matrix accumulation and fibrosis (87, 94), as summarized in Figure 3.

Occlusion of the extensive liver sinusoidal capillary network within the liver by an expanded HSC/myofibroblast population and collagen deposition affects liver hemodynamics by increasing intra-sinusoidal resistance. Increased vascular pressures in the liver disallow normal processing of dietary nutrients and toxic metabolites, as well as efficient venous blood return to the heart from the viscera. In addition, sinusoidal endothelial cells lose their fenestrations during liver fibrogenesis (96, 97) and are unable to allow macromolecules to diffuse across the endothelium to the hepatocytes (98). In advanced cirrhosis, angiogenesis may also occur in an HSC-dependent manner within fibrotic tracts that bridge between larger vessels, shunting blood away from sinusoids (99). This alteration in blood flow is detrimental to the hepatocytes, which are perfused primarily through the sinusoidal capillaries. As a consequence, derangement in the metabolic and synthetic functions of the liver comprises the clinical syndrome of cirrhosis. Ultimately, liver cirrhosis can be characterized as a vascular disease process.

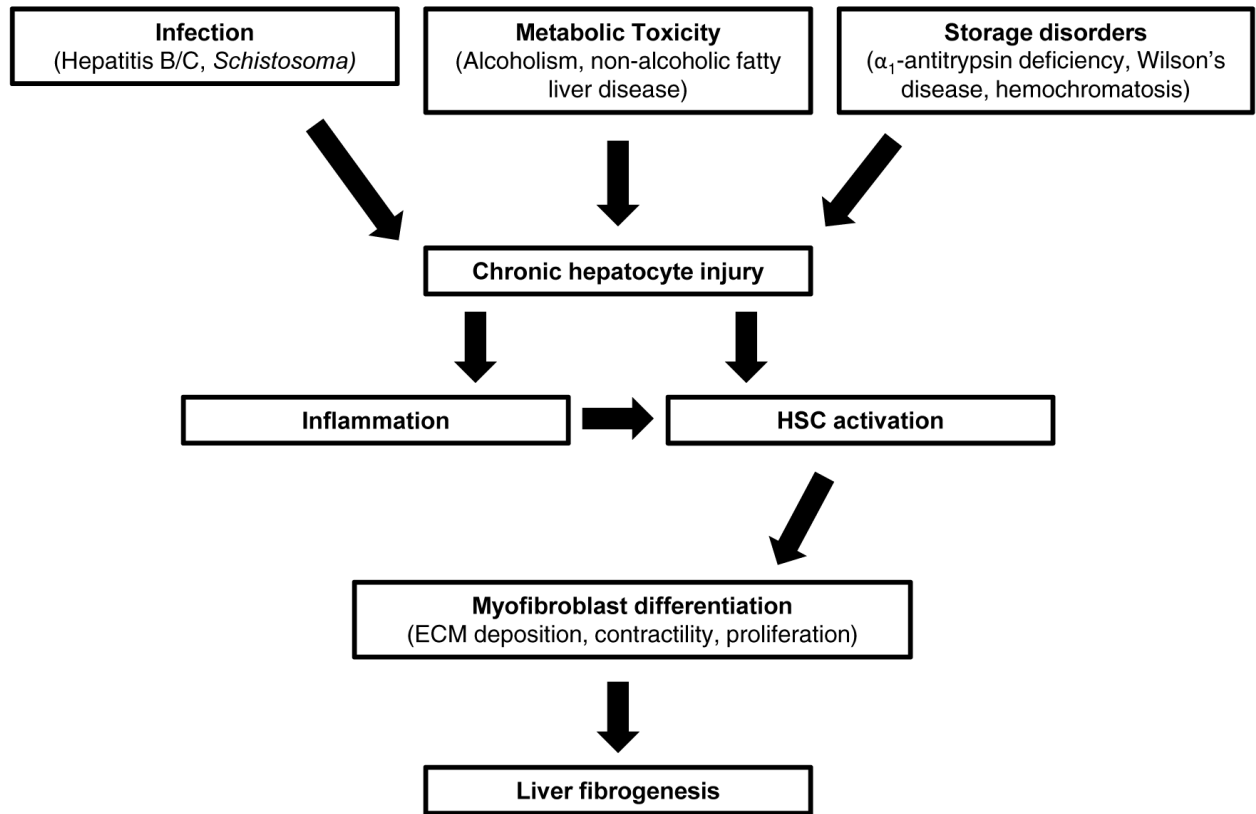


Figure 3. Progression from liver injury to fibrosis. Hepatic fibrogenesis is a process common to any condition that results in chronic inflammation and injury to the hepatocytes (the parenchymal cells of the liver). Significant causes include infection, alcoholism, non-alcoholic fatty liver disease (NAFLD), hepatic storage diseases, and chemical toxicity (e.g. hepatotoxic medications). Activation of hepatic stellate cells (HSCs) is necessary for liver repair after acute injury; however, accumulation of myofibroblasts from chronic inflammation and liver injury results in fibrogenesis. It is therefore crucial to remove the underlying pathology for resolution of fibrosis to occur. Adapted from (100).

1.2.2 Challenges to treating hepatic cirrhosis

Liver cirrhosis and failure is a leading cause of death in the United States and is the common outcome for a variety of chronic liver diseases, including hepatitis B/C, alcoholism, and non-alcoholic fatty liver disease. Prevalence of liver cirrhosis continues to increase due to the Hepatitis C and obesity epidemics worldwide. Currently the only strategy to target liver cirrhosis is to treat the underlying liver pathology. Some success has been found with this approach as better anti-viral regimens have become standard for hepatitis B and C. However, not all hepatitis patients tolerate or respond to therapy, and lifestyle changes associated with alcoholic or fatty liver-related cirrhosis are difficult to implement. Therefore, current disease-specific treatments are often inadequate or too late to stem the progression to end-stage liver disease, when only symptomatic therapy and liver transplant are viable options.

Only recently have scientists and clinicians realized that regression of established cirrhosis may be an achievable goal in patients. In animal models, regression of fibrosis has been consistently seen after removal of the chronic hepatic injury and is associated with HSC apoptosis and quiescence (101-103). However, in contrast to the relatively quick timeline of animal models of fibrosis (weeks), human liver cirrhosis represents up to decades of collagen crosslinking and parenchymal remodeling, presenting a more difficult and multi-variable challenge for potential anti-fibrotic therapies (104). Therefore, the idea that regression of cirrhosis can also occur in humans has historically been met with some skepticism. Within the last decade, however, an increasing number of clinical studies have been published reporting a decline in histological fibrosis score with successful therapy for the underlying disease (such as hepatitis C) (105). With concurrent greater appreciation of the basic mechanisms of liver fibrogenesis, particularly the signaling pathways regulating the deposition of matrix by

myofibroblasts and/or survival of these cells, the advent of fibrosis-specific drugs that can be adjuvant therapies to disease-specific treatments is on the horizon (106-108).

1.3 PLASMINOGEN ACTIVATORS

1.3.1 Structure, function, and clearance of plasminogen activators

Fibrinolysis is the process by which crosslinked molecules of fibrin are broken down by the serine protease plasmin and cleared from a site of injury. As shown in Figure 4, plasmin activity is positively regulated by the plasminogen activators and negatively regulated by α 2-antiplasmin and α 2-macroglobulin, collectively referred to as the plasminogen activating system (PAS). Tissue-type plasminogen activator (t-PA) and urokinase-type plasminogen activator (u-PA) are soluble serine proteases present in the serum and various tissues that are known primarily because they activate the zymogen plasminogen into its active form, plasmin. Both PAs are secreted in a single chain form and can be cleaved into a two-chain form by plasmin and other proteases; both single chain and two-chain t-PA can be enzymatically active, while single chain u-PA has significantly reduced activity compared to its activated form (109). Both t-PA and u-PA possess a C-terminal serine protease domain, a zymogen activation site, one (u-PA) or two (t-PA) kringle domains, and an epidermal growth factor (EGF) domain (110). In addition, t-PA possesses a fibronectin-type II “finger” domain at its amino-terminal domain (110), as shown in Figure 5.

Regulation of PA function occurs by formation of inhibitory complexes and clearance from the extracellular environment. The PAs have been found to be specifically inhibited by the

serpins plasminogen activator inhibitor type-1 and -2 (PAI-1 and PAI-2); however, PAI-1 is thought to be the primary physiological inhibitor of the PAs *in vivo* as most PAI-2 is expressed intracellularly (111). The low density lipoprotein-receptor related protein-1 (LRP1; also known as the α_2 -macroglobulin receptor or CD91) and gp330 have been shown to bind and internalize u-PA and its complexes (with PAI-1 and/or u-PAR) on hepatocytes (110), while t-PA and t-PA-PAI-1 complexes have been shown to be cleared by LRP1 (on hepatocytes and Kupffer cells) and the mannose receptor (on endothelial cells) (110, 112, 113).

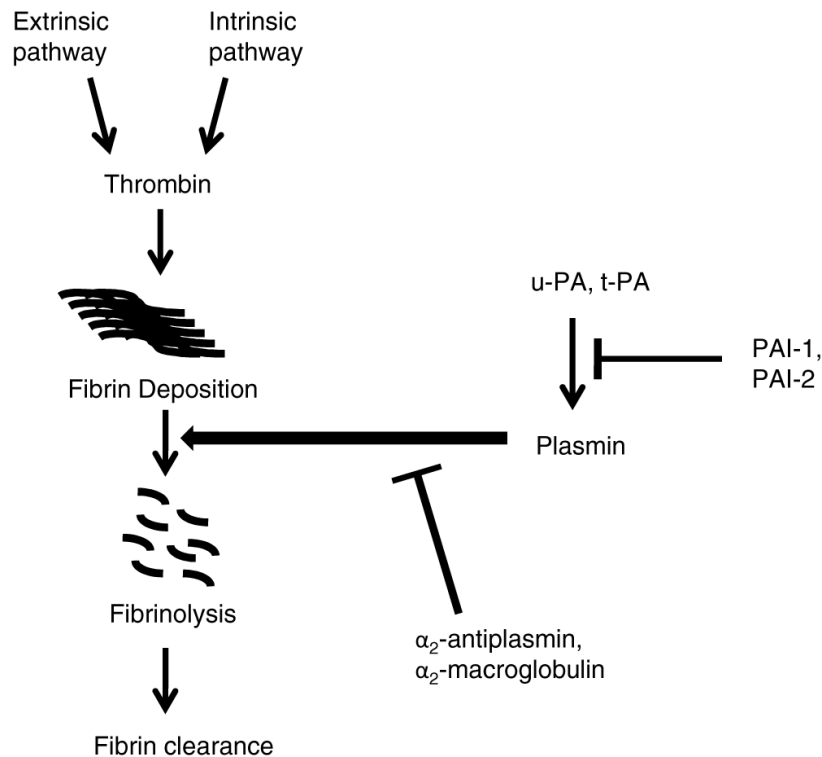


Figure 4. Relationships and effects of plasmin in fibrinolysis and in hepatic homeostasis. Plasmin is a multi-functional serine protease that promotes dissolution of fibrin clots during hemostasis. It is activated by urokinase plasminogen activator (u-PA) and tissue-type plasminogen activator (t-PA) and inhibited by α_2 -antiplasmin and α_2 -macroglobulin. Adapted from (100).

Each of the members of the PAS has known non-classical functions. Plasmin has been reported to cleave a variety of extracellular matrix proteins, growth factors, and proteases. For instance, the activation of matrix metalloproteinase (MMP)-2 and -9, both targets of plasminogen-mediated proteolysis, is essential for successful tissue remodeling in normal liver regeneration (95). Through binding to its cell-surface receptor u-PAR (urokinase plasminogen activator receptor), u-PA mediates cell-mediated matrix turnover and cell migration (114). t-PA has emerged as a regulator of the blood-brain barrier via ligand-binding to LRP1 (115). The PAs and plasmin have also been noted to activate hepatocyte growth factor (HGF), the biological importance of which is discussed in greater detail below.

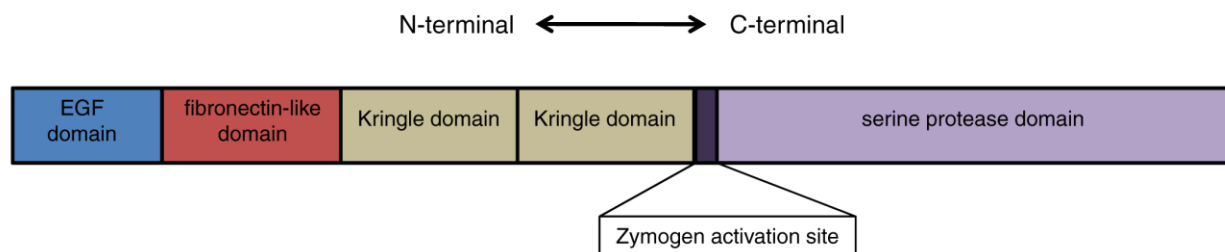


Figure 5. Schematic illustrating the different functional domains of t-PA. t-PA is a bi-functional protein, with N-terminal receptor and fibrinogen-binding regions and a C-terminal protease domain.

1.3.2 Plasminogen activators in liver homeostasis

Plasminogen is primarily expressed in the liver. The resting liver does not express detectable amounts of the PAs or PAI-1; however, studies in rodents have revealed multi-dimensional roles of the PAs in normal liver repair after injury, as shown in Figure 6. The generation of plasmin by the PAs is necessary for appropriate clearance of fibrin and restoration of normal liver architecture following acute liver injury (116). Mice lacking plasminogen have prolonged liver injury and fibrin deposition after acute carbon tetrachloride intoxication despite normal hepatocyte proliferative response post-injury (117). Interestingly, however, plasminogen-dependent tissue remodeling is not rescued by concurrent genetic deletion of fibrinogen. Correspondingly, genetic loss of u-PA or both u-PA and t-PA in mice prolongs liver injury and fibrin deposition compared to wild-type controls (116, 118, 119). As noted above, the PAs and plasminogen have also been shown *in vitro* and *in vivo* to be indirect and direct activators of HGF, a prominent hepatocyte mitogen and anti-apoptotic factor that signals through the tyrosine kinase receptor MET (120-123). In fact, constitutively active MET is able to rescue plasminogen-null mice from an inability to reorganize liver architecture (120). These studies demonstrate the integral, although not completely understood, role of plasmin activity in promoting resolution of liver injury.

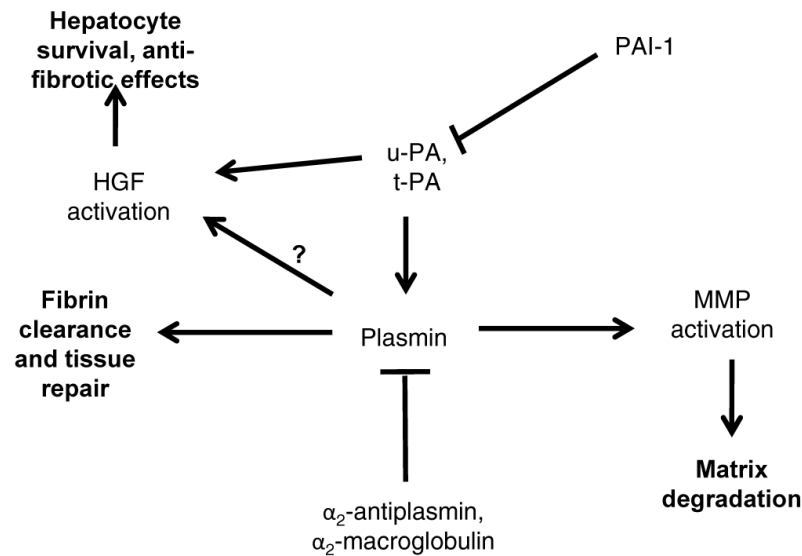


Figure 6. The plasminogen activators promote liver homeostasis. After injury, the plasminogen activating system has multi-functional roles in promotion of matrix turnover via plasmin activation and fibrin clearance during injury and activating growth factors such as hepatocyte growth factor (HGF). Adapted from (100).

1.3.3 Plasminogen activators in liver injury and fibrosis

Evidence for a role for the PAs in modulating human liver cirrhosis is not lacking. In a study examining the prevalence of pro-thrombotic risk factors in a cohort of chronic hepatitis patients segregated by histologic severity of fibrosis, plasminogen deficiency (as measured by colorimetric assay of patient plasma) was present in 19% of patients with advanced fibrosis versus 2% in mild fibrosis ($p=0.03$) (124). Our laboratory reported elevation of plasmin protein levels in human cirrhotic livers as compared to normal control tissues (125). Interestingly, in the same study, hepatocellular carcinomas were generally plasmin negative. Elevation of tissue expression and serum concentration of the PAs and their targets (HGF, plasmin) have been

observed in chronic liver injury and disease in humans and rodents but is accompanied by increases in PAI-1 (125-127). This suggests a net decrease in PA and plasmin activity, despite increased concentrations, may contribute to liver fibrosis.

HSCs regulate plasminogen activation through expression of various components of the PA system, such as u-PA and PAI-1 (128). In addition, exogenous plasmin can suppress *in vitro* activation of HSCs. Martinez-Rizo *et al.* found that by over expressing u-PA in a human-derived HSC line and increasing plasminogen activation, they could suppress HSC activation and expression of pro-fibrotic cytokines such as TGF- β 1 in a plasmin-dependent manner (129).

In animal studies, a decrease in HGF activation was seen after surgical resection in rats with dimethylnitrosamine-induced cirrhosis (130). Correspondingly, loss of PAI-1 ameliorates liver fibrosis development three weeks post-bile duct ligation and is associated with increases in t-PA activity and HGF activation (131). A recent study using a lung fibrosis model also demonstrates that loss of PAI-1 leads to increased HGF activation and downstream production of prostaglandin E2, a known anti-fibrotic factor in lung (132). Hence, it is reasonable to hypothesize that the concurrent increase in PAI-1 expression in liver fibrosis models inhibits HGF activation and exacerbates liver injury.

Conversely, over-expression of components of the PAs can reverse liver fibrosis *in vivo*. HGF gene therapy, when given as a naked DNA plasmid by tail vein injection or by intramuscular injection, can improve cirrhosis by either bile duct ligation or carbon tetrachloride (91, 133). PA gene therapy can improve liver cirrhosis as well; a single dose of uPA, introduced by adenoviral vector to rats after six weeks of carbon tetrachloride administration, led to marked histological improvement by 10 days post-therapy. Reduction of fibrosis was associated with increased HGF transcription and MMP-2 activity (134).

Nevertheless, a relevant signaling role of the PAs during liver fibrogenesis remains unclear. Higazi *et al.* recently reported amelioration of fibrosis with the loss of either or both of the PAs (135), while Hsiao and colleagues reported exacerbation of hepatic fibrosis with the loss of t-PA (136). Interestingly, in a model of *in vivo* alcoholic injury, plasminogen activation was promoted at moderate dosage of alcohol (0.4 g/kg) but suppressed at higher dosages due to an increase in PAI-1 activity. Furthermore, *in vitro* treatment of a human stellate cell line with a low concentration of alcohol (10 mM) increased plasmin activity, and this effect was dependent on the receptor annexin A2, a plasminogen and t-PA receptor (137). Taken together, it is likely that the PAs have signaling roles that are relevant in liver fibrosis development; however, any study that wishes to analyze the mechanisms must remember to take into account the relative levels of the PA and plasmin inhibitors.

1.4 LOW DENSITY LIPOPROTEIN RECEPTOR-RELATED PROTEIN 1 (LRP1)

1.4.1 General structure and function

LRP1 (also commonly known as α_2 MR and CD91) is a 600 kDa multi-functional receptor that binds to over 40 different ligands (138). These include ligands such as lipoproteins (e.g. LDL, VLDL), proteases and their inhibitor complexes (e.g. t-PA/PAI-1, α_2 -macroglobulin, metalloproteinases), and growth factors (e.g. TGF- β 1, CTGF). In addition to functioning as a clearance receptor to control serum concentrations of these diverse ligands, LRP1 plays cell-specific roles in normal and pathologic physiology (139); it has been found to be involved in blood-brain barrier permeability (140), regulation of β -amyloid generation in the brain (141),

cancer cell survival and metastasis (142), and atherosclerosis development (143). LRP1 null mice are embryonic lethal due to dysregulation of uPA:PAI-1 complexes at the site of implantation (144).

LRP1 is composed of two chains: the α -chain is 515 kDa, completely extracellular, and contains the ligand-binding regions, while the β -chain is 85 kDa and contains the transmembrane and intracellular tail portions of the molecule (145), as indicated in Figure 7. They are synthesized as one chain, cleaved, and remain associated with each other non-covalently. The cytoplasmic tail contains two NPXY motifs that are sites of phosphorylation and adaptor protein docking (146). Additional phosphorylation sites are involved in regulating endocytosis and recycling of the receptor (147). LRP1 can be phosphorylated by kinases such as v-Src, inducing binding of docking proteins including Shc and Disabled-1 (148, 149). Its activity is regulated endogenously by the chaperone protein RAP (receptor-associated protein), which binds to it during processing in the endoplasmic reticulum and Golgi apparatus to prevent intracellular activation of the receptor (150). Proteolytic cleavage at an extracellular membrane-proximal region can mediate release of the extracellular domain as a soluble receptor (151), while intracellular cleavage of the cytoplasmic tail domain by γ -secretase-like activity releases a potential intracellular signaling molecule (152).

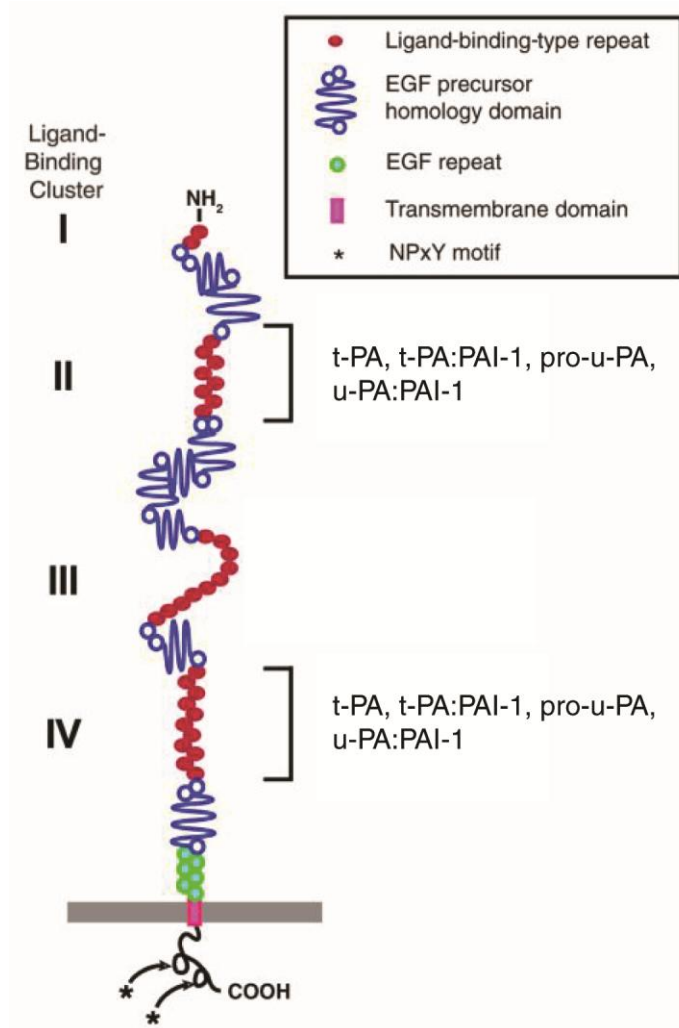


Figure 7. Schematic of LRP1 and ligand-binding regions. The plasminogen activators and its inhibitor can bind to multiple regions on the LRP1 receptor. Adapted from (153).

1.4.2 t-PA and LRP1 in kidney fibrosis

Recent studies have defined a non-proteolytic role for t-PA in the development of kidney fibrosis. Mice lacking t-PA developed significantly less tubular injury and matrix deposition in a model of unilateral urethral obstruction (UUO) that correlated with decreased levels of MMP-9

but no change in plasmin expression and activity, suggesting that the activation of MMP-9 in wild-type mice via t-PA was independent of its proteolytic activity (154). Further studies found that the previously characterized t-PA clearance receptor LRP1 was necessary for the induction of MMP-9 by t-PA (155). LRP1 becomes phosphorylated upon ligand-binding of t-PA, leading to myofibroblast differentiation of kidney tubular epithelial cells. These signal transduction events are mediated through β 1 integrin and integrin linked kinase (ILK) (156). Furthermore, t-PA signaling through LRP1 also promotes myofibroblast survival in the presence of apoptosis-promoting conditions via ERK1/2 dependent mechanism (157). Hence, these data strongly support a non-proteolytic role for t-PA-mediated promotion of kidney fibrosis.

1.4.3 Role of LRP1 in smooth muscle cells

In contrast, LRP1 has been found to suppress the function of signaling pathways that are known to be involved in promoting fibrogenesis, such as the platelet derived growth factor receptor- β (PDGFR β). Increased PDGF ligand binding promotes HSC proliferation and liver fibrosis (158, 159), while inhibition of PDGFR β signaling can decrease liver fibrosis (160). PDGFR signaling is also mitogenic in vascular smooth muscle cells (161) and contributes to development of atherosclerotic plaques (162).

Recent studies have uncovered that LRP1 suppresses smooth muscle cell proliferation and is protective in a murine model of atherosclerosis (143). LRP1 null vascular smooth muscle cells had increased levels of PDGFR β , increased markers of proliferation, and larger atherosclerotic plaque formation. Inhibition of PDGFR β activation through use of imatinib (Gleevec) was able to decrease plaque formation in smooth muscle LRP1-null mouse aortas, suggesting that LRP1 is protective against atherosclerosis by suppressing PDGFR β (or other

tyrosine kinase receptor) activity (143). Previous work demonstrated that LRP1 and PDGFR β act as co-receptors: upon PDGF receptor-ligand interaction, LRP1 is phosphorylated in a PDGFR β -dependent manner and clusters with PDGFR β within clathrin-coated pits for endocytosis (163, 164). It is postulated that in this way, LRP1 targets PDGFR β for degradation, and the loss of LRP1 then allows sustained surface expression of PDGFR β , such as was seen in the smooth muscle cell-specific LRP1 knockout.

2.0 TISSUE-TYPE PLASMINOGEN ACTIVATOR DOWN-REGULATES HEPATIC STELLATE CELL ACTIVATION THROUGH LDLR-RELATED PROTEIN 1 IN RATS AND MICE

2.1 INTRODUCTION

Liver cirrhosis is a rapidly growing global health concern due to the increasing prevalence of chronic liver diseases such as viral hepatitis and non-alcoholic fatty liver disease. Regardless of etiology, chronic parenchymal injury leads to accumulation of scar tissue and organ dysfunction through a highly orchestrated process centered on a *de novo* population of myofibroblast-like (MFB-like) cells. Hepatic stellate cells (HSCs) are considered one of the major sources of matrix-depositing MFB-like cells in liver injury; in response to inflammatory cytokines and growth factors, they become more proliferative, migratory, contractile, and fibrogenic (7). Gaining greater understanding of the factors that regulate HSC trans-differentiation is key to selecting druggable anti-fibrotic targets.

The plasminogen activators are multifunctional serine proteases involved in fibrinolysis, cellular migration (165), growth factor activation (166), and hepatic repair after injury (116, 167). Loss of the plasminogen activators delays liver regeneration after acute injury, which has been largely attributed to sustained fibrin deposition and loss of growth factor and matrix

metalloproteinase activation (116). However, their roles in chronic liver injury have been ambiguous (135, 136), possibly due to pleiotropic functions on multiple cell types.

Emerging literature suggests the biological effects of the plasminogen activators in any system cannot be isolated to their proteolytic function; in fact, signaling functions may be equally, if not more, important to understanding their roles in disease processes. In particular, tissue-type plasminogen activator (t-PA) is a key endogenous signaling molecule in injury and disease (156). One prominent t-PA signaling receptor is LRP1 (LDLR-related protein 1). LRP1 is a multi-ligand receptor involved in protease-inhibitor complex and growth factor clearance, but additionally, it can signal following ligand-binding to promote cellular migration, differentiation, and changes in viability or proliferation (139). Recent studies have defined new roles for LRP1 in modulating tissue fibrosis and the myofibroblast phenotype (156). HSCs are now known to express LRP1 (168, 169); however, little is known about the role of LRP1 in HSCs during liver injury and regeneration.

In the present study, we sought to establish if there is t-PA-mediated signaling through LRP1 in HSCs. We anticipated a pro-fibrotic response, similar to kidney; however, here, we present data demonstrating that LRP1 activation by t-PA *in vitro* decreases expression of markers associated with HSC activation. Further, *in vivo* deletion of LRP1 in HSCs, or t-PA globally, allows MFB-like cells to persist after injury. Hence, t-PA mediated signaling through LRP1 suppresses pro-fibrotic MFB-like cells, a finding with potential therapeutic value for chronic liver disease.

2.2 EXPERIMENTAL PROCEDURES

2.2.1 Reagents and Antibodies

Recombinant single-chain and two-chain t-PA (American Diagnostica, Stanford, CT, and Molecular Innovations, Novi, MI) and an irreversible, inhibitor-treated, non-proteolytic form of t-PA (FPRCK-TPA, Molecular Innovations) were used for cell culture experiments. FPRCK-TPA is tested to have zero enzymatic activity by functional assay (personal communication with company representative). Recombinant human TGF- β 1 was purchased from R&D Systems (Minneapolis, MN) Antibodies used for immunohistolabeling and Western blotting include: α -SMA (Clone 1A4; Dako, Carpinteria, CA or Sigma-Aldrich), p-LRP1 (Santa Cruz Biotechnology, Santa Cruz, CA), LRP1 (Clone 11H4; ATCC, Manassas, VA or #3501; American Diagnostica), PDGFR β (Santa Cruz), p-Akt (Thr308) and total Akt (both Cell Signaling Technology, Danvers, MA), p-ERK1/2 and total ERK1/2 (Cell Signaling Technology), t-PA (American Diagnostica), PAI-1 (American Diagnostica). The PI3K pathway inhibitor LY294002 was from Cell Signaling. Human RAP was prepared as described (170).

2.2.2 Rat hepatic stellate cell isolation and cell culture

Male Fischer 344 rats (Charles River, Wilmington, MA) greater than 200 grams in weight were used for isolation of primary HSCs. Primary rat HSCs were isolated using a protocol adapted from Riccalton-Banks, et al. (171). Briefly, liver cells of male Fischer 344 rats were dissociated using an in situ two-step collagenase perfusion method, as previously described (172, 173). After low-gravity centrifugation of total liver cell suspension in calcium-free buffer to isolate

hepatocytes, non-parenchymal cells were isolated from the resulting supernatants (174, 175). The NPC fraction was washed once in complete medium (Dulbecco's Modified Eagle Medium + 10% fetal bovine serum + 0.1% gentamicin solution) and plated on 3-4 uncoated six-well tissue-culture plates. Cells were maintained in a humidified incubator at 37°C with 5% CO₂. Complete medium was replaced 24 hours post-plating. At 48 hours post-plating, cells were serum starved for 24 hours before treatment as indicated in the text. Rat HSC-T6 and human LX-2 cells (both gifts from Dr. Scott Friedman, Mt. Sinai School of Medicine, New York, NY) maintained in the same medium as primary HSCs were used for t-PA experiments. HSC-T6 cells were seeded at 3x10⁵ cells/mL, allowed to attach overnight, then serum starved for 24 hours prior to treatment as indicated. LX-2 cells were seeded at 1x10⁵ cells/mL and allowed to grow to ~60% confluency prior to serum starvation and subsequent treatment. NRK-49F cells (ATCC) were cultured in Dulbecco's modified Eagle's medium/Ham's F12 (1:1) supplemented with 5% FBS until ~70% confluency, after which cells were serum starved 24 hours prior to treatments as indicated in text.

2.2.3 MTT and [³H]Thymidine Incorporation Assays

HSC-T6 cells were seeded at 3x10⁵ cells/mL and allowed to attach overnight in complete medium. Cells were treated with vehicle control or t-PA (10nM) for 48 hours in serum-free conditions. An MTT-based *in vitro* toxicology assay kit (Sigma-Aldrich) was used according to manufacturer instructions to assess for mitochondrial dehydrogenase activity after 48 hours. For the [³H]thymidine incorporation assay, [³H]thymidine was added to the medium to a final concentration of 2.5 µCi/ml at the same time as t-PA treatment. After 48 hours, cells were fixed with ice-cold 5% trichloroacetic acid, washed in running tap water, and air dried completely. One milliliter of 0.33N NaOH was added to each well for 30 minutes to solubilize the cells. A

300- μ l aliquot from each well was used to measure cpm/dpm in a Beckman LS6000IC scintillation counter (Beckman Coulter, CA).

2.2.4 SDS-PAGE and Western Blot

Cell cultures were harvested in lysis buffer (10mM Tris buffer with 1% sodium dodecyl sulfate and protease/phosphatase inhibitor cocktail) and analyzed by Western blot as previously described in detail (121, 176). Briefly, thirty micrograms of protein from each sample was mixed with loading buffer with or without 100 mmol/L dithiothreitol, heated to 65°C for 15 minutes, resolved by electrophoresis on 8 or 10% SDS-polyacrylamide gels, and transferred to polyvinylidene difluoride membranes for western blot analyses. Membranes were blocked in 5% milk or fish gelatin in Tris-buffered saline + Tween, followed by incubation with primary antibody in 5% blocking buffer. Horseradish peroxidase-conjugated secondary antibodies (Jackson ImmunoResearch Laboratories, West Grove, PA) were used at a concentration of 1:50,000. Blots were developed using enhanced chemiluminescence substrate (Pierce, Rockford, IL) and visualized on X-ray film. Loading equivalence was assessed from densitometry of scanned images of Ponceau Red staining performed immediately after transfer of protein onto the polyvinylidene difluoride membranes (97).

For western blot analysis of cell culture medium post-treatment, 250 microliters of conditioned medium were supplemented with protease/phosphatase inhibitors and concentrated to approximately 20 microliter volume and applied to an 8 or 10% SDS- polyacrylamide gel for resolution. Transfer and blotting were preformed as described above.

2.2.5 Immunoprecipitation

HSC-T6 cells were treated with vehicle control or t-PA for one minute and lysed in ice-cold CHAPS buffer (10 mM CHAPS, 20 mM HEPES [pH 7.4], 150 mM NaCl, 2 mM CaCl₂) supplemented with phosphatase and protease inhibitor cocktails (Sigma-Aldrich). Samples were sonicated on ice to further homogenize the cells. One hundred micrograms of lysate from each treatment were incubated with mouse IgG and Protein A/G PLUS agarose beads (Santa Cruz Biotechnology Inc.) for an hour at 4°C to “pre-clear” the lysate. Beads were pelleted and supernatants transferred to new tubes. The pre-cleared lysates were then incubated with monoclonal antibody against LRP-1 (11H4) or equivalent amount of mouse IgG at 4°C overnight with rotation. Protein A/G PLUS agarose beads were added to the lysates and incubated at 4°C for 3 hours. The beads were pelleted, washed with CHAPS buffer, and the bound proteins were extracted from the beads in reducing sample buffer. Proteins were resolved on 10% SDS-polyacrylamide gel, and analyzed by western blotting as described above, using anti-phosphotyrosine (BD Biosciences, San Jose, CA) and anti-LRP-1 (11H4) antibodies.

2.2.6 Reverse Transcription and Polymerase Chain Reaction

Treated cells were harvested using RNABee (Amsbio, Lake Forest, CA)-chloroform extraction and precipitated with isopropanol. Isolated RNA was DNase-treated using Turbo DNase kit (Life Technologies, Grand Island, NY) according to manufacturer instructions. RNA was converted to cDNA using random hexamers and SuperScript III reverse transcriptase (Life Technologies). One hundred nanograms of cDNA from each sample were used for polymerase chain reaction for collagen I α 1 or β -actin. Primers used were previously described (177). The primer sequences

used were as follows: Collagen I Forward Primer 5'-AAC GGC AAG GTG TTG TGC CAT G-3'; Collagen I Reverse Primer 5'-AGC TGG GGA GCA AAG TTT CCT C-3'; β -actin Forward Primer 5'-GAG CTA TGA GCT GCC TGA CG-3'; β -actin Reverse Primer 5'-GTG CTA GGA GCC AGG GCA GTA A-3'. No enzyme and water controls were run for each primer set (data not shown). PCR consisted of 30 cycles at 94°C for 1 minute, 57°C for 1 minute, and 72°C for 1 minute, followed by a final extension step at 72°C for 7 minutes. PCR products were run on a 2% agarose gel containing ethidium bromide and visualized with ultraviolet light for photography.

2.2.7 Gene Array Analysis

HSC-T6 cells were cultured and treated with vehicle control or t-PA for 24 hours as described above. Three treated wells from a six-well plate were pooled for each condition and cell pellets were snap-frozen until further preparation (as described below). A parallel plate was harvested for western blot analysis for α -SMA to confirm previously seen effects prior to proceeding with the microarray. All sample preparation and hybridization procedures were performed by the laboratory of Dr. Jianhua Luo in the Department of Pathology at the University of Pittsburgh School of Medicine. Double stranded cDNA was synthesized from total RNA and used as the template *in vitro* transcription to generate biotin-labeled cRNA according to manufacturer's instructions. Eight micrograms of the labeled cRNA from each sample was fragmented and hybridized to Rat Genome 230 2.0 GeneChip array (Affymetrix, CA, USA) and the signal was amplified by biotin-avidin-phycoerythrin technique. Affymetrix scanner 3000 7G and Genechip Operating software 3.2 (Affymetrix, CA, USA) were applied to scan the images and convert intensity to a numerical format representing an average difference value for each probe. Raw

data were analyzed by removing all probes with values having a combined sum of less than 200 intensity units between the compared treatments. Unidentified sequences were excluded. The remaining data was sorted by both fold change and absolute change in intensity between treatments.

2.2.8 Carbon tetrachloride acute injury and resolution experiments

Male C57Bl/6 (Jackson Laboratories, Bar Harbor, Maine), t-PA ^{-/-} (Jackson Laboratories), or LRP^{flox/flox};SM22-cre +/- mice (Strickland laboratory, University of Maryland at Baltimore), aged 10-12 weeks, were used for in vivo acute liver injury experiments. Mice were given plain water or 0.05% phenobarbital (PB) water *ad libitum* for one week prior to corn oil (control) or carbon tetrachloride (CCl₄) injections (1uL/gram body weight, diluted 1:4 with corn oil for injection; Sigma-Aldrich, St. Louis, MO). The PB equalized the cytochrome P450 enzyme 2E1 expression by western blot amongst the different genotypes after injury (see Figure 16-17) (178). Two acute doses of CCl₄ were given three days apart and mice were harvested over a time course of 1-14 days after the second dose. Total and liver body weights were recorded at time of sacrifice. Serum and liver tissue were collected for biochemical and histological analyses. Serum alanine transaminase was analyzed by the University of Pittsburgh Medical Center-Presbyterian Hospital, Department of Pathology Lab Support Services.

2.2.9 Immunohistochemical staining and fluorescent labeling

Formalin-fixed paraffin embedded livers from CCl₄-treated mice (n=3-5 at each time point) were cut into 4µm-thick section for immunostaining. Immunohistochemistry was done by

standard avidin-biotin complex-horseradish peroxidase method. Double staining on paraffinized mouse tissue sections with anti- α -SMA (1:50) and anti-p-LRP1 (1:200) was labeled with Qdot-conjugated anti-mouse Q705 and anti-rabbit Q605 antibodies, respectively (Life Technology). Triple staining was done with the addition of anti-t-PA (1:150) labeled with biotinylated anti-goat secondary and Streptavidin-Q655. Anti-human α -SMA antibody was confirmed to cross-react with mouse α -SMA and be specific to α -SMA with a mouse-on-mouse blocking kit (Vector Laboratories, Burlingame, CA). Sequential double labeling on LRP^{fl_{ox}/fl_{ox}};SM22-cre^{+/-} mice and t-PA^{-/-} mice liver was done using Acetone:MeOH (1:1) fixed 4 μ m-thick frozen sections with anti-LRP1 (1:50, American Diagnostica) and anti-mouse-Cy5 secondary antibody, followed by α SMA-Cy3 (1:1000, Sigma-Aldrich).

2.2.10 Image Capture and Analysis

Provis microscopes for brightfield imaging (Olympus, Center Valley, PA), Olympus Fluoview 1000 upright confocal microscopy for fluorescence imaging, and Metamorph software (Sunnyvale, CA) for quantification of staining were located in and provided by the Center of Biologic Imaging at University of Pittsburgh. For quantification of immunohistochemical stains, low-powered images were taken at regular intervals to cover as much of the stained tissue as possible in a non-discriminate fashion. Only edges, large vessel lumens, and artifacts were avoided in the image capture. Only slides that were stained together and imaged together were compared in analysis. Images were thresholded for positive staining and analyzed for area of staining using the same threshold. Qdot-labeled tissues were scanned with a Zeiss AxioVision MIRAX MIDI scanner (Carl-Zeiss, Jena, Germany) and captured single frame with the Panoramic Viewer from 3DHISTECH (Budapest, Hungary).

2.2.11 Statistical Analysis

Densitometry of scanned western blot and PCR gel images was analyzed using NIH ImageJ 1.42q (National Institutes of Health, USA). For western blots, scanned images of Ponceau stain were used to normalize protein loading and transfer between samples (97). All graphing and statistical analysis was performed using Prism (GraphPad, La Jolla, CA) or Excel (Microsoft, Redmond, WA). When two groups were compared, Student's t-test was performed. When more than two groups were compared, one-way analysis of variance test was performed with Tukey's post-test analyses. Statistical significance was set at $p < 0.05$, and variability within a group is presented as \pm standard error of the mean (SEM).

2.2.12 Animal use approval

The studies described were approved by the University of Pittsburgh Institutional Animal Care and Use Committee in accordance to the "Guide for the Care and Use of Laboratory Animals" published by the National Institutes of Health. The University of Pittsburgh is an accredited institution by the Association for Assessment and Accreditation of Laboratory Animal Care.

2.3 RESULTS

2.3.1 Exogenous t-PA decreases markers of HSC activation in primary and transformed cells

To examine the effect of t-PA on HSC phenotype, we treated primary or immortalized HSCs with t-PA or vehicle control for 24 hours under serum free conditions. A reproducible decrease in the HSC activation markers α -SMA and PDGFR β was seen in t-PA treated cells compared to vehicle controls (Figure 8A). In addition, t-PA markedly decreased collagen I mRNA expression in primary rat HSCs after 24 hour treatment (Figure 8A). Lastly, we observed a significant loss of mitochondrial activity as assessed by the MTT assay, a surrogate marker of cell viability, and a corroborating trending decrease in $^3\text{[H]}$ -thymidine incorporation in HSC-T6 cells after 48 hours treatment with t-PA (Figure 8B). Collectively, these data demonstrate that t-PA treatment is sufficient to suppress markers of HSC activation in vitro.

Since our results in HSCs were in contrast to what was reported to be observed in kidney fibroblasts (156), we repeated the experiments reported in the literature with the NRK-49F cell line with our reagents. As seen in Figure 8C, a preliminary experiment with the NRK-49F cells confirms the increase in fibroblast activation by western blot analysis of α -SMA in whole cell lysates post-treatment with t-PA, either alone or in combination with TGF- β 1. Thus, there are cell-specific effects of t-PA between fibrogenic cell types of different organs.

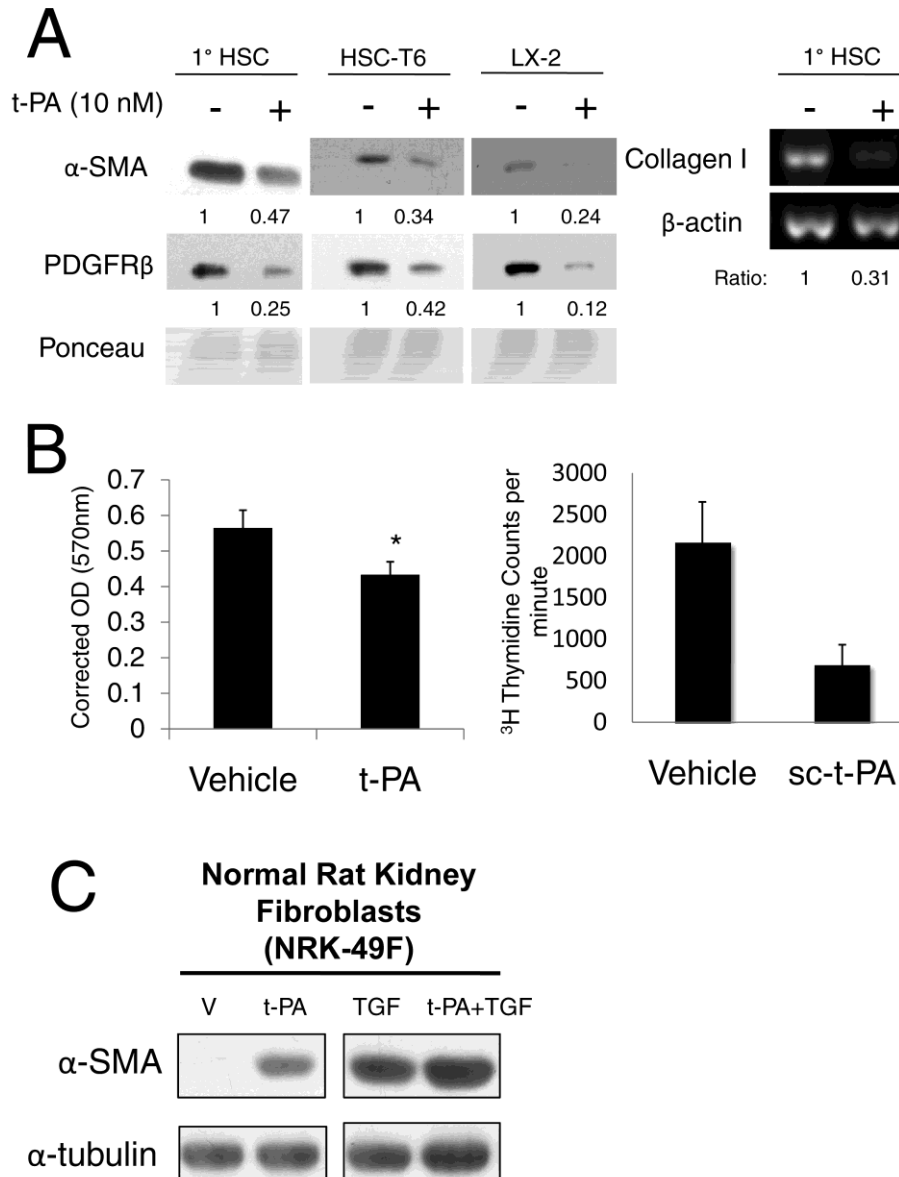


Figure 8. Exogenous t-PA suppresses HSC activation *in vitro*. (A) Primary rat stellate cells or cell lines (HSC-T6, rat; LX-2, human) were cultured serum-free for 24 h and stimulated for another 24 h with t-PA (10 nM). Whole cell protein lysates or RNA were prepared, pooled, and equal amounts were subjected to western blot analyses or RT-PCR, respectively, for the indicated markers. Normalized densitometry values are given for representative images, relative to vehicle control, with loading normalized to total Ponceau staining/lane. In all experiments, n=2-3 wells for 2-4 independent experiments per cell source. (B) HSC-T6 cells were stimulated with t-PA for 48h under serum-free conditions before measuring mitochondrial function (MTT reduction assay) or ³[H]-thymidine incorporation. n=3, *p<0.05. (C) For comparison, NRK-49F cells were

cultured to 70% confluency prior to serum starvation and 24 hour treatment with t-PA, TGF- β 1, or both. Error bars are +/- SEM. (HSC, hepatic stellate cell; α -SMA, α -smooth muscle actin; PDGFR β , platelet derived growth factor receptor- β ; t-PA, tissue-type plasminogen activator; OD, optical density)

2.3.2 Global gene expression changes after t-PA treatment of HSC-T6 cells

To further understand the cellular effects of t-PA on HSCs, we treated the HSC-T6 cells with vehicle control or t-PA for 24 hours and harvested cells for microarray analysis of total cDNAs. Identifiable genes with the maximal changes after t-PA treatment based on fold change or absolute intensity change are presented in Tables 1 and 2, respectively. Of note, several genes involved in HSC activation were noted to decrease after t-PA treatment (α -SMA, -1.47 fold change; TIMP3, -2.15 fold; Vasopressin Receptor V1a, -3.0 fold; Serotonin receptor Type 1B, -3.43 fold; Collagen III a1, -3062 total change; Collagen I a2, -2472.9 total; Collagen I a1, -1032; TIMP2, -966.7). Likewise, genes associated with HSC quiescence were up-regulated (nitric oxide synthase, +39.34 fold change; Retinol-binding protein, +2.84 fold change). These changes are consistent with the effects we reported in Figure 8 in HSC-T6 cells.

2.3.3 The effects of t-PA on HSC activation are dependent on LRP1-mediated signaling

Plasmin activity has been reported to have anti-fibrotic effects on HSCs (129). To assess the role of t-PA-mediated plasmin generation, we next asked whether the suppression of HSC activation markers by t-PA was dependent on its proteolytic activity. Interestingly, we see the same changes with treatment of a non-proteolytic form of t-PA (irreversibly inactivated) versus

wildtype t-PA (Figure 9A), suggesting in our *in vitro* system, t-PA's effects are not plasmin-dependent.

t-PA is also a known signaling ligand for the receptor LRP1 (139). To see if LRP1 becomes phosphorylated on HSCs in response to t-PA, we treated primary rat HSCs or immortalized HSC-T6 cells with t-PA for various lengths of time. LRP1 was selectively phosphorylated on the Tyr4507 residue within one minute of t-PA addition in HSC-T6 cells or five minutes in primary rat HSCs (Figure 9B). These same results were observed with the HSC-T6 cells using immunoprecipitation of whole cell lysates with anti-LRP1 and then immunoblotting for phospho-tyrosine (Figure 9B).

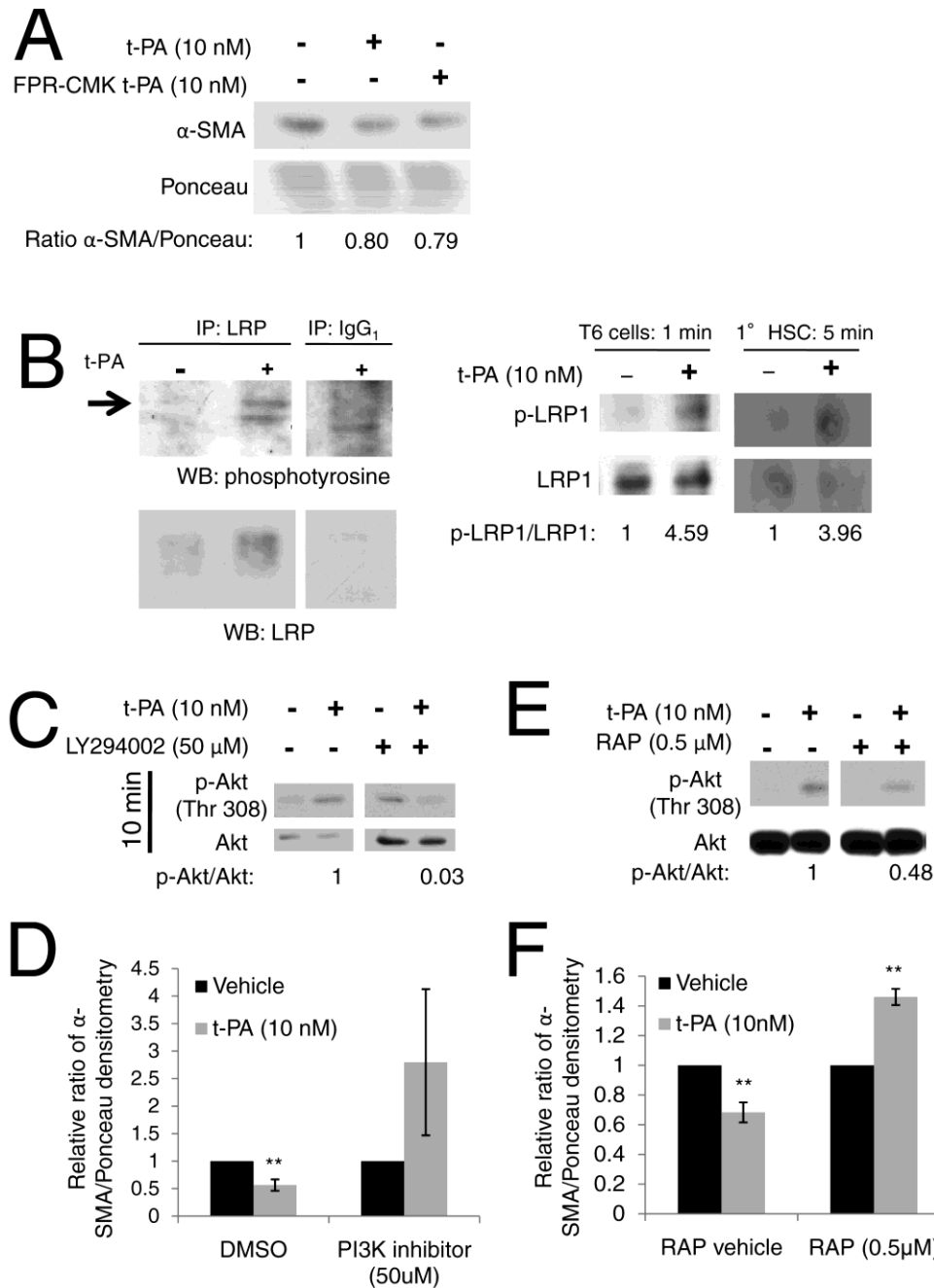


Figure 9. t-PA effects are protease-independent. Whole cell lysates were subjected to western blot with densitometry and loading values analyzed as in Figure 8 unless indicated otherwise. Representative images and matching values shown for A, B, C, and E. (A) Serum-free HSC-T6 cells were treated for 24 hours with recombinant human t-PA or protease-inactivated t-PA (irreversibly inhibited by the peptide ATA-FPR-chloromethylketone). (B) HSC-T6 cells and primary rat HSCs were cultured serum-free for 24 h, stimulated for 1 or 5 min with t-PA, and lysates analyzed either by immunoprecipitation with anti-LRP1 antibody prior

to western blot analysis for phosphotyrosine, or directly probed with p-LRP1. In both situations, total LRP1 was probed in parallel. (C-D) HSC-T6 cells were cultured serum-free for 24 h, pretreated with PI3K pathway inhibitor LY294002 or vehicle control (DMSO) for 60 minutes, and then treated with t-PA or t-PA vehicle in either DMSO or LY294002 for 10 minutes (C) or 24 hours (D). (E-F) Serum-free HSC-T6 cells were pretreated with the LRP1 inhibitor RAP or RAP vehicle control for 30 minutes, and then treated with t-PA or t-PA vehicle in the presence of RAP or RAP vehicle for 10 minutes (E) or 24 hours (F). n=6 and 3 for D and F, respectively. Error bars shown are +/- SEM. **p<0.01. (HSC, hepatic stellate cell; t-PA, tissue-type plasminogen activator; CMK, chloromethylketone; LRP1, low density lipoprotein receptor-related protein 1; RAP, receptor-associated protein; α -SMA, α -smooth muscle actin; PDGFR β , platelet derived growth factor receptor- β ; DMSO, dimethyl sulfoxide; PI3K, phosphoinositide 3-kinase)

Since Tyr4507 phosphorylation is essential for LRP1-dependent signaling pathway activation (146, 179), we tested whether t-PA addition had effects on known LRP1 downstream signaling targets. Akt was activated in t-PA treated HSC-T6 cells within ten minutes post-treatment, and this effect was abolished in the presence of a PI3K/Akt pathway inhibitor, LY294002 (Figure 9C). Stimulation of HSC-T6 cells with t-PA in the presence of the LY294002 inhibitor abrogated the suppression of α -SMA (Figure 9D). Comparable results were obtained using primary rat HSCs in a preliminary experiment (data not shown).

To confirm that Akt signaling is dependent on activation of LRP1, we used an inhibitor of LRP1 ligand-binding, the chaperone protein RAP (receptor-associated protein), to prevent t-PA signaling (180). Pretreatment with RAP in HSC-T6 cultures abrogated both Akt phosphorylation (Figure 9E) and the subsequent suppression of α -SMA expression (Figure 9F). In summary, LRP1-mediated signaling through Akt was sufficient to account for the observed effects of t-PA in HSCs.

We also observed transient ERK activation after treatment with t-PA in HSC-T6 cells (Figure 10); however consistent results were not obtained using MEK inhibitors, leading us to conclude that ERK activation was incidental rather than necessary for the downstream effects of t-PA-mediated signaling.

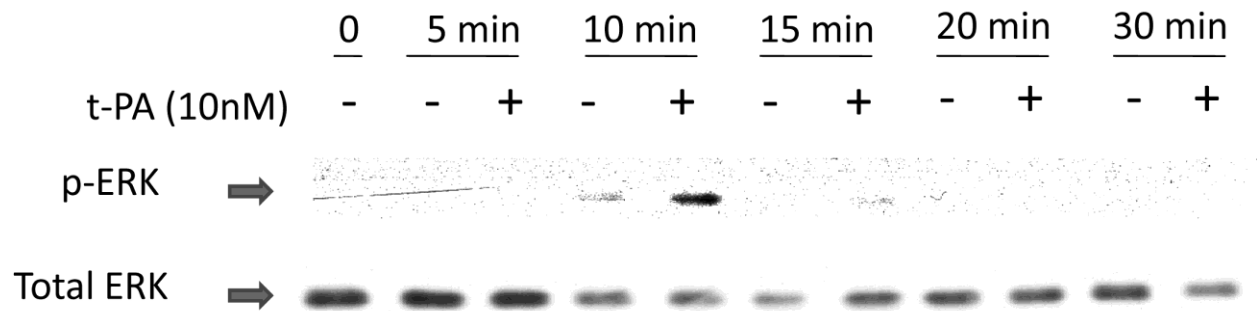


Figure 10. Transient activation of ERK by t-PA in HSC-T6 cells. HSC-T6 cells were cultured serum-free for 24 hours and stimulated with t-PA for 5-30 minutes. Whole cell lysates were analyzed by western blot for p-ERK1/2 and total ERK1/2.

2.3.4 p-LRP1 and t-PA co-localization with α -SMA precedes resolution of injury in WT mice

Since our in vitro data suggested that LRP1 signaling suppresses or reverses MFB-like differentiation, we hypothesized phosphorylation of LRP1 should occur on MFB-like cells just prior to their regression during resolution of an acute, in vivo hepatic injury. WT mice were subject to acute liver injury by carbon tetrachloride (CCl₄) following phenobarbital initiation and allowed to recover for up to 14 days in order to detect the time frame of injury resolution with

regard to the α -SMA⁺ cell population (please refer to Chapter 3.3.2 for more detailed description and justification of injury protocol used). As shown in Figure 11A, the α -SMA⁺ population drops off significantly between days four and five after injury. We next performed co-immunolocalization of p-LRP1 and α -SMA spanning the same time points (Figure 11B). Strikingly, at day 4 there was little to no co-localization of p-LRP1 with α -SMA when the overall area of α -SMA-positive staining in the tissue was high; however, beginning at day five and throughout the rest of the recovery period, co-localization was readily observed, correlating with the loss of α -SMA immunoreactivity. Figure 11B highlights α -SMA⁺ regions not exclusive to vessels in order to focus on true de novo MFB-like α -SMA⁺ cells, rather than vascular smooth muscle α -SMA⁺ cells, indicating LRP1 is activated on α -SMA⁺ MFB-like cells when they regress from the tissue.

Finally, we sought to verify that t-PA localized to SMA⁺ cells with activated LRP1. Liver sections from WT mice were co-immunolabeled at day four of recovery with antibodies against t-PA, p-LRP1, and α -SMA. Although sparse, we were able to find regions where all three were co-localized (arrow, Figure 11C) as well as multiple regions with t-PA adjacent to α -SMA⁺ cells (arrowheads, Figure 11C), indicating in situ proximity and interaction of t-PA with MFB-like cells at a time point prior to increased p-LRP1 (day five; Figure 11B). These data support endogenous t-PA-LRP1 interactions on MFB-like cells during liver injury resolution.

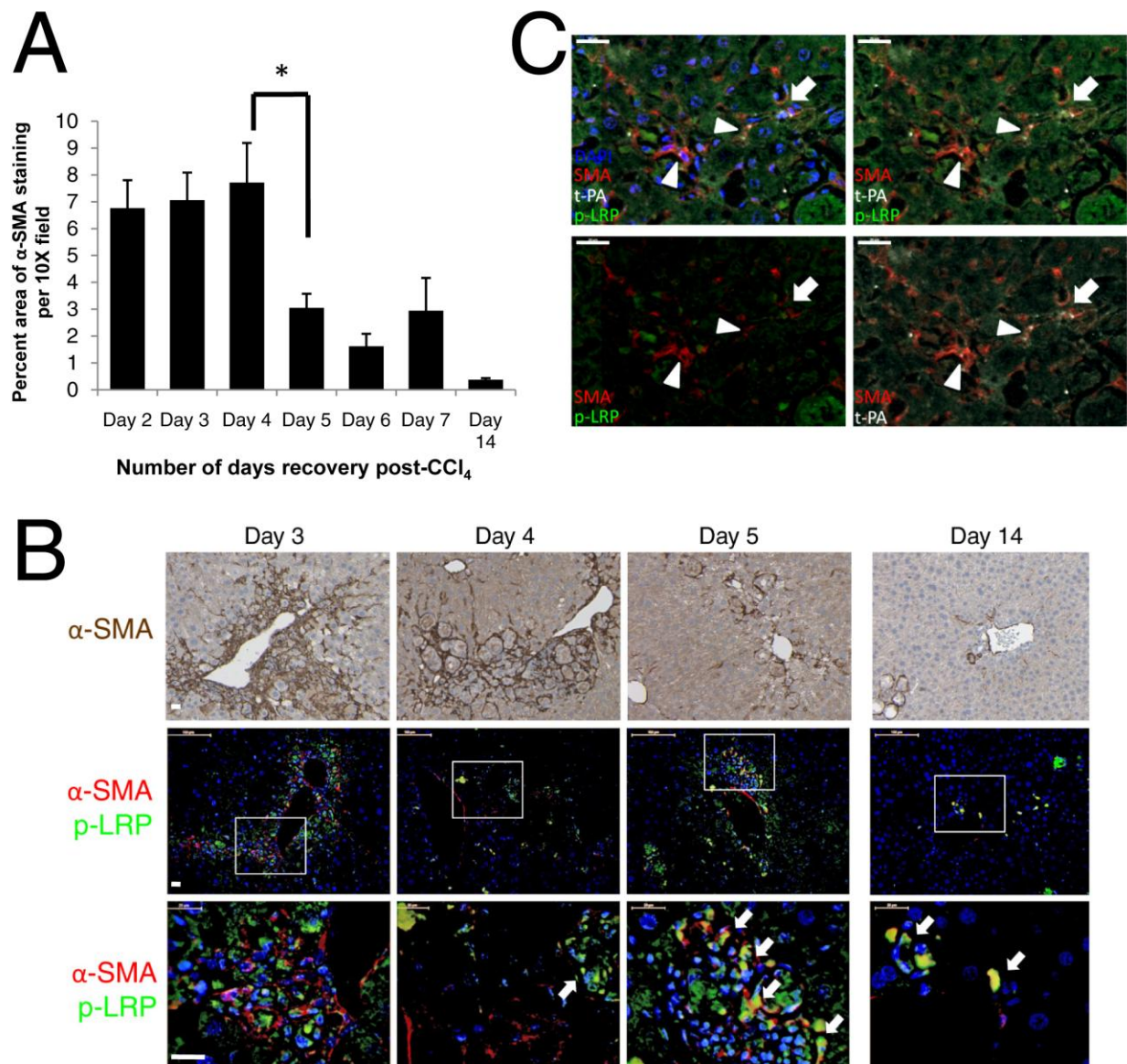


Figure 11. LRP1 is activated on HSCs during resolution of acute hepatic injury *in vivo*. Wildtype (C57Bl/6) mice were given phenobarbital (PB) in water for one week and then intraperitoneally injected twice with CCL₄ (1 μ L/g body weight) at days 7 and 10 post-PB induction. Livers were harvested at days 2-7 and 14 after the last dose, embedded in paraffin, and immunostained as indicated. n=3 mice, days 2-7, n=2 mice, day 14. (A) Metamorph software was used to quantify thresholded area of positive α -SMA staining of the entire image (10X images, minimum 10) to determine the timing of injury resolution in this model. * p <0.05 using one-way ANOVA with post-test comparisons; only sequential differences denoted. Error bars shown are \pm SEM. (B) Immunofluorescent staining with Qdots was used to determine the timing of co-localization

between p-LRP1 and α -SMA (arrows). Representative images of standard α -SMA immunohistochemistry are shown in the top panels. Bottom panels represent higher magnifications of boxed regions from the middle panel. Days are post final CCL₄ injection. (C) Qdots were used to determine if α -SMA, t-PA, and p-LRP1 co-localize on day 4. Channels are separated from the same image to allow for comparison. Arrow indicates triple co-location, arrowheads indicate regions of α -SMA/t-PA co-localization. Scale bars 20 μ m. (α -SMA, α -smooth muscle actin; PB, Phenobarbital; CCL₄, carbon tetrachloride; LRP1, low density lipoprotein receptor-related protein 1)

2.3.5 t-PA- and LRP1-deficient mice retain more α -SMA-positive cells after injury

To clarify the role of t-PA signaling in vivo, we next compared t-PA null mice (181) to their corresponding controls after acute CCL₄ liver injury to assess if regression of MFB-like cells is impaired. Following acute injury, there are no significant differences in the extent of parenchymal injury between WT and t-PA null mice in our model, as measured by serum ALT concentrations (Figure 12A). Nevertheless, t-PA null mice have significantly increased liver/body ratio at day six of recovery (Figure 12B) and significantly larger areas of α -SMA positive staining per visual field compared to WT mice, beginning at day five (Figure 12B), demonstrating a lag in injury resolution and MFB-like cell regression.

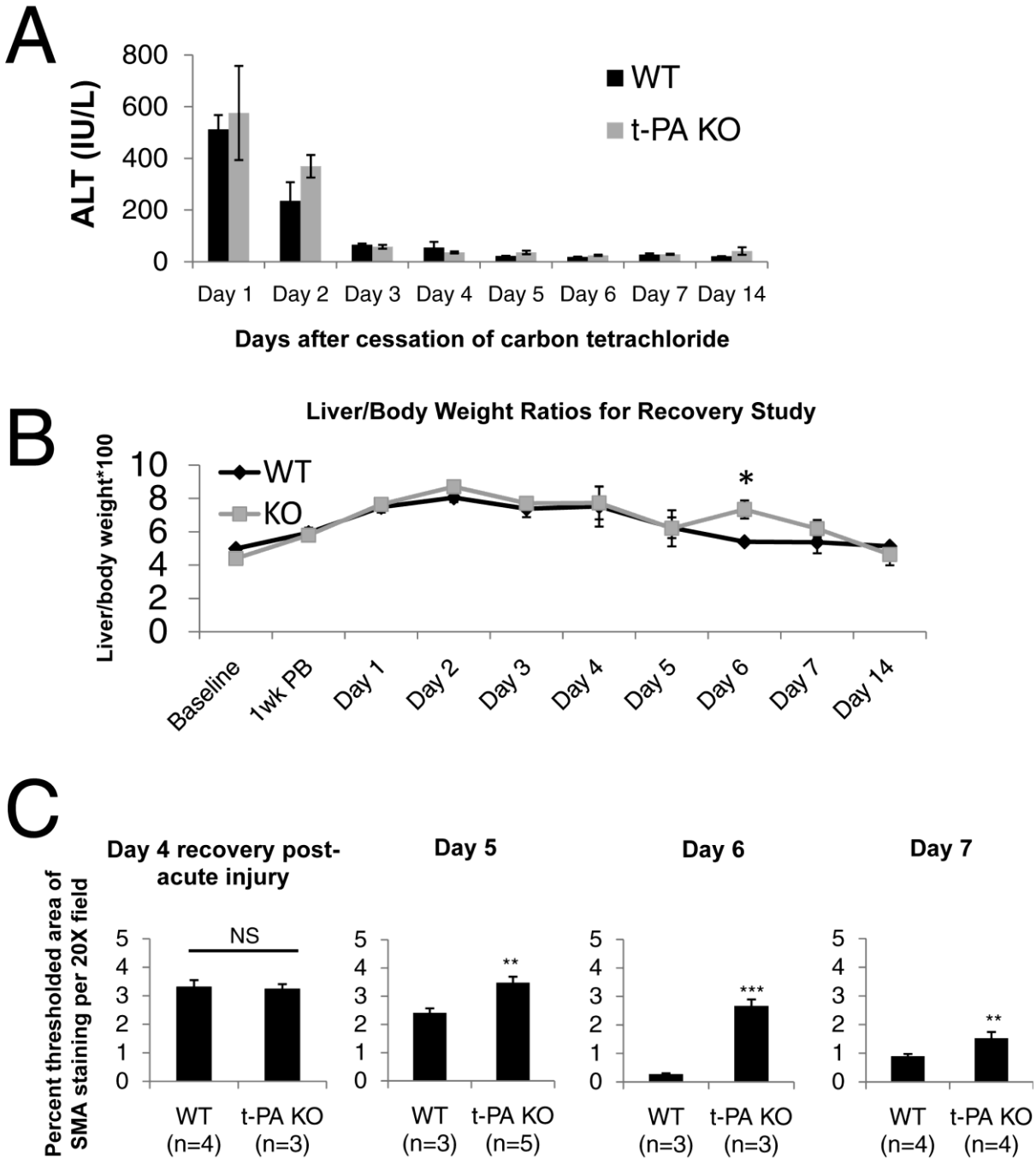


Figure 12. t-PA contributes to resolution of acute hepatic injury in mice. WT (C57Bl/6) and t-PA null mice (KO) were treated as described in Figure 11. Liver tissue and serum were collected at days 2-7 and day 14 after the last dose. n=3-5 animals per time point for each genotype. (A) Comparison of the liver injury marker ALT in WT and t-PA null mice at the indicated time points after injury. No values were significant.

(B) Body to liver weight ratios were calculated and expressed as a percentage. WT and t-PA null mice were compared at baseline and prior to CCL₄ injection, as well as throughout recovery after acute injury. Only at day 6 is there a significant difference seen. *p<0.05 (C) Metamorph software (20X images, minimum 10/animal) was used to determine differences in α -SMA staining in WT and t-PA null mice. Days indicated are days after the last CCL₄ injection. All error bars shown are +/- SEM. WT and KO groups were compared at each time point using Student's t-test. n shown is number of mice analyzed. **p<0.01, *p<0.001 as compared to WT. Sections from WT and KO mice on matching days were stained, imaged, and analyzed together. (t-PA, tissue-type plasminogen activator; WT, wildtype; KO, knockout; ALT, alanine transaminase; α -SMA, α -smooth muscle actin)**

As t-PA is globally inactivated in the t-PA null mice, we next tested whether the differences seen involved signaling in HSCs by repeating the experiment using conditional LRP1 knockout mice (143). SM22, also known as transgelin, is a smooth muscle cell marker that is also selectively expressed in quiescent and activated stellate cells of the liver (182). Hence, amongst the different liver cell types, LRP^{fl_{ox}/fl_{ox}};SM22-Cre⁺ animals should selectively delete LRP1 from their stellate cells. To confirm loss of LRP1, we performed double immunolabeling of LRP1 and α -SMA on cryosections. A decrease in co-localized signal relative to total SMA signal was seen in the LRP^{fl_{ox}/fl_{ox}};SM22-Cre⁺ (KO) mice at day four after injury as compared to the controls (WT; Figure 13A) when we compared equivalent areas of α -SMA⁺ staining. These mice were subjected to the same acute injury protocol and sacrificed at days four and six after injury. Similar to the t-PA null mice, the LRP1 conditional KO mice harbored more α -SMA⁺ cells than the control mice during recovery, despite a similar degree of liver injury (Figure 13B-C). In summary, general loss of t-PA and targeted loss of LRP1 function delayed MFB-like cell resolution *in vivo*.

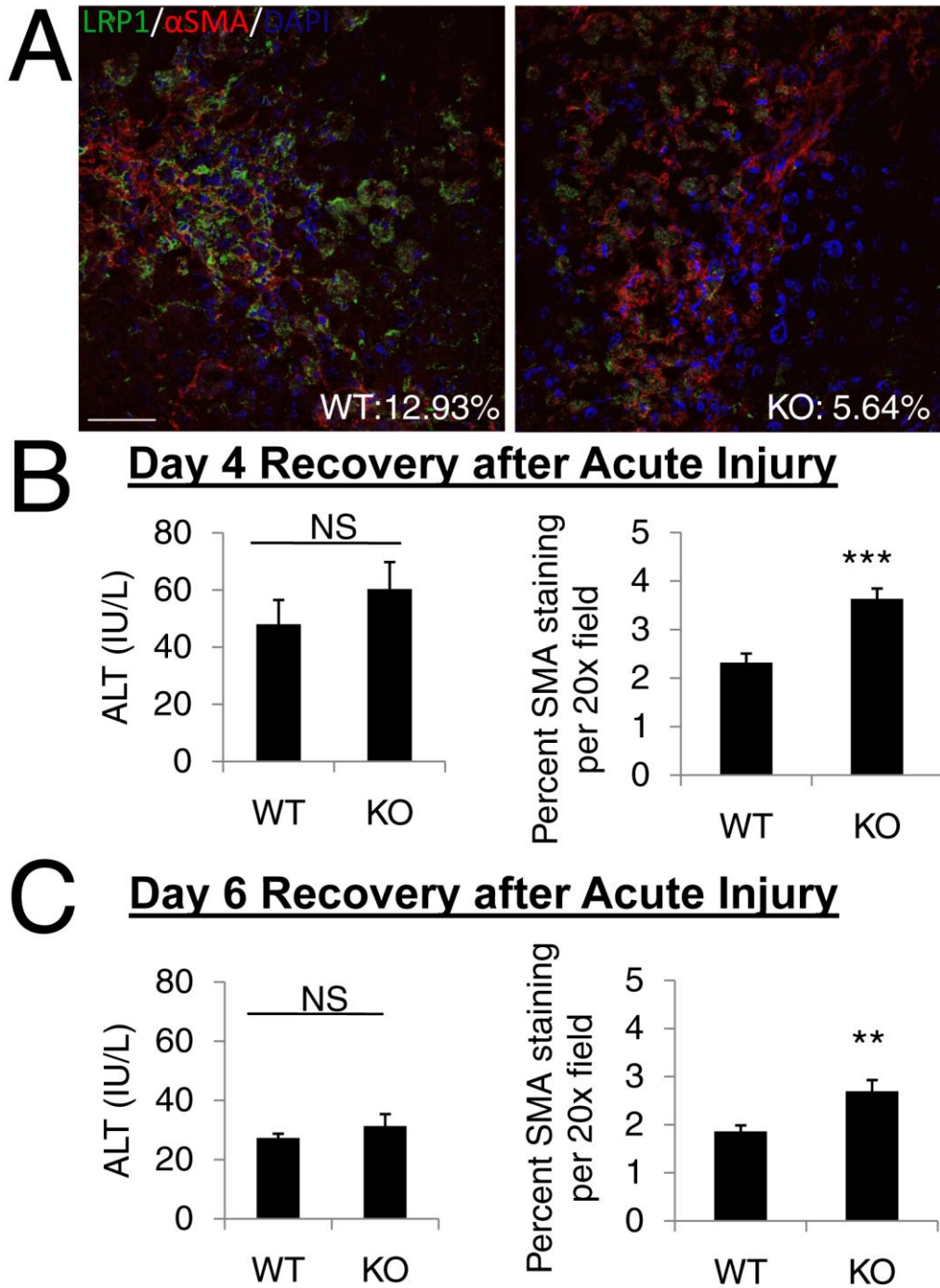


Figure 13. HSC LRP1 contributes to resolution of acute hepatic injury in mice. $LRP^{flox/flox}$ (WT) and $LRP^{flox/flox};SM22-Cre^+$ (KO) mice treated as described in Figure 11. Liver tissue and serum were collected at days 4 and 6 after the last dose. $n=3$ animals for each time point and genotype. (A) Representative confocal images of double immunolabeling with anti-LRP1 and anti- α -SMA antibodies of sections from Day 4 post-

injury. Average co-localized signal as a percentage of total α -SMA staining is indicated for each genotype. Scale bar represents 50 μ m. (B-C) Comparison between WT and LRP1 KO mice for serum liver injury marker ALT and staining quantification for percent area of positive staining for α -SMA (both as described in Figure 12) at the indicated time points after injury. Days indicated are days after the last CCL₄ injection. Sections from WT and KO mice on matching days were stained, imaged, and analyzed together. Error bars shown are \pm SEM. groups were compared at each time point using Student's t-test. **p<0.01, *p<0.001 as compared to WT. (HSC, hepatic stellate cell; LRP1, low density lipoprotein receptor-related protein 1; α -SMA, α -smooth muscle actin; ALT, alanine transaminase; WT, wildtype; KO, knockout)**

2.4 DISCUSSION

Development of anti-fibrotic therapies to treat hepatic fibrosis/cirrhosis has the potential to decrease morbidity and mortality of patients with chronic liver diseases (183) and reduce their risk for hepatocellular carcinoma (184). HSCs play a crucial role in liver fibrogenesis; their depletion leads to marked amelioration of fibrogenesis and tissue expression of markers of MFB-like cells after chronic liver injury (185). This study identifies non-proteolytic t-PA and its interaction with LRP1 as a possible therapeutic target for this disease.

In liver, LRP1 has historically been known solely as a hepatocellular clearance receptor for t-PA (186). Our findings, that LRP1 on HSCs can bind to t-PA and exert other biological effects, expand this observation. A recent *in vitro* study used LRP1 inactivation to demonstrate that anti-proliferative and anti-migratory functions are mediated by LRP1 in HSCs (169). Our data adds to this knowledge by 1) identifying t-PA as a signaling ligand for LRP1, 2) associating *in vitro* changes with phenotypic transformation and, 3) confirming the phenotypic effects of

LRP1-mediated signaling *in vivo*. Further, our finding that t-PA-mediated signaling through LRP1 can decrease, rather than increase, markers of activation in an Akt-dependent manner (Figure 9) opens up a greater question about what proteins partner with LRP1 to exert its functions. Although t-PA-mediated signaling through LRP1 on hepatic MFB-like cells in the present studies was anti-fibrotic, we observed the exact opposite outcome in a model of kidney fibrosis, where t-PA-mediated signaling through LRP1 was profibrotic (156). LRP1 is a known co-receptor with proteins such as integrins (156), PDGFRs (187), and other tyrosine kinase receptors (188). In kidney, LRP1 and $\beta 1$ integrin form a complex that then signals in a pro-fibrotic manner through ERK. Our own preliminary experiments do not support a role for $\beta 1$ integrin in LRP1-mediated HSC signaling (data not shown); however, interestingly, constitutive loss of LRP1 in HSCs can induce ERK activity (169). Although we see transient ERK activation (Figure 10), MEK inhibitors did not yield the same effects as our results with RAP or the PI3K/Akt inhibitor (Figure 9). This suggests that signaling through ERK is also pro-fibrotic in HSCs and further supports the hypothesis that cell-specific partners of LRP1 may differentially regulate the divergent outcomes. Notably, our studies found that PDGFR β was decreased upon activation of LRP1 through ligand binding by t-PA (Figure 8). Hence, similar to vascular smooth muscle cells, in HSCs, LRP1 may partner with PDGFR β and repress proliferation (143). Further studies will be needed to fully clarify the mechanism controlling LRP1 signaling in HSCs before therapeutic targeting can be implemented.

Other studies have examined the effects of the plasminogen activating system (t-PA and/or the urokinase-type plasminogen activator, u-PA) on the resolution of acute liver injury; however, the studies primarily focused on the proteolytic actions of u-PA and t-PA with respect to plasmin generation and subsequent fibrin clearance. Although u-PA and t-PA are commonly

believed to substitute for each other in regard to plasmin generation, with t-PA playing the dominant role, liver appears to provide the exception to this rule. WT mice completely restore hepatocellular organization and fibrin clearance by day seven after injury; however, although t-PA null mice only exhibit a mild defect in their repair, u-PA null mice show a severe delay in resolving hepatic injury with notable fibrin deposition (116). These data suggest that u-PA, rather than t-PA, is responsible for the majority of plasminogen activation and fibrin clearance in recovering liver tissue. Further, other studies also support a role for u-PA in generating hepatic plasmin both specifically in HSCs (118, 129) and in general (118, 129). Interestingly, the plasmin generated by the HSC u-PA also appears to act in an anti-fibrotic manner (118, 129). Never the less, as our studies show that a proteolytically inactive t-PA can effectively generate MFB-like regression, we propose that the primary role of t-PA in liver repair is to signal in HSCs, rather than generate plasmin.

Finally, it is worth noting that the function of t-PA in chronic liver injury still remains unclear; two separate studies tested t-PA null mice in CCl₄ fibrosis protocols and reported opposite results (135, 136). Interestingly, it was the longer study (6, versus 4, weeks of CCl₄) that reported less fibrosis in the t-PA null animals as compared to their WT counterparts, despite an overall increase in liver damage and necrosis. This suggests that extended insults to the liver invoke important changes in the microenvironment that can alter the outcome. Importantly, with regard to the present work, neither of the chronic studies examined activation of LRP1 on HSCs, nor did they look at the ability of the t-PA null animals to resolve fibrosis after removing the injury. As the evidence presented here gives indication that exploiting the function of LRP1 on HSCs can protect from and maybe even reverse cirrhosis development, extending these studies to

chronic models is necessary if we are to explore the use of t-PA, an FDA-approved drug, for liver-targeted therapy for the resolution of liver injury and fibrosis prevention.

3.0 FURTHER INSIGHTS INTO TISSUE-TYPE PLASMINOGEN ACTIVATOR FUNCTION IN LIVER AND LIVER INJURY

3.1 INTRODUCTION

With the recent discoveries of LRP1-mediated signaling in many cell types, it is possible that the effects of exogenous t-PA on liver repair reported in Chapter 2 may not solely be due to LRP1 on HSCs. Of note, hepatocytes and Kupffer cells also are known to express LRP1 (110). In this chapter, we present intriguing data that support the idea that t-PA (via signaling through LRP1) may be exerting cellular effects on both hepatocytes and Kupffer cells after injury.

Finally, our ultimate question is whether t-PA exerts an anti-fibrotic effect in the context of chronic injury. Previous chronic injury studies on t-PA null mice were conflicting (135, 136), but to extend the acute injury observations in t-PA null mice to a chronic injury model, we hypothesized that t-PA null mice would repair and resolve fibrosis at a slower rate than their wildtype counterparts. In this chapter, we present preliminary evidence to support this hypothesis in our model of chronic liver injury.

3.2 EXPERIMENTAL PROCEDURES

3.2.1 Carbon tetrachloride chronic injury and resolution

Male C57Bl/6 (Jackson Laboratories, Bar Harbor, Maine) or t-PA $-/-$ (Jackson Laboratories) mice, aged 10-12 weeks, were given water or 0.05% phenobarbital water *ad libitum* for one week prior to corn oil (control) or carbon tetrachloride (CCl₄) injections (1 μ L/gram body weight, diluted 1:4 with corn oil for injection; Sigma-Aldrich, St. Louis, MO). For acute injury, two doses of CCl₄ were given three days apart and mice were harvested over a time course of 1-14 days after the second dose. For chronic studies, mice were injected twice weekly (Friday/Monday injection schedule) for four weeks and were harvested at days 3 and 14 after the final injection (Figure 14). Serum and liver tissue were collected for biochemical and histological analyses.

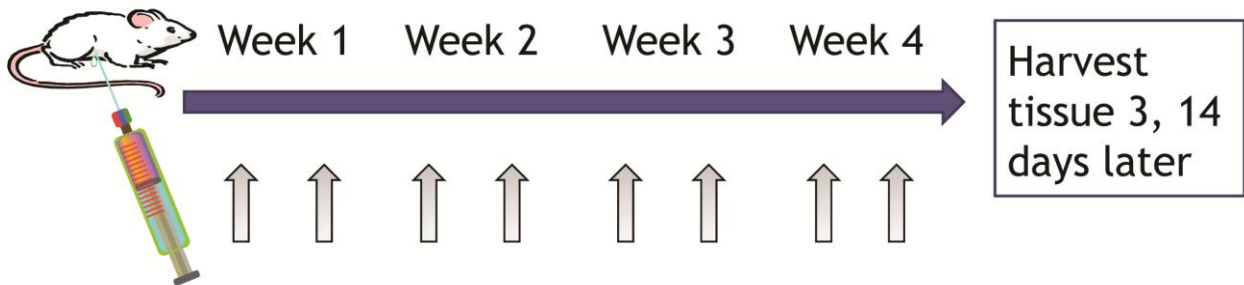


Figure 14. Schematic of chronic CCl₄ administration in mice. Mice are given twice weekly intraperitoneal injections at a dose of 1 μ L/gram body weight. After four weeks, mice are sacrificed at day 3 to get a baseline reading of fibrosis development and at day 14 to assess rate of fibrosis resolution.

3.2.2 SDS-PAGE and western blot from liver tissue

Frozen liver tissue was prepared for non-detergent fractionation, SDS-PAGE, and western blot analysis as previously described in detail (121, 176). Briefly, snap-frozen livers were pulverized on dry ice and homogenized in non-detergent lysis buffer (10mM Tris buffer, pH 7.6, supplemented with protease/phosphatase inhibitors P8340, P2714, P2850, P5726, AEBSF, and sodium amiloride [all from Sigma-Aldrich]). Homogenates were centrifuged at maximum speed in a chilled microcentrifuge ($>14,000 \times g$). Supernatants were transferred to new tubes and designated as the cytoplasmic fraction, while the pellet was sonicated in additional Tris + inhibitors buffer with 1% SDS and designated as the cellular membrane compartment. Protein concentrations for both sets of samples were measured using the bicinchoninic acid assay (Pierce). Thirty micrograms of protein from each sample was mixed with loading buffer with or without 100 mmol/L dithiothreitol, heated to 65°C for 15 minutes, resolved by electrophoresis on 8 or 10% SDS-polyacrylamide gels, and transferred to polyvinylidene difluoride membranes for western blot analyses. Membranes were blocked in 5% milk or fish gelatin in Tris-buffered saline + Tween, followed by incubation with primary antibody in 5% blocking buffer. Rabbit anti-CYP2E1 antibody (Abcam) was used at a concentration of at least 1:2500. Horseradish peroxidase-conjugated secondary antibodies (Jackson ImmunoResearch Laboratories, West Grove, PA) were used at a concentration of 1:50,000. Blots were developed using enhanced chemiluminescence substrate (Pierce, Rockford, IL) and visualized on X-ray film. Loading equivalence was assessed from densitometry of scanned images of Ponceau Red staining performed immediately after transfer of protein onto the polyvinylidene difluoride membranes.

3.2.3 Immunohistochemical staining and image capture

Formalin-fixed paraffin embedded livers from CCl₄-treated mice (n=3-5 at each time point) were cut into 4µm-thick section for immunostaining and routine H&E staining. Immunohistochemistry was done by standard avidin-biotin complex-horseradish peroxidase method. The following primary antibodies were used: mouse anti- α -SMA (1:50; Dako), rat anti-F4/80 (1:50; Abcam), rabbit anti-collagen I (1:100; Abcam), and goat anti-t-PA (1:200; American Diagnostica). Species-appropriate biotinylated secondary antibodies were used (Millipore).

Provis microscopes for brightfield imaging (Olympus, Center Valley, PA) and Metamorph software (Sunnyvale, CA) for quantification of staining were located in and provided by the Center of Biologic Imaging at University of Pittsburgh. Imaging and analysis were performed as described in Chapter 2.

3.3 RESULTS

3.3.1 Increased macrophage populations in t-PA null mice after injury

A recent study showed that t-PA is needed for integrin- and LRP1-mediated macrophage attachment during the process of migration to sites of injury (165). To investigate whether macrophage phenotype after injury could be affected, we performed immunohistochemical labeling for the macrophage marker F4/80 in tissues from wildtype and t-PA null mice at day one after acute injury, both with and without phenobarbital pre-treatment, and quantified the area of positive staining. Interestingly, more macrophages are seen in t-PA null mice liver tissue after injury (Figure 15), regardless of whether phenobarbital was administered (Figure 15B). It is unclear whether this is a baseline difference or induced only after injury; more studies are needed to understand the nature and implications of this phenomenon.

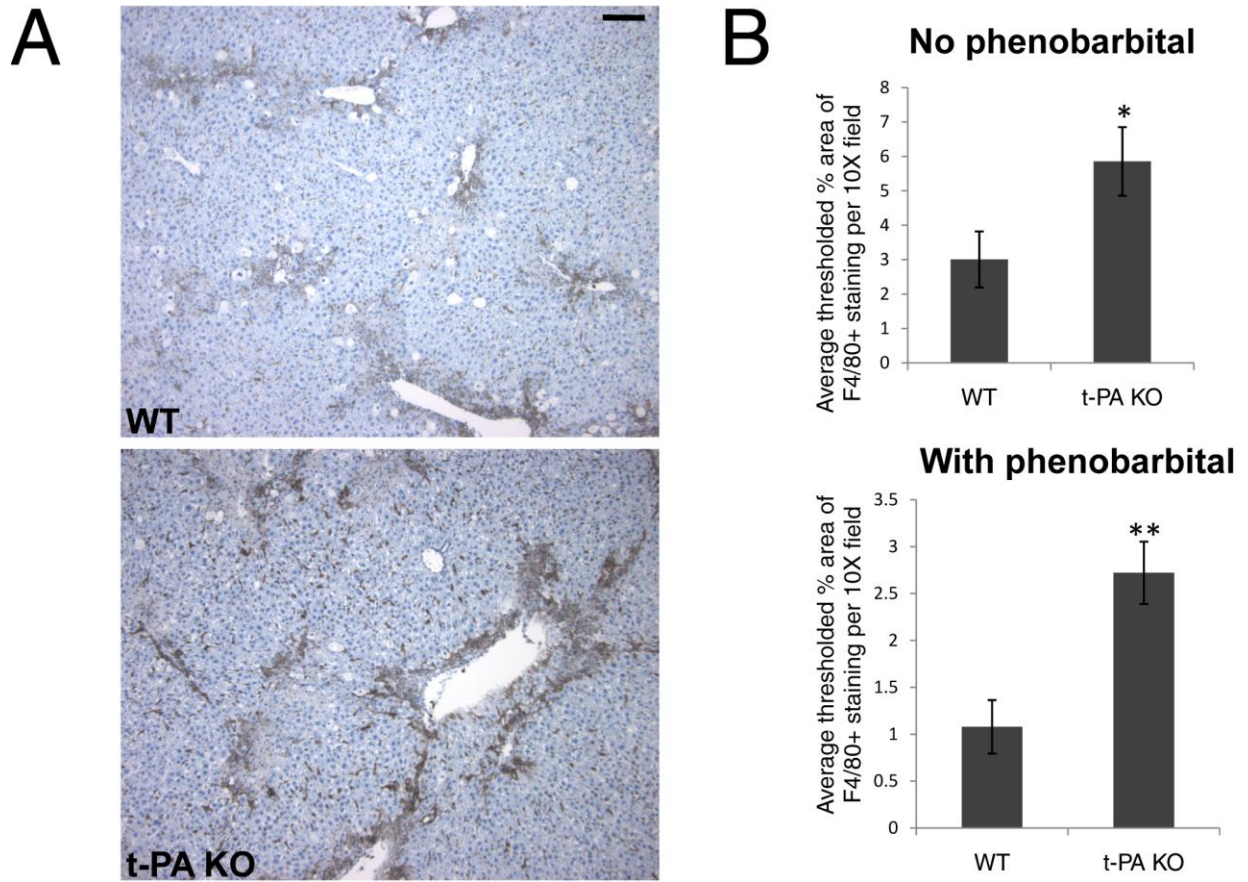


Figure 15. Increased macrophage numbers in t-PA null mice after injury. Wildtype (WT) and t-PA null (KO) mice were given 0.05% phenobarbital (PB) or plain water for one week and then intraperitoneally injected twice with CCL₄ (1 μ L/g body weight) at days 7 and 10 post-PB induction. Livers were harvested at day one after the last dose, embedded in paraffin, and immunostained with anti-F4/80 antibody. n=4-5 mice. (A) Representative images of F4/80 immunostain for mice without PB treatment prior to CCL₄. Scale bars indicate 100 μ m. (B) Metamorph software was used to quantify F4/80 staining (10X images, 6-11 images per genotype). *p<0.05, **p<0.01 using Student's t-test. Error bars shown are +/- SEM. (CCL₄, carbon tetrachloride)

3.3.2 Cytochrome P450 2E1 expression in WT and t-PA knockout mice

Phenobarbital pre-treatment potentiates CCl₄-induced liver injury by up-regulating the metabolic enzymes responsible for bioactivating CCl₄ (189, 190). When considering the appropriate model for our acute liver injury experiments in t-PA knockouts (Figure 12), we first tested CCl₄ injury with and without pretreatment of phenobarbital (0.05% in drinking water) in both wildtype and t-PA knockout mice. We found that, in accordance to previous studies, phenobarbital-treated mice had a greater area of necrosis and injury than those mice not treated with phenobarbital. Correspondingly, MFB-like cell accumulation, as detected by α -SMA immunostaining, was increased in phenobarbital-treated mice (Figure 16A). Additionally, however, we discovered that there was a difference between the wildtype and t-PA knockout mice in extent of centrilobular necrosis and α -SMA⁺ staining (Figure 16A) in mice without pretreatment, while the phenobarbital-pretreated groups had no difference. So in addition to increasing the injury, the phenobarbital equalized the extent of injury between the two genotypes.

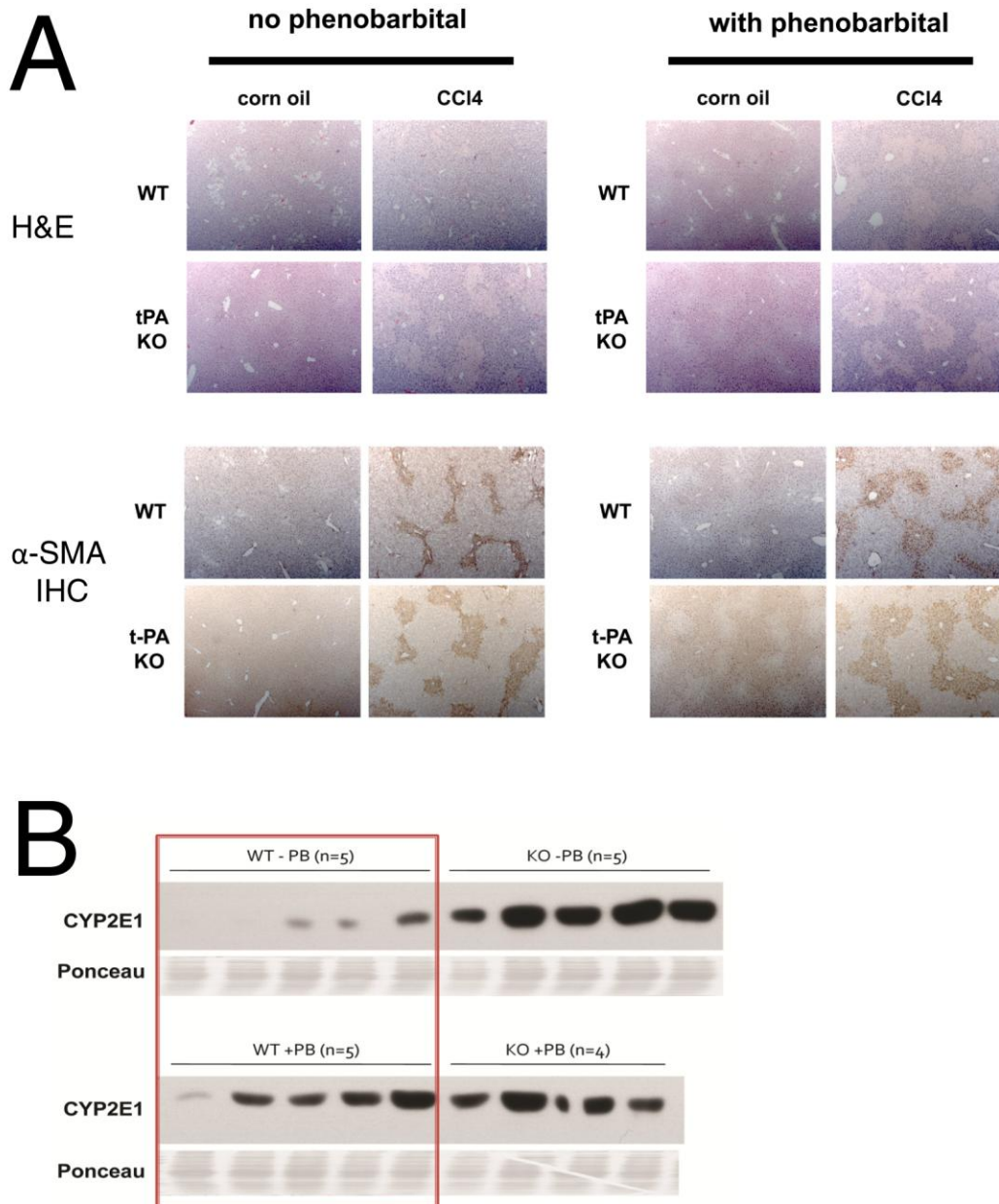


Figure 16. Phenobarbital pre-treatment equalizes CYP2E1 protein expression, CCl₄-induced necrosis and HSC activation between wildtype and t-PA null mice. Wildtype (WT) and t-PA null (KO) mice were given 0.05% phenobarbital (PB) or plain water for one week and then intraperitoneally injected twice with corn oil or CCL₄ (1 μL/g body weight, diluted 1:4 in corn oil) at days 7 and 10 post-PB induction. Livers were harvested at day one after the last dose, embedded in paraffin, and immunostained with anti-α-SMA antibody or stained with H&E protocol. (A) Representative images of H&E and α-SMA immunostain for

mice with and without PB treatment prior to corn oil or CCL₄ injections. Images taken at 50X magnification. (B) CYP2E1 protein expression in membrane-enriched lysates from mice harvested at day one after acute injury. Ponceau stain is shown for respective blots to show equal protein loading.

To further investigate the cause of this discrepancy, we first looked at the protein expression levels of the cytochrome P450 (CYP) 2E1 enzyme, the prominent bioactivator of CCl₄, post-injury to see if there might be a difference in bioactivation (Figure 16B). At day one after acute injury, the wildtype mice without phenobarbital had down-regulated expression of CYP2E1 in response to CCl₄, while the t-PA knockouts had sustained levels; phenobarbital pre-treatment kept the wildtype expression elevated (Figure 16B). These results suggest differential regulation of CYP enzymes in t-PA null mice; however, the post-injury time point did not give us an understanding of whether differences existed between WT and t-PA null mice at time of injection, or whether the difference was in post-injury protein regulation.

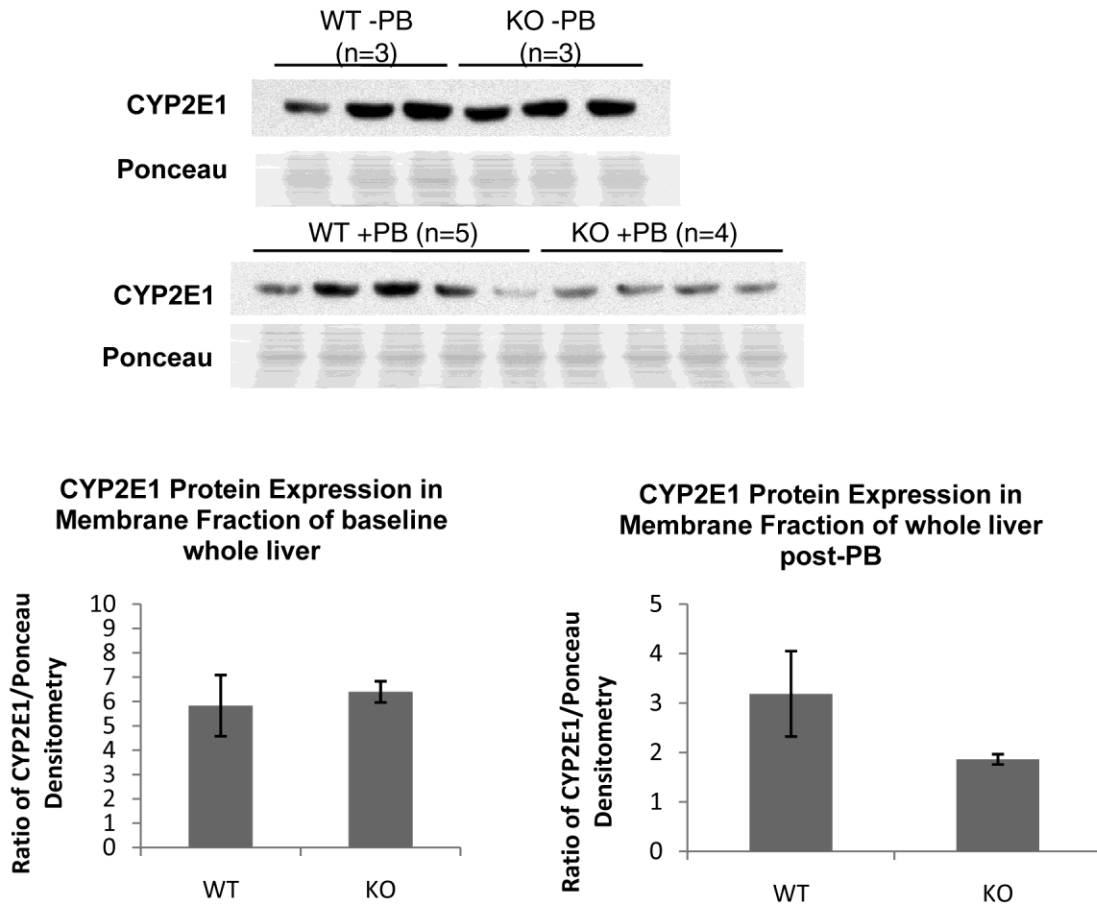


Figure 17. Baseline and post-phenobarbital protein expression of CYP2E1 in wildtype and t-PA null mice. Membrane-enriched liver lysates were subjected to SDS-PAGE and western blot for CYP2E1 expression for baseline and PB-treated mice, as indicated. Densitometry analysis of the two sets of samples is shown in lower panels, using Ponceau stain as a loading control. No differences were detected between the two genotypes in either condition.

We then looked further at baseline levels of CYP2E1 to determine if differences in injury seen could potentially be due to inherent gene expression differences of CYP enzymes in t-PA null mice. CYP2E1, in contrast to post-injury, is not markedly different between wildtype and t-PA knockout mice, with or without phenobarbital treatment (Figure 17).

3.3.3 Chronic injury studies in WT and t-PA deficient mice

Since we observed a delay in resolution of MFB-like cells after acute injury in t-PA null mice compared to wildtype controls, we hypothesized that in chronic injury, more extracellular matrix deposition (i.e. fibrosis) would occur. To test this hypothesis, we expanded our acute injury model to a four-week chronic injury model (Figure 14) and sacrificed mice at day 3 and day 14 after the last injection. We then immunostained liver tissue sections for collagen I deposition and compared the groups. At day three after the last injection, a baseline time point to measure the extent of fibrosis incurred after four weeks of injury, t-PA null mice had decreased average area of collagen I staining per visual field compared to wildtype control mice. However, by day 14 of recovery after the last injection, the t-PA null mice had significantly more collagen I still remaining in the tissue (Figure 18).

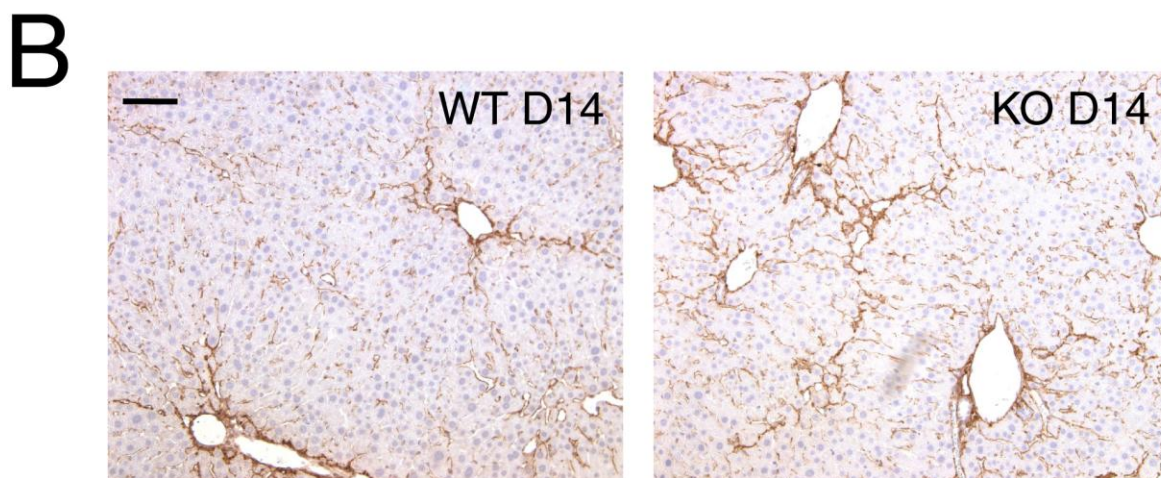
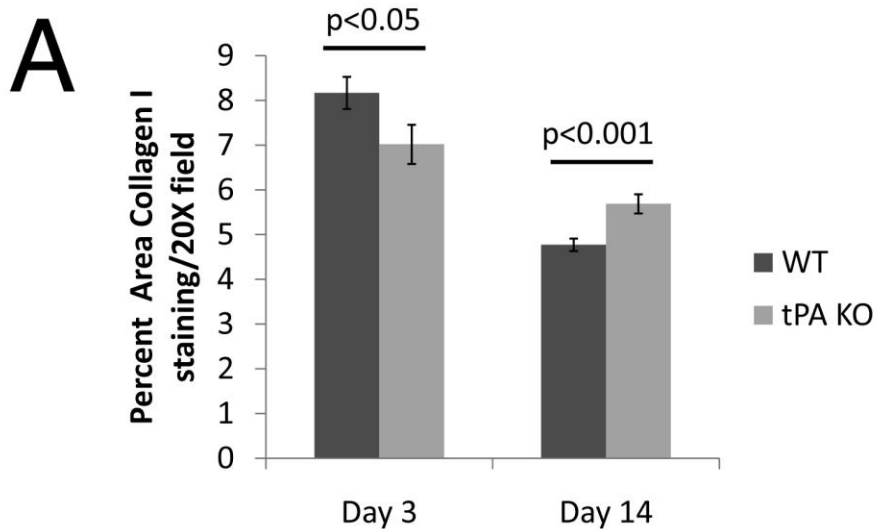


Figure 18. Increased collagen I deposition in t-PA null mice 14 days after cessation of chronic injury regimen. Wildtype (WT) and t-PA null (KO) mice were given 0.05% phenobarbital (PB) for one week and then intraperitoneally injected twice with CCL₄ (1 μ L/g body weight) twice weekly for four weeks. Livers were harvested at day 3 and 14 after the last dose, embedded in paraffin, and immunostained with anti-collagen I antibody. n= minimum 6 mice for each group. (A) Metamorph software was used to quantify area of thresholded positive collagen I staining from images taken across the entire usable tissue section (20X images, >10 images per animal). Error bars shown are +/- SEM. (B) Representative images for the collagen I staining is shown. Scale bar indicates 100 microns.

3.4 DISCUSSION

The aggregate role of t-PA in liver homeostasis and repair is yet to be fully understood. It is likely that liver t-PA has multiple effects on many cell types. In Chapter 2, we describe a signaling role for t-PA on HSCs through the receptor LRP1. Here in Chapter 3, we describe differences in t-PA null mice that suggest roles with regard to macrophages (Figure 15) and hepatocytes (Figure 16-17) in addition to HSCs/MFB-like cells (Figure 18) during injury.

Despite no differences in hepatocyte injury marker ALT between wildtype and t-PA null mice after CCl₄ administration (Figure 12), another potential mechanism for sustained HSC activation in t-PA null mice during recovery, in addition to t-PA signaling loss on HSCs, could be changes in liver macrophage activation or population number. We find that t-PA null mice have increased accumulation of macrophages after injury (Figure 15). It has been reported that t-PA contributes to macrophage migration in an integrin-dependent manner (165, 191). At this point, we have not investigated whether baseline numbers of macrophages are different in t-PA null mice; it is possible that the increased numbers reflect an inability of macrophages to undergo normal turnover or circulation. In addition, it is not clear whether cytokine production by t-PA null macrophages is altered.

We have also demonstrated that CYP2E1 expression after acute liver injury is dysregulated in t-PA null mice (Figure 16). Hepatocytes are the cells that express CYP enzymes, thus the loss of t-PA in all cell types can affect hepatocyte behavior. Hepatocytes express LRP1 and clear t-PA and t-PA:PAI-1 complexes from the blood (186). Although a signaling role has

yet to be attributed to t-PA on hepatocytes, it is possible that regulation of processes such as metabolism could be attributed to hepatocellular LRP1. Strategies to test this hypothesis will be discussed in the future directions (Chapter 4).

Lastly, Figure 18 presents our first results in looking at the role of t-PA in chronic injury. We extended our acute injury out to four weeks (eight injections in total), and then looked at both the baseline fibrosis as well as the ability of the mice to resolve matrix deposition after injury is removed. Since two research groups have reported conflicting results about whether t-PA promotes or protects from hepatic fibrosis (135, 136), we felt repeating the study was worthwhile and we felt that our injury model had distinct advantages: 1) we pretreated with phenobarbital to equalize the HSC activation initially as much as possible, 2) our CCl₄ dose was stronger than the other two studies (1 μ L/gram body weight compared to 0.5 μ L/gram), 3) we looked at not only baseline but during recovery. Indeed, it seems that if anything, t-PA null mice are protected from fibrosis upon examination immediately after the chronic injury regimen. However, after two weeks of repair and recovery, the loss of t-PA renders the knockout mice unable to resolve matrix deposition in a timely manner (Figure 18). As collagen I deposition was an indirect measure of MFB-like cell accumulation and phenotype, further histochemical and biochemical studies need to be conducted to understand the mechanisms involved. These studies will be discussed in more detail in the future directions (Chapter 4).

4.0 GENERAL REMARKS

4.1 SUMMARY

Herein we present evidence to support a previously uninvestigated role for t-PA in liver: direct regulation of HSC phenotype and population, both *in vitro* and after acute injury *in vivo*. Exogenous t-PA is able to suppress markers of HSC activation in both immortalized HSC cell lines and primary rat HSCs (Figure 8). LRP1-mediated signaling is a necessary component of t-PA's actions on HSCs *in vitro* (Figure 9), and endogenous t-PA/LRP1 interactions occur during injury repair at time points congruent with the disappearance of MFB-like cells *in vivo* (Figure 11). Global loss of t-PA or HSC-specific loss of LRP1 delays regression of MFB-like cells after acute injury (Figures 12-13). Further, the rate of collagen I turnover is decreased in t-PA null mouse livers after chronic injury (Figure 18). Collectively, our data support an anti-fibrotic role for t-PA in liver that extends beyond its traditional plasminogen activating function.

Additionally, we have discovered new attributes of t-PA null mice which merit further investigation. Differences in macrophage populations (Figure 15) and CYP2E1 protein expression (Figure 16-17) in t-PA null livers compared to control livers after acute CCl₄ suggest that t-PA's protective role in liver repair may also be due to effects on many cell types.

4.2 DISCUSSION AND FUTURE DIRECTIONS

The overarching objective of this project was to determine the role of t-PA on HSC activation. Based on a substantial body of work done in collaboration with our laboratory that defines a profibrotic role for t-PA in kidney fibrosis (192), we first hypothesized that t-PA would promote HSC activation and liver injury. Indeed, as described above in detail, this did not end up being the case; in fact, we discovered that t-PA has exactly the opposite effect on HSCs but seemingly through the same mechanism of signaling, LRP1. However, although paradoxical, the results presented in this dissertation, in fact, are supported by many studies in liver that describe an overall protective role for plasminogen activators in liver repair. Genetic deficiency of plasminogen activators have been reported to aggravate liver repair in several injury models, including CCl₄ and cholestatic injury (116, 167, 193). Our data add to these previous studies, but many questions still remain; these will be discussed below along with potential future directions for the project.

4.2.1 Dissection of t-PA and LRP1 signaling partners in HSCs

One of the foremost questions left unanswered by this work is the nature of LRP1 interactions on HSCs that distinguishes their response to t-PA from other fibroblasts, such as kidney fibroblasts. It is clear that a divergent set of roles for LRP1 exists, depending on the system. On one hand, our data in combination with the recent study by Llorente-Cortes et al. (169) describe an anti-proliferative and deactivating effect on MFB-like cells. On the other hand, LRP1 on kidney fibroblasts promotes activation and proliferation (156, 157).

Therefore, our next step is to better elucidate LRP1 binding partners in HSCs. While we could test for many potential partners through co-immunoprecipitation followed by western blot, a large-scale approach may be more time and cost-effective due to the large number of described co-receptors and signaling molecules associated with LRP1. One way to achieve this is to perform co-immunoprecipitation studies using an anti-LRP1 antibody on HSC lysates at a time point when LRP1 phosphorylation and signaling activation has been established (between 1-10 minutes, according to our findings presented here). This could be followed by mass spectrometry to identify all proteins pulled down in conjunction with LRP1 (194). Samples from HSCs that have been stimulated with t-PA can be compared with kidney fibroblasts similarly treated after confirming reproducibility of the divergent phenotypes at later time points (e.g. 24 hours) of cells treated in parallel. Another large scale approach might be to use widely-available phosphorylation immunoassay array kits or chips, in which a grid of different phospho-specific antibodies are affixed to a slide, allowing you to test activation of different signaling pathways in one sample at the same time.

The intracellular signaling pathways downstream of LRP1 have only been partly elucidated. Originally characterized as the α_2 -macroglobulin receptor, a multi-functional protease inhibitor, it was shown that only the receptor-binding cleaved form of α_2 -macroglobulin could induce calcium influx and production of inositol phosphates and cyclic AMP (159). In Schwann cells, LRP1 and downstream ERK activation was required for selective gene induction by α_2 -macroglobulin (158). Even with a classical LRP1 ligand such as α_2 -macroglobulin, however, there is still evidence for co-receptor requirement for its effects (159).

Recent evidence suggests that the binding of the adapter protein Disabled 2 (Dab2) to the FXNPXY⁶³ may be key to the suppressive effects of LRP1; when Dab2 is displaced due to

mutagenesis of the receptor or loss of the receptor, there is a corresponding hyperactivation of ERK in CHO cells. As the cytoplasmic tail of LRP1 can bind to other adaptor proteins, it is likely that more thorough co-immunoprecipitation studies described above, comparing t-PA treated cells of different origins will give insight into which co-receptors induce different adaptor proteins in response to t-PA.

Another intriguing mechanism we have not fully studied is the role of t-PA:PAI-1 complexes in signaling through LRP1. The inhibitor complex binds to LRP1 with more affinity than t-PA alone, and in many situations, PAI-1 is a crucial component of the process by which t-PA binds to LRP-1 to exert its effects (165). HSCs express PAI-1, and more so when activated (Figure 19). Our preliminary studies show that when t-PA is added to primary HSC cultures, it is able to interact and cleave the endogenous PAI-1, suggesting there is complexing occurring in the culture medium (Figure 19). We have yet to determine whether our effects are at all dependent on t-PA:PAI-1 complexing, and whether the two-chain form of t-PA may have differential effects than single-chain t-PA in relation to binding ability to LRP1.

Lastly, it is known that LRP1 can act as a moderator of TGF- β signaling; loss of LRP1 from vascular smooth muscle cells results in constitutive TGF- β 1 downstream signaling (96). When we treat cells with t-PA in combination with TGF- β 1, t-PA is able to oppose the function of TGF- β 1 (Figure 19), in contrast to kidney fibroblasts (Figure 8C). It remains to be studied in our system whether activation of TGF- β 1 downstream signaling molecules, the SMADs, are disrupted after t-PA addition in combination with TGF- β 1. If so, this would be one potential mechanism for action of t-PA in HSCs.

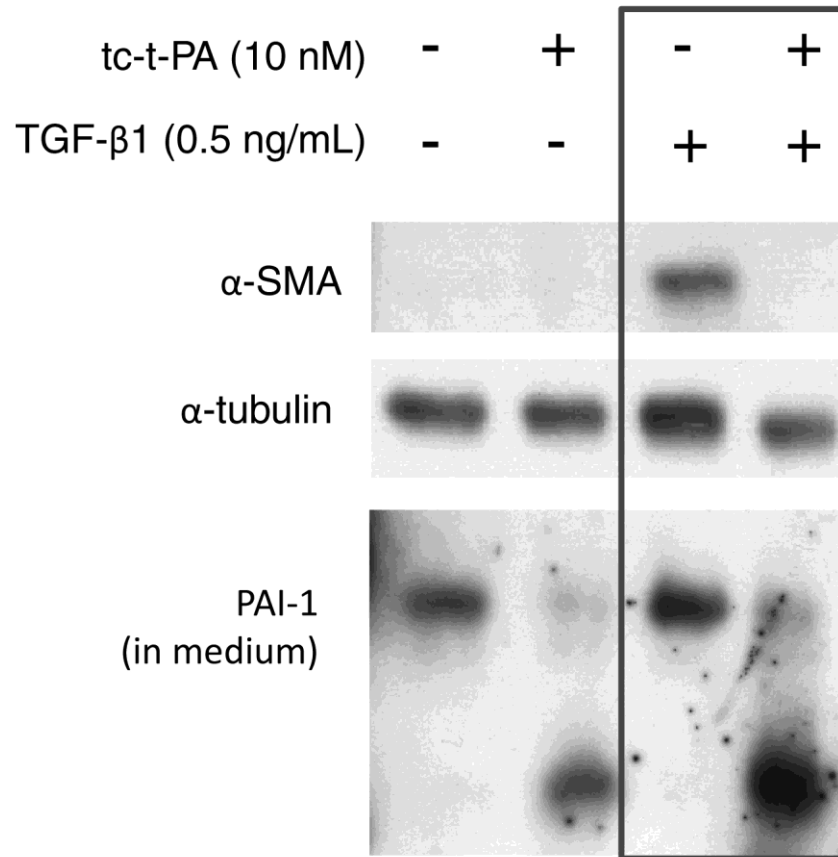


Figure 19. Effects of proteolytically-active t-PA in antagonism to TGF- β 1. Primary HSCs were treated with two-chain t-PA for 24 hours in serum free conditions, alone or in combination with TGF- β 1. Whole cell lysates (α -SMA and α -tubulin) or concentrated medium (PAI-1) were analyzed by western blotting. Boxed lanes highlight the ability of t-PA to counter the effect of TGF- β 1 in primary HSCs.

4.2.2 t-PA and LRP1 kinetics and distribution after injury

Another critical question remaining is the exact contribution of different cell types to secreting t-PA during injury and whether dysregulation of t-PA expression is a contributing factor to fibrosis progression. Despite undetectable levels of t-PA expression at baseline in liver (195), expression is increased in cirrhosis (196), and enzymatic activity is also increased by two days after acute

injury (116) in animal models. However, it is not clear which cells are producing t-PA in these scenarios, as only whole liver mRNA or homogenates were examined. Based on the data presented here, the local production and distribution of t-PA may affect rates of injury resolution.

In our mouse liver injury model, we preliminarily looked for t-PA immunoreactivity at several time points after CCl₄ injury, observing increased t-PA expression at day four and beyond, especially in the perivascular regions. In serial sections of the same tissue, we can identify some α -SMA+ cells in close proximity to t-PA localization, presumably vascular smooth muscle cells in periportal regions, and a mix of smooth muscle cells and activated HSCs around central vein regions (Figure 20). These data complement our Qdot studies at day four after injury (Figure 11C), where we show co-localized t-PA and α -SMA signal. Therefore, t-PA is increased in expression at relevant time points and locations to act upon MFB-like cells through LRP1.

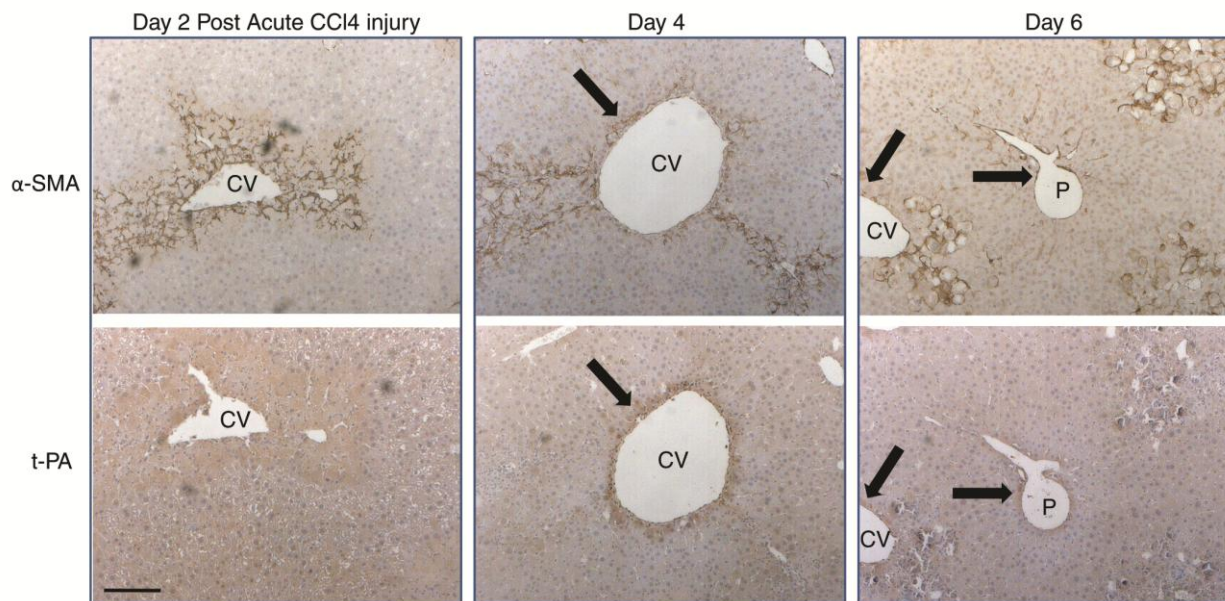


Figure 20. Immunohistochemical evaluation of t-PA expression during injury resolution in wildtype mice. Wildtype mice were given 0.05% phenobarbital (PB) for one week and then intraperitoneally injected twice with CCL₄ (1 μ L/g body weight) at days 7 and 10 post-PB induction. Livers were harvested at various

days after the last dose, embedded in paraffin, and serial sections were immunostained with anti- α -SMA or anti-t-PA antibody. Scale bars indicate 100 μ m. Black arrows indicate similar regions on serial sections.

However, it remains unclear whether cells other than endothelial cells can produce t-PA after injury. It is possible that HSCs, or activated MFB-like cells, can be induced to produce t-PA and signal in a paracrine or autocrine fashion. To better understand the cellular sources of t-PA, we can use *in situ* hybridization for t-PA messenger RNA and double label tissue sections with antibodies against cell-specific markers.

Another relevant question is whether the expression of LRP1 on HSCs is static or if it changes upon activation. Perhaps LRP1 is down-regulated upon MFB-like transition of HSCs, rendering them insensitive to LRP1 ligands and potentiating trans-differentiation. Double-labeling with an HSC marker such as desmin and LRP1 and measuring relative expression between resting and injured livers would be one way to approach this question. Another way would be to isolate primary HSCs and grow them in culture over a period of about one week. HSCs plated on uncoated tissue-culture plates self-activate over time, so harvesting cells at different time points, from freshly plated to one week, and measuring the expression of LRP1 by western blot or immunostaining would be another approach.

4.2.3 Evaluation of observed differences in t-PA null mice

In Chapter 3, we discussed two incidental findings in t-PA null mice at day one after acute injury that have intriguing implications.

First was the observation of increased macrophage density in t-PA null mice after injury, which is of interest for two reasons. One is that in light of the other studies showing a role for t-PA in macrophage recruitment (165, 191), it is paradoxical that we would have more, not less, macrophages at a site of injury. To address this issue, we need to first establish what the baseline macrophage populations are in the t-PA null mice in comparison to wildtype. If there is no difference at baseline, it is possible that the macrophage regression is what is impaired in this model and therefore more macrophages are sequestered in the liver after injury. If there is a baseline difference, then perhaps normal macrophage circulation is also impaired in t-PA null mice in addition to migration in response to injury as the other studies report. The second reason why these results are interesting is that macrophage activation and cytokine production promotes HSC activation after hepatic injury, so this may contribute to the sustained MFB-like population in the t-PA null mice starting from day five after injury. It would be of interest to stain tissues over the whole recovery study for F4/80 to track the entire course of macrophage flux after injury in our model. Also it would be enlightening to measure macrophage-specific cytokine production in t-PA null mice to see if there are elevations in cytokine levels or changes in macrophage polarity.

The second observation we discussed in Chapter 3 was the differential regulation of CYP2E1 after liver injury *in vivo*. Since hepatocytes are the main cells that express the CYP enzymes, the changes noted in the t-PA null mice must be due to changes in the hepatocytes themselves in the setting of t-PA absence. A sustained expression in CYP2E1 in t-PA null mice renders them more sensitive to subsequent intoxication, while the wildtype hepatocytes have shut down expression to protect themselves from further injury. A first step in examining direct regulation of CYP2E1 by t-PA would be to add exogenous t-PA to pure primary hepatocyte

cultures and measure any changes in CYP2E1 expression over several time points. Additionally, although we have measured protein expression of CYP2E1 in the various groups, it is worthwhile to confirm that the differences we see at the protein level are matched by enzymatic activity. If t-PA could indeed regulate CYP enzyme expression in hepatocytes, this would define the first known direct phenotypic effect of t-PA on hepatocytes.

4.2.4 Follow-up studies in LRP1 conditional null mice

In Figure 13, we show that LRP1 conditional knockout mice also display increased numbers of MFB-like cells, using α -SMA as a marker, during recovery after injury. There are a few caveats to this study. First, the promoter for the Cre recombinase, SM22, is also a marker expressed in smooth muscle cells, rendering it not a perfect cell-specific marker in liver. This opens up the possibility that the effects that we see are partially due to contribution of vascular smooth muscle cell LRP1 loss. To confirm that effects we saw are indeed HSC-specific, we could follow up our studies with conditional LRP1 knockouts using a different Cre recombinase transgenic mouse, such as GFAP-cre. Although this marker is also not HSC-specific, the other cell types potentially affected are in the brain and therefore would not be confounding in analyzing hepatic MFB-like cell effects. Another caveat is that due to limited access to the mice, at the present we have not been able to establish a baseline for HSC numbers or phenotype for these mice. It could be possible that loss of LRP1 alone is sufficient to produce increase numbers of activated HSCs in the resting liver.

These caveats aside, the next step in this line of investigation would be to follow up with the SM22-Cre LRP1 conditional knockout mice and test if they have aggravated fibrosis in a

chronic liver injury model such as what we have described in Chapter 3. This would be the ultimate test of whether LRP1 on HSCs ultimately plays a role in suppressing fibrogenesis.

4.2.5 Evaluation the efficacy of t-PA treatment in chronic liver injury

Finally, it has not escaped our notice that since t-PA is an FDA-approved drug, pursuit of using t-PA as a therapeutic in chronic liver disease has distinct advantages. However, many questions and proofs of concept remain before we can reasonably be assured of its clinical usefulness.

Foremost, our chronic injury studies in the t-PA null mice are incomplete. Immunostaining for collagen I was a clean and useful first analysis; however, to confirm the results, we should measure total collagen content in the tissue using the standard hydroxyproline assay. In addition, it would be useful to know how long the sustained matrix deposition persists in the t-PA null mice beyond the time point in which the wildtypes completely resolve the injury and fibrosis. Time points of up to four weeks or more after the final injection may be useful for this purpose. In addition, evaluation of the mechanism for increased matrix deposition is needed. One possibility could be sustained MFB-like cell activation, in which case we should be able to detect increased numbers of α -SMA+ cells throughout the same time period as increased collagen deposition. But another possibility might be enhanced expression of collagen crosslinking enzymes such as lysyl oxidase, promoting mature fibrils that are hard to proteolytically digest, or impaired collagenase function secondary to loss of t-PA protease function.

Finally, as we hypothesize that the primary mechanism that t-PA suppresses fibrosis is through LRP1-mediated signaling on HSCs, we predict that exogenous t-PA administration as a treatment concurrent to a chronic injury protocol would result in amelioration of fibrosis.

Further, if we were to use a proteolytically-inactive t-PA, we predict we would achieve the same result. If these were the case, the proteolytically-inactive t-PA should be considered as a potential drug for any future liver disease applications since it would decrease risk for hemorrhage (a concern in patients with liver failure due to decreased ability of the liver to produce clotting factors). Multiple sites on t-PA participate in binding to LRP1, although a higher affinity exists for the finger/growth factor domain on the very N-terminus; therefore, although another attractive alternative to total t-PA, it is not likely to be as effective (5). However, it is worth exploring whether other LRP1 ligands may be able to confer the same effects. Efficient activation of the receptor is seen with the receptor binding domain fragment of α_2 -macroglobulin (188) and could be tested as a proof of principle that LRP1 activation is the necessary step for any *in vivo* results. Also, testing u-PA might be another proof-of-concept. Interestingly, both of these LRP1 ligands have co-receptors that are unique to them (e.g. u-PAR), which further attest to the possibility that there are ligand-specific effects through the same signaling receptor.

A last consideration would be how to administer t-PA in an organ-specific manner so as to minimize adverse effects in the kidney or brain. For our mouse experiments, the current proposal is to administer the t-PA via intraperitoneal injection, which ought to be absorbed into the portal circulation first; however, this would not be a practical route for patients. One possibility on the horizon is the use of nanotechnology or enteric coatings to produce orally-administered capsules for protein drugs. If at least some of the protein can be absorbed through the intestinal lining, the first organ target for the t-PA would be the liver. Since hepatic clearance of t-PA is very efficient, smaller doses would ensure that only low concentrations of t-PA would escape first-pass by the liver. In this way, then, perhaps t-PA may be safely administered to patients with liver cirrhosis as an anti-fibrotic therapy, regardless of etiology.

APPENDIX A

TABLE OF MICROARRAY RESULTS

Table 1. Fold changes in selected genes in HSC-T6 cells after treatment with t-PA.

Fold Change	Gene Name
39.34	nitric oxide synthase
36.12	lipocalin 2 (Lcn2)
20.73	SERUM AMYLOID A-3
11.93	nitric oxide synthase gene
11.63	secretory leukocyte protease inhibitor (Slpi)
11.25	CC chemokine ST38 precursor
9.79	gro
9.51	plasminogen activator inhibitor 2 type A (Pai2a)
8.05	Weakly similar to nerve growth factor
6.44	small inducible cytokine subfamily, member 2 (Scyb2)
6.19	Moderately similar to RNP RAT RIBONUCLEASE PANCREATIC PRECURSOR
6.02	CINC-2 alpha
5.79	Superoxide dismutase 2, mitochondrial
5.52	CINC-2 alpha
5.49	latent transforming growth factor beta binding protein 2
5.39	Weakly similar to T22286 hypothetical protein F46B6.3
5.27	RAT SMALL INDUCIBLE CYTOKINE A7 PRECURSOR
5.23	CINC-2 alpha
4.99	Hydroxysteroid dehydrogenase, 11 beta type 1 (Hsd11b1)
4.36	2,3-oxidosqualene:lanosterol cyclase
4.06	Moderately similar to RR46_HUMAN Exosome complex exonuclease RRP46
4.04	CXC chemokine LIX (LOC60665)
3.99	Weakly similar to TRANSFORMING PROTEIN RHOB
3.90	Colony stimulating factor 3 (granulocyte) (Csf3)
3.77	Ceruloplasmin (ferroxidase) (Cp)
3.72	Moderately similar to TRMU_HUMAN PROBABLE TRNA
3.67	ATP-binding cassette, sub-family G (WHITE)
3.47	CCAATenhancerbinding, protein (CEBP) delta

3.40	reg I binding protein I (Rbp1)
3.23	Superoxide dismutase 2, mitochondrial
3.18	Weakly similar to A45445 janusin precursor, long form - rat
3.17	Highly similar to JE0174 frizzled protein-2
3.16	Fatty acid binding protein 3, muscle and heart (Fabp3)
3.07	IKBA_RAT NF-kappaB inhibitor alpha
2.89	Moderately similar to S04363 class II histocompatibility antigen RT1-B alpha
2.87	Interleukin 6 (interferon, beta 2) (Il6)
2.86	Complement component 3 (C3)
2.84	Retinol-binding protein 1 (Rbp1)
2.82	Highly similar to A56640 CDC4 repeat unit-containing protein - mouse
2.78	Weakly similar to FCN2_RAT Ficolin 2 precursor
2.77	retinoid X receptor gamma
2.75	GPI-anchored ceruloplasmin
2.71	cyclooxygenase 2
2.68	syntaxin 1 a
2.68	Weakly similar to LIPB_YEAST PROBABLE LIPOATE-PROTEIN LIGASE B, MITOCHONDRIAL
2.65	DEAD (aspartate-glutamate-alanine-aspartate) box polypeptide 25 (Ddx25)
2.63	Highly similar to URIDINE PHOSPHORYLASE
2.63	Mitogen-activated protein kinase kinase kinase 8 (Map3k8)
2.61	Potassium (K+) channel protein alpha 5
2.54	oxidised low density lipoprotein (lectin-like) receptor 1 (Olr1)
2.52	hemopexin (Hpx)
2.36	Acid nuclear phosphoprotein 32 (leucine rich) (Anp32)
2.33	Weakly similar to CLD3 RAT CLAUDIN-3
2.32	Weakly similar to C42D8.3.p (Caenorhabditis elegans)
2.32	solute carrier family 19 (sodiumhydrogen exchanger), member 1 (Slc19a1)
2.32	versican Vint isoform
2.25	Highly similar to COMPLEMENT C2 PRECURSOR
2.23	Weakly similar to RNA polymerase I (127 kDa subunit)
2.20	GPI-anchored ceruloplasmin
2.20	homeobox protein (R1b)
2.19	Moderately similar to JC6307 homeobox protein Barx2 - mouse
2.18	Weakly similar to T20358 hypothetical protein D2030.8
2.15	Moderately similar to U2R2 MOUSE U2 SMALL NUCLEAR RIBONUCLEOPROTEIN AUXILIARY FACTOR 35 KD
2.15	Highly similar to VTL1_MOUSE Vesicle transport v-SNARE protein Vti1-like 1
2.13	Weakly similar to KRP1_RAT Kelch-related protein 1
2.10	translocator of inner mitochondrial membrane 44 (Timm44)
2.09	CCAATenhancerbinding, protein (CEBP) delta (Cebpd)
2.06	Stromal cell-derived factor 1
2.04	Small inducible gene JE (Scya2)
2.04	Hydroxysteroid dehydrogenase, 11 beta type 2 (Hsd11b2)
2.01	small inducible cytokine subfamily D, 1 (Scyd1)
-1.47	alpha-SMA

-2.00	Adrenergic, alpha 1B-, receptor (Adra1b)
-2.00	Moderately similar to KIAA0351
-2.00	endo-alpha-mannosidase (Enman)
-2.01	Weakly similar to APP2 RAT AMYLOID-LIKE PROTEIN 2 PRECURSOR
-2.01	elongation factor-2 kinase
-2.01	Highly similar to T08771 hypothetical protein DKFZp586L151.1
-2.03	small rec (srec)
-2.03	Weakly similar to JE0343 terf protein - rat
-2.03	serotonin 5-HT2C receptor
-2.03	trefoil factor 1 (Tff1)
-2.04	Annexin A3
-2.04	regulator of G-protein signaling 14 (Rgs14)
-2.05	Gap junction protein, alpha 1, 43 kD (connexin 43)
-2.05	retinol dehydrogenase homolog (Rdhl)
-2.05	Highly similar to A4 RAT ALZHEIMERS DISEASE AMYLOID A4 PROTEIN HOMOLOG PRECURSOR
-2.05	Moderately similar to S04363 class II histocompatibility antigen RT1-B alpha
-2.05	Highly similar to casein kinase 1 gamma 3 isoform
-2.05	Highly similar to T47180 hypothetical protein DKFZp434C2316.1
-2.05	Insulin-like growth factor-binding protein 5
-2.06	amphiregulin (Areg)
-2.06	Tyrosine hydroxylase (Th)
-2.06	Weakly similar to apolipoprotein L, 3; TNF-inducible protein CG12-1
-2.06	Moderately similar to HUD RAT PARANEOPLASTIC ENCEPHALOMYELITIS ANTIGEN HUD
-2.06	gamma-aminobutyric acid (GABA-A) receptor, subunit alpha 6 (Gabra6)
-2.07	plasma membrane Ca ²⁺ -ATPase isoform 4
-2.07	Weakly similar to T23273 hypothetical protein Y63D3A.8
-2.07	synaptopodin (Synpo)
-2.07	exostoses (multiple)-like 3 (Extl3)
-2.07	calpain 10 (Capn10)
-2.09	norvegicus guanosine monophosphate reductase (Gmpr)
-2.09	AGAL MOUSE ALPHA-GALACTOSIDASE A PRECURSOR
-2.10	transforming growth factor, beta receptor III (Tgfr3)
-2.10	solute carrier family 21 (organic anion transporter), member 9 (Slc21a9)
-2.11	Weakly similar to S25644 Ig mu chain C region - rat
-2.11	Drosophila discs-large tumor suppressor homologue (synapse associated protein) (Dlg1)
-2.11	Moderately similar to MTM1_MOUSE MYOTUBULARIN
-2.11	strain BNCr1 glucocorticoid receptor
-2.11	Highly similar to SC14_HUMAN SEC14-LIKE PROTEIN
-2.11	Weakly similar to F56A11.5.p
-2.11	bone morphogenetic protein 2 (Bmp2)
-2.12	Weakly similar to JG0164 LIM protein, FHL4
-2.12	Highly similar to GLUTATHIONE S-TRANSFERASE 8
-2.13	Gap junction membrane channel, protein alpha 4 (connexin 37) (Gja4)
-2.13	Weakly similar to T16005 hypothetical protein F09E5.2 -
-2.13	Weakly similar to CALM_HUMAN CALMODULIN
-2.14	low density lipoprotein receptor-related protein 3 (Lrp3)
-2.14	solute carrier family 31 (copper transporters), member 1 (Slc31a1)

-2.14	Regeneration protein, lithostatin, pancreatic stone protein (Reg1)
-2.15	Tissue inhibitor of metalloproteinase 3
-2.15	Weakly similar to A Chain A, Crystal Structure Of S-Glutathiolated Carbonic Anhydrase Iii
-2.16	Weakly similar to FMOD RAT FIBROMODULIN PRECURSOR
-2.16	NaPi-2 gamma
-2.17	Glutathione-S-transferase, alpha type (Yc?) (Gsta2)
-2.19	Weakly similar to polypeptide GalNAc transferase T1 (Rattus norvegicus)
-2.23	Solute carrier family 2 A3 (neuron glucose transporter) (Slc2a3)
-2.23	Moderately similar to Y084_HUMAN HYPOTHETICAL PROTEIN KIAA0084
-2.24	alcohol dehydrogenase 7 (class IV), mu or sigma polypeptide (Adh7)
-2.26	N-myc downstream-regulated gene 2 (Ndr2)
-2.27	Highly similar to S58008 GPI-anchored protein
-2.27	Weakly similar to development-related protein
-2.29	solute carrier family 12, (potassium-chloride transporter) member 5 (Slc12a5)
-2.30	Glial cell line-derived neurotrophic factor receptor alpha (Gfra1)
-2.31	prostaglandin D2 synthase 2, hematopoietic (Ptgds2)
-2.32	Highly similar to D4DR RAT D(4) DOPAMINE RECEPTOR
-2.32	putative pheromone receptor (Go-VN1)
-2.33	Weakly similar to MATERNAL PUMILIO PROTEIN
-2.34	Highly similar to LHX1 MOUSE LIMHOMEBOX PROTEIN LHX1
-2.34	proto-oncogene (Met)
-2.36	Weakly similar to T46436 hypothetical protein DKFZp434I1926.1
-2.39	hairy and enhancer of split 5
-2.43	Moderately similar to LEF1 RAT LYMPHOID ENHANCER BINDING FACTOR 1
-2.44	proliferin-related protein (Plfr)
-2.46	Weakly similar to FMOD RAT FIBROMODULIN PRECURSOR
-2.48	Mg1
-2.49	Highly similar to A4 RAT ALZHEIMERS DISEASE AMYLOID A4 PROTEIN HOMOLOG PRECURSOR
-2.54	Weakly similar to A40805 b-locus protein - mouse
-2.55	Highly similar to 2008147B protein RAKc
-2.56	cholinergic receptor, nicotinic, alpha polypeptide 6 (Chrna6)
-2.58	myocilin (Myoc)
-2.59	GABA transporter (RNU28927)
-2.59	collagen XII alpha 1 (Col12a1)
-2.62	Highly similar to I60125 PDGF receptor beta-like tumor suppressor (H.sapiens)
-2.62	wingless-type MMTV integration site family, member 4 (Wnt4)
-2.63	Weakly similar to GSHC RAT GLUTATHIONE PEROXIDASE
-2.64	Weakly similar to ZN42_HUMAN ZINC FINGER PROTEIN 42
-2.65	ERM-binding phosphoprotein
-2.68	Weakly similar to similar to C.elegans hypothetical protein CET01H8.1,CEC05C12.3,CEF54D1.5. similar to trp and trp-like proteins
-2.69	130kDa-Ins(1,4,5)P3 binding protein (LOC84587)
-2.72	angiopoietin-like 2 (Angptl2)
-2.86	Highly similar to A47220 dermatopontin precursor
-2.87	Weakly similar to S26689 hypothetical protein hc1 - mouse
-2.89	CA3 mRNA for carbonic anhydrase III
-2.98	Alcohol dehydrogenase (class I), alpha polypeptide (Adh1a)

-3.00	Weakly similar to T00636 hypothetical protein F21856_2
-3.00	Vasopressin receptor V1a (Avpr1a)
-3.01	resistin like alpha (Retnla)
-3.03	dihydrodiol dehydrogenase
-3.05	growth hormone secretagogue receptor type 1a
-3.22	salivary protein 1 (Spt1)
-3.30	Weakly similar to T08802 hypothetical protein DKFZp586D0623.1 (H.sapiens)
-3.33	aldehyde oxidase (Aox1)
-3.43	Serotonin (5-hydroxytryptamine (5HT)) receptor, type 1B (Htr1b)
-3.60	sema domain, immunoglobulin domain (Ig), short basic domain, secreted, (semaphorin) 3A (Sema3a)
-3.70	Moderately similar to Y188_HUMAN HYPOTHETICAL PROTEIN KIAA0188
-3.70	GDNF receptor alpha
-3.88	WNT1 inducible signaling pathway protein 2 (Wisp2)
-4.24	prostaglandin E receptor EP2 subtype
-4.34	Alkaline phosphatase 1, intestinal, defined by SSR (Alpi)
-4.52	transmembrane 4 superfamily member 3 (Tm4sf3)
-5.24	myosin Ic (Myo1c)
-6.97	Weakly similar to F43B10.2.p (Caenorhabditis elegans)
-8.31	Highly similar to TCPZ MOUSE T-COMPLEX PROTEIN 1, ZETA SUBUNIT
-10.63	Cu ⁺⁺ transporting, alpha polypeptide (Menkes syndrome) (Atp7a)
-11.03	damage-specific DNA binding protein 1 (DDB1 gene)

Table 2. Absolute changes in selected genes in HSC-T6 cells after treatment with t-PA.

Relative copy number difference (t-PA - Vehicle)	Gene Name
-3884.8	osteopontin
-3062.4	Col3a1
-2472.9	Col1a2
-2460.3	Diaphorase (NADHNADPH) /DEF=Rat NAD(P)H:menadione oxidoreductase
-2459.9	Id3a
-2057.6	RUK-1 (Ruk)
-2027.8	collagen type V, alpha 2
-1826.6	catalase
-1795.6	SH3 domain-containing adapter protein isoform SETA-1x23 (SETA)
-1775.4	stearoyl-CoA desaturase 2
-1753.9	Weakly similar to POL3 MOUSE RETROVIRUS-RELATED POL POLYPROTEIN
-1639.3	osteonectin
-1518.2	villin 2
-1503.4	Highly similar to T4S1_MOUSE Transmembrane 4 superfamily, member 1 (Tumor-associated antigen L6)
-1437.1	stearoyl-Coenzyme A desaturase 2 (Scd2)
-1415	Nogo-C protein
-1361.8	Weakly similar to POL3 MOUSE RETROVIRUS-RELATED POL POLYPROTEIN
-1329.9	Signal transducer and activator of transcription 1 (Stat1)
-1321.5	PKC-delta binding protein (SRBC)
-1308.4	Rap7a
-1235.3	aldose reductase-like protein
-1218.5	Transforming growth factor beta stimulated clone 22 (Tgfbli4)
-1218.3	selectin, endothelial cell, ligand (Selel)
-1191.3	Highly similar to ITMB_MOUSE INTEGRAL MEMBRANE PROTEIN 2B (M.musculus)
-1191.2	Moderately similar to RB48_MOUSE CHROMATIN ASSEMBLY FACTOR 1 P48 SUBUNIT
-1147.8	homocysteine-inducible, endoplasmic reticulum stress-inducible, ubiquitin-like domain member 1 (Herpud1)
-1129.2	Weakly similar to NOMR_RAT NEURONAL OLFACTOMEDIN-RELATED ER LOCALIZED PROTEIN PRECURSOR
-1123	BM1av1 MHC class Ib antigen, strain DA
-1079.2	Annexin 1 (p35) (Lipocortin 1) (Anxa1)
-1075.1	Insulin-like growth factor binding protein 6 (Igfbp6)
-1059.6	Secreted acidic cystein-rich glycoprotein (osteonectin) (Sparc)
-1045	Ryudocansyndecan 2
-1036.7	Highly similar to SRE1_RAT Sterol regulatory element binding protein-1
-1032.4	collagen alpha1 type I
-1028.4	Moderately similar to C560_HUMAN SUCCINATE DEHYDROGENASE CYTOCHROME B560 SUBUNIT, MITOCHONDRIAL PRECURSOR
-1014.7	Prion protein, structural
-970.6	upregulated by 1,25-dihydroxyvitamin D-3
-966.7	tissue inhibitor of metalloproteinase 2 (Timp2)

-965.5	membrane-type matrix metalloproteinase
-942.8	Highly similar to S70642 ubiquitin ligase Nedd4 - rat
-936.9	disabled homolog 2, mitogen-responsive phosphoprotein (Drosophila) (Dab2)
-929	Highly similar to CDC28 protein kinase 1; cyclin-dependent kinase regulatory subunit 1 (Mus musculus)
-924	Peripherin (Prph)
-921.5	brain expressed X-linked 3 (Bex3)
-916	heterogeneous nuclear ribonucleoprotein K
-905.6	transmembrane 4 superfamily member 3 (Tm4sf3)
-905.5	Guanine nucleotide-binding protein beta 1
-897	S61A RAT PROTEIN TRANSPORT PROTEIN SEC61 ALPHA SUBUNIT
-894.4	coated vesicle membrane protein (Rnp24)
-881.5	Early growth response 1 (Egr1)
-874.8	Peripheral myelin protein
-868.2	GLUT4 vesicle 20kDa protein
-860.2	S-100 related protein, clone 42C (S100A10)
-858.7	Crystallin, alpha polypeptide 2 (Cryab)
-846	Inhibitor of DNA binding 2, dominant negative helix-loop-helix protein
-838.9	Highly similar to I84741 RNA helicase - mouse (M.musculus)
-835.2	CD151 antigen (Cd151)
-835	follistatin-related protein precursor
-833.4	follistatin-related protein precursor (Frp)
-831.4	Isocitrate dehydrogenase 1, soluble (Idh1)
-825.6	inhibitor of DNA binding
-822	Insulin-like growth factor 2 receptor
-813.4	Moderately similar to delta-6 fatty acid desaturase
-806.2	Highly similar to Y193_HUMAN HYPOTHETICAL PROTEIN KIAA0193
-803.7	Highly similar to T14738 hypothetical protein DKFZp564A2416.1
-797.1	Tropomyosin 4 (Tpm4)
-795.9	peptidyl-glycine alpha-amidating monooxygenase (rPAM-2) mRNA
-794.7	collagen, type V, alpha 1 (Col5a1)
-789.6	Highly similar to GELS MOUSE GELSOLIN
-788.5	fatty acid desaturase 1 (Fads1)
-786.6	lamin A
-784.3	xanthine dehydrogenase (Xdh)
-783.6	Weakly similar to T46436 hypothetical protein DKFZp434I1926.1
-771.5	Ryudocansyndecan 2
-768.8	Highly similar to T46500 hypothetical protein DKFZp434D098.1 (H.sapiens)
-764.3	transmembrane receptor Unc5H2 (Unc5h2)
-761.8	sodiumpotassium ATPase alpha-1 subunit truncated isoform
-761	Moderately similar to S71356 glucocorticoid-attenuated response gene 49 protein
-760.6	procollagen-lysine, 2-oxoglutarate 5-dioxygenase (lysine hydroxylase, Ehlers-Danlos syndrome type VI) (Plod)
-759.7	S100 calcium-binding protein A4 (S100a4)
-753.1	Moderately similar to T17320 hypothetical protein DKFZp564J0863.1 (H.sapien
-753	Heme oxygenase (Hmox1)
-751.2	dithiolethione-inducible gene-1 (DIG-1)
-750.1	Weakly similar to TYROSINE-PROTEIN KINASE JAK2

-750	endothelial differentiation, lysophosphatidic acid G-protein-coupled receptor, 2 (Edg2)
-749.5	Weakly similar to T22416 hypothetical protein F49C12.12 - Caenorhabditis elegans (C.elegans)
-749.5	prolyl 4-hydroxylase alpha subunit
-732.1	Weakly similar to cyclophilin B
-728.2	Highly similar to S66254 dolichyl-diphosphooligosaccharide--protein glycotransferase (H.sapiens)
-715	Highly similar to IBP6 RAT INSULIN-LIKE GROWTH FACTOR BINDING PROTEIN 6 PRECURSOR
-709.6	PDZ and LIM domain 1 (elfin) (Pdlim1)
-707.3	cysteine-rich protein 2 (Csrp2)
-696.7	Weakly similar to SP10_MOUSE NUCLEAR AUTOANTIGEN SP-100
-696.7	Weakly similar to putative serinethreonine protein kinase MAK-V
-693.5	Highly similar to A4 RAT ALZHEIMERS DISEASE AMYLOID A4 PROTEIN HOMOLOG PRECURSOR
-690	Signal transducer and activator of transcription 1
-689.9	Highly similar to GLUTATHIONE S-TRANSFERASE 8
-681.5	Weakly similar to R155.1.p (Caenorhabditis elegans)
-680.9	Glutathione-S-transferase, alpha type (Ya) (Gsta1)
-672.3	Microtubule-associated protein 2
-670.7	BM1k MHC class Ib antigen
-670.1	Transforming growth factor, beta 3 (Tgfb3)
-662.5	Highly similar to T00056 hypothetical protein KIAA0418
-660.6	CBP-50 protein
-658.4	Highly similar to ER23_HUMAN ER LUMEN PROTEIN RETAINING RECEPTOR 3
-648.6	Weakly similar to FMOD RAT FIBROMODULIN PRECURSOR
-634.8	Highly similar to MTRP_MOUSE GOLGI 4-TRANSMEMBRANE SPANNING TRANSPORTER
-628.9	TIMP2
-627.4	Moderately similar to F22B5.10.p (Caenorhabditis elegans)
-626.8	Moderately similar to S04363 class II histocompatibility antigen RT1-B alpha
-623.8	annexin VI
-622.6	Moderately similar to T43496 hypothetical protein DKFZp434J039.1
-616.5	cyclase-associated protein homologue
-614.4	plasma glutamate carboxypeptidase (Pgcp-pending)
-612.3	moesin (Msn)
-612.1	ARP2_HUMAN ACTIN-LIKE PROTEIN 2
-609.8	unction plakoglobin (Jup)
-609.4	Weakly similar to F55A12.9a.p (Caenorhabditis elegans)
-604.9	Moderately similar to COG2_MOUSE Coatomer gamma-2 subunit (Gamma-2 coat protein)
-603.9	Moderately similar to FINC RAT FIBRONECTIN PRECURSOR
-603.8	Weakly similar to RETROVIRUS-RELATED POL POLYPROTEIN
-603.6	CD14 antigen
-600.8	HIF-1 responsive RTP801 (Rtp801)
-597.1	Highly similar to JE0223 destrin - rat
-593.2	CaBP1
-592.3	alanyl (membrane) aminopeptidase (Anpep)
-587.3	Highly similar to CA1B RAT COLLAGEN ALPHA 1(XI) CHAIN

-584	Fucosidase, alpha-L-1, tissue (Fucal)
667.9	calmodulin
670.1	tropomyosin non-muscle isoform NM1 (TPM-gamma)
670.8	Highly similar to Sin3-associated polypeptide 18
672	Highly similar to C8
672.8	Weakly similar to T32886 hypothetical protein C34B2.8
675.9	cyclin-dependent kinase inhibitor 2a p16Ink4a (Cdkn2a)
676.5	Moderately similar to SKD1 MOUSE SKD1 PROTEIN
677	Weakly similar to T-COMPLEX PROTEIN 1, ALPHA SUBUNIT
677.8	C-terminal binding protein 1 (Ctbp1)
678.8	Highly similar to HETEROCHROMATIN PROTEIN 1 HOMOLOG GAMMA
681.6	Ceruloplasmin (ferroxidase) (Cp)
684.1	Mx1 protein
684.4	Moderately similar to T30249 cell proliferation antigen Ki-67
685.6	ATP synthase subunit d (Atp5jd)
688	Moderately similar to selective hybridizing clone
689.5	H3 histone, family 3B
689.9	matrin 3 (Matr3)
690.4	immunophilin FKBP12
690.6	Weakly similar to MIC2_HUMAN T-CELL SURFACE GLYCOPROTEIN E2 PRECURSOR
690.9	Weakly similar to T-COMPLEX PROTEIN 1, ALPHA SUBUNIT
693.8	parathymosin (Ptms)
696.3	Weakly similar to SFR2_MOUSE Splicing factor, arginineserine-rich 2
698.6	Highly similar to adaptor-related protein complex AP-3, delta subunit
700.1	G protein gamma-5 subunit
700.3	transcription factor A, mitochondrial (Tfam)
701.3	Phosphoglycerate mutase 1 (Pgam1)
703.4	Atp5c1
703.8	Moderately similar to T14773 hypothetical protein DKFZp564B0482.1
704.3	Highly similar to U123_HUMAN HYPOTHETICAL 12.4 KDA PROTEIN BK223H9.2
705.2	versican V3 isoform precursor
705.9	casein kinase II beta subunit
709.3	Moderately similar to splicing factor, arginineserine-rich 6
709.9	Weakly similar to PRSC MOUSE 26S PROTEASOME REGULATORY SUBUNIT S12
710.3	NonOp54nrb homolog mRNA
711.4	Cell division cycle control protein 2
711.6	Moderately similar to pumilio; pumuckel; ovarette; bemused
712.8	aldo-keto reductase family 1, member A1
713.2	interacting protein 30 (Sip30)
713.8	ATP synthase, H ⁺ transporting, mitochondrial F0 complex, subunit c (subunit 9) isoform 3 (Atp5g3)
715.3	Highly similar to S22655 translation elongation factor eEF-1 gamma chain
715.7	Highly similar to PFD2_MOUSE PREFOLDIN SUBUNIT 2
716.1	nucleolar phosphoprotein of 140kD, Nopp140
720.1	tissue factor pathway inhibitor (Tfpi)
720.3	Weakly similar to GBB1 RAT GUANINE NUCLEOTIDE-BINDING PROTEIN

	G(I)G(S)G(T) BETA SUBUNIT 1
721.9	cyclooxygenase 2
722.8	norvegicus eukaryotic translation initiation factor 4E binding protein 1 (Eif4ebp1)
725.2	Highly similar to PLS1 MOUSE PROLIFERATION-ASSOCIATED PROTEIN 1
726.3	solute carrier family 7 member A1 (amino acid transporter cationic 1)
726.6	Highly similar to budding uninhibited by benzimidazoles 3 homolog (S. cerevisiae)
727.2	transcription elongation factor B (SIII) polypeptide 2
731.7	zinc finger protein Y1
734.9	nuclear RNA helicase, DECD variant of DEAD box family (Ddx1)
735.8	DNA primase small subunit
736.1	Cytochrome C
738.7	tumor-associated protein 1
740.3	phosphatidylethanolamine binding protein (Pbp)
740.5	HG17 RAT NONHISTONE CHROMOSOMAL PROTEIN HMG-17
742.2	ferritin light chain subunit
743.7	NTF2 gene
745.2	Highly similar to PROTEASOME SUBUNIT RC6-1
746.7	Weakly similar to S26689 hypothetical protein hc1 - mouse
748.6	fertility protein SP22
749.3	Weakly similar to S11349 nonhistone chromosomal protein HMG-17 - rat
750.2	small zinc finger-like protein (TIM13)
752.6	Moderately similar to DHSD_HUMAN SUCCINATE DEHYDROGENASE
754.1	nitric oxide synthase gene
754.9	Highly similar to RPCX MOUSE DNA-DIRECTED RNA POLYMERASES I, II, AND III 7.0 KD POLYPEPTIDE
755.2	Highly similar to DIAMINE ACETYLTRANSFERASE
756	Weakly similar to NFH MOUSE NEUROFILAMENT TRIPLET H PROTEIN
756.4	Weakly similar to JC5521 TATA-binding protein-interacting protein 49 - rat
757.1	Moderately similar to I Chain I, Beta-Galactosidase (Chains I-P)
757.5	Nopp140 associated protein (Nap65)
758.2	Weakly similar to SYW MOUSE TRYPTOPHANYL-TRNA SYNTHETASE
764	Highly similar to CNIH MOUSE CORNICHON HOMOLOG
764.2	solute carrier family 25 (mitochondrial adenine nucleotide translocator) member 4
767.5	Moderately similar to UCRH_HUMAN UBIQUINOL-CYTOCHROME C REDUCTASE COMPLEX 11 KDA PROTEIN PRECURSOR
767.8	integrin-linked kinase (Ilk)
768.5	proteasome (prosome, macropain) subunit, beta type, 4 (Psm4)
768.6	orphan seven transmembrane receptor (Ieda)
768.8	DDRT helix-destabilizing protein - rat
771.2	Tumor protein p53 (Li-Fraumeni syndrome) (Tp53)
772.2	Highly similar to S25111 alpha-2-macroglobulin receptor precursor - mouse
776.1	Weakly similar to S46930 teg292 protein - mouse
777.4	glycine cleavage system protein H (aminomethyl carrier) (Gcsh)
777.9	Weakly similar to T15543 hypothetical protein C18A3.3
778.6	Prosaposin (sulfated glycoprotein, sphingolipid hydrolase activator) (Psap)
778.9	cytoplasmic beta-actin (Actx)
781	Weakly similar to T27859 hypothetical protein ZK430.5
781.7	Highly similar to AF151857 1 CGI-99 protein

782.1	tyrosine 3-monooxygenasetryptophan 5-monooxygenase activatioprotein
787.2	proteasome (prosome, macropain) subunit, beta type, 2 (Psmb2)
787.8	Highly similar to IF37 MOUSE EUKARYOTIC TRANSLATION INITIATION FACTOR 3 SUBUNIT 7
788.3	Highly similar to translation initiation factor eIF3 p40 subunit (H.sapiens)
792	outer mitochondrial membrane receptor rTOM20
796.1	Protein phosphatase 2 (formerly 2A), catalytic subunit, beta isoform (Ppp2cb)
803.1	Protein phosphatase 1, catalytic subunit, gamma isoform 1 (Ppp1cc)
804.4	Highly similar to B Chain B, Crystal Structure Of The D1d2 Sub-Complex From The Human Snrnp Core Domain
805.4	Moderately similar to ribosomal protein L33-like protein
808	ribosomal protein L30
808.1	large subunit ribosomal protein L36a (Rpl36a)
809.2	Weakly similar to intracellular chloride ion channel protein p64H1
811.2	eukaryotic initiation factor 5 (eIF-5)
811.5	bone marrow stromal cell antigen 1
812.4	cytoplasmic beta-actin
815.3	solute carrier family 3 (activators of dibasic and neutral amino acid transport), member 2 (Slc3a2)
816.3	myosin regulatory light chain (RLC)
817.6	Highly similar to LSM4_MOUSE U6 SNRNA-ASSOCIATED SM-LIKE PROTEIN LSM4
818.7	ubiquitin A-52 residue ribosomal protein fusion product 1 (Uba52)
818.9	splicing factor 3b, subunit 3, 130kD; spliceosome-associated protein 130 (Homo sapiens)
819.9	Moderately similar to COXM MOUSE CYTOCHROME C OXIDASE POLYPEPTIDE VIIB PRECURSOR
824.6	Highly similar to H33_HUMAN HISTONE H3.3
827.1	Highly similar to HSPC014
828.4	heterogeneous nuclear ribonucleoprotein A1
829.2	Highly similar to 60S RIBOSOMAL PROTEIN L8
832.6	Highly similar to PRCE RAT PROTEASOME EPSILON CHAIN PRECURSOR
833.8	Bax protein splice variant k
834.7	Highly similar to MGN_HUMAN MAGO NASHI PROTEIN HOMOLOG
835.5	proteasome (prosome, macropain) subunit, beta type 1 (Psmb1)
837.4	Farnesyl diphosphate synthase (Fdps)
837.9	Highly similar to T46901 hypothetical protein DKFZp761C10121.1
839	Calmodulin 1 (phosphorylase kinase, delta)
841.4	heterogeneous nuclear ribonucleoprotein L
843.9	voltage-dependent anion channel 1 (Vdac1)
849	mitochondrial protonphosphate symporter
850.4	fatty acid synthase
853.2	small inducible cytokine subfamily, member 2 (Scyb2)
854.4	syntenin (Sdcbp)
858.8	Peptidylprolyl isomerase A (cyclophilin A)
859.6	MHC class I RT1.E protein mRNA
860.3	proteasome (prosome, macropain) subunit, alpha type 1 (Psmal1)
860.5	proteasome (prosome, macropain) subunit, beta type, 7 (Psmb7)
862.1	Cytochrome C, expressed in somatic tissues (Cycs)
866.2	Highly similar to translation intiation factor eIF-3 p110 subunit

867	Moderately similar to T13381 hypothetical protein EG:115C2.12 - fruit fly
867.2	Proliferating cell nuclear antigen (Pcna)
874.6	Weakly similar to PC1154 tumor rejection antigen P815 - mouse
882.7	Siahbp1
882.8	vesicle-associated membrane protein, associated protein A (33 kDa)
883.6	Highly similar to TF19 MOUSE TFAR19 PROTEIN
886.4	Weakly similar to Ribosomal protein L11
887	Highly similar to I55595 splicing factor
889.1	FK506-binding protein 1 (12kD)
897.4	metallothionein 1
899.3	LPS-induced TNF-alpha factor
903.8	Pyruvate kinase 3 (Pkm2)
903.8	GPI-anchored ceruloplasmin
908.4	Highly similar to P2CG MOUSE PROTEIN PHOSPHATASE 2C GAMMA ISOFORM
911.1	proteasome (prosome, macropain) subunit, alpha type 4 (Psm4)
913.7	T-complex 1
914.9	guanosine diphosphate (GDP) dissociation inhibitor 2
933.6	Highly similar to IF6 MOUSE EUKARYOTIC TRANSLATION INITIATION FACTOR 6
933.8	Highly similar to ACTB_HUMAN ACTIN, CYTOPLASMIC 1
936.5	Tyrosine 3-monooxygenasetryptophan 5-monooxygenase activation protein, theta
938.9	Highly similar to TPM1 RAT TROPOMYOSIN, FIBROBLAST ISOFORM 1 (R.norvegicus)
940	Superoxide dismutase 1, soluble (Sod1)
940.3	mitochondrial ATP synthase beta subunit
942.3	putative ionotropic glutamate receptor GLURR-F11694B (Glurr)
947.7	Highly similar to GTO1_RAT GLUTATHIONE TRANSFERASE OMEGA 1 (GSTO 1-1)
953.1	Histone H1-0 (H1f0)
964.3	transporter protein; system N1 Na+ and H+-coupled glutamine transporter
965	prothymosin alpha
970.3	Highly similar to SFR2_MOUSE Splicing factor, arginineserine-rich 2 (Splicing factor SC35) (SC-35)
980.6	Moderately similar to SYQ_HUMAN GLUTAMINYL-TRNA SYNTHETASE
987	Highly similar to ring-box 1; ring-box protein 1
989.6	Weakly similar to UCRQ_HUMAN UBIQUINOL-CYTOCHROME C REDUCTASE COMPLEX UBIQUINONE-BINDING PROTEIN QP-C
991.3	proteasome (prosome, macropain) subunit, alpha type 3 (Psm3)
997	Rat unidentified mRNA expressed in embryo and tumor but not normal differentiated
1001	class I beta-tubulin
1002.2	Weakly similar to S45359 polyubiquitin 10 - rat
1004.7	Weakly similar to PAB1 MOUSE POLYADENYLATE-BINDING PROTEIN 1
1015.6	microsomal glutathione S-transferase 1 (Mgst1)
1018.7	Weakly similar to T22490 hypothetical protein Y37A1B.1 - Caenorhabditis eleg
1025.3	Highly similar to EXT1 MOUSE EXOSTOSIN-1 (M.musculus)
1030.2	CCAATenhancerbinding, protein (CEBP) delta
1031.9	Moderately similar to UCR6_HUMAN UBIQUINOL-CYTOCHROME C REDUCTASE COMPLEX 14 KDA PROTEIN (H.sapiens)
1034.2	ribosomal protein L27

1036.3	Weakly similar to HS9B RAT HEAT SHOCK PROTEIN HSP 90-BETA (R.norvegicus)
1041.9	protease, serine, 11 (Igf binding) (Prss11)
1044.7	protease (prosome, macropain) 28 subunit, alpha (Psme1)
1046.5	Tegt
1046.8	protein tyrosine phosphatase 4a1
1049	Highly similar to IRF7 MOUSE INTERFERON REGULATORY FACTOR 7
1049.4	H3 histone, family 3B
1051	LY6E_MOUSE LYMPHOCYTE ANTIGEN LY-6E PRECURSOR (THYMIC SHARED ANTIGEN-1) (TSA-1)
1051.6	tissue inhibitor of metalloproteinase 1 (Timp1),
1053.1	Weakly similar to T-COMPLEX PROTEIN 1, ALPHA SUBUNIT (R.norvegicus)
1059.4	hypoxia inducible factor 1, alpha subunit (Hif1a)
1060.8	Highly similar to NAD-DEPENDENT METHYLENETETRAHYDROFOLATE DEHYDROGENASE METHENYLtetrahydrofolate cyclohydrolase MITOCHONDRIAL PRECURSOR
1072.8	Weakly similar to ROD_RAT HETEROGENEOUS NUCLEAR RIBONUCLEOPROTEIN D0 (HNRN)
1077.8	Highly similar to SYS_HUMAN SERYL-TRNA SYNTHETASE (H.sapiens)
1078.9	Weakly similar to UBIQUITIN-CONJUGATING ENZYME E2-17 KD 2 (R.norvegicus)
1084.9	cytochrome c oxidase subunit Va preprotein
1087.7	macrophage migration inhibitory factor (Mif)
1088.5	endolyn (Cd164)
1090.8	CCAATenhancerbinding, protein (CEBP) delta (Cebpd)
1102.7	MHC class I RT1 (RT21)
1103	peroxiredoxin 3 (Prdx3)
1103.1	Weakly similar to T34105 hypothetical protein C17G10.8
1110.4	cytochrome c oxidase, subunit IVa (Cox4a)
1112.3	3-phosphoglycerate dehydrogenase (Phgdh)
1120.1	protease (prosome, macropain) 28 subunit, beta (Psme2)
1123.2	T-complex 1 (Tcpl)
1127.4	Highly similar to FIBRILLARIN
1127.4	Weakly similar to T12A2.7.p
1129.7	Weakly similar to DOC1 MOUSE PUTATIVE ORAL CANCER SUPPRESSOR
1131.3	discs, large (Drosophila) homolog 2 (chapsyn-110)
1132.9	Moderately similar to T02345 hypothetical protein KIAA0324 (H.sapiens)
1134	Highly similar to C143_HUMAN PROTEIN C14ORF3 (PROTEIN HSPC322) (H.sapiens)
1135.8	Highly similar to RUXE_HUMAN SMALL NUCLEAR RIBONUCLEOPROTEIN E (M.musculus)
1140.8	Weakly similar to All-1 protein +GTE form (M.musculus)
1144.6	small inducible cytokine A5 (RANTES) (Scya5)
1145.1	Protein disulfide isomerase (Prolyl 4-hydroxylase, beta polypeptide) (P4hb)
1149.8	GLIA DERIVED NEXIN PRECURSOR (R.norvegicus)
1154.2	Triosephosphate isomerase 1 (Tpi1)
1157.7	profilin
1158.4	Weakly similar to TRANSFORMING PROTEIN RHOB
1165.3	phosphoglycerate kinase 1
1168	high mobility group box 2 (Hmgb2)
1172.5	interferon, alpha-inducible protein 27-like (Ifi271)

1184.4	mama
1186.2	versican Vint isoform
1187.3	polymerase (RNA) II (DNA directed)polypeptide G (Polr2g)
1188.8	Moderately similar to RL22 RAT 60S RIBOSOMAL PROTEIN L22 (R.norvegicus)
1200.3	Lysyl oxidase
1204.4	proteasome (prosome, macropain) subunit, beta type, 3
1214.2	ribosomal protein L5
1215.7	Highly similar to I56581 dnaK-type molecular chaperone grp75 precursor
1218.1	amphoterin
1218.3	Highly similar to IF36_HUMAN EUKARYOTIC TRANSLATION INITIATION FACTOR 3 SUBUNIT 6
1220.1	interferon-inducible protein variant 10
1228.6	Rps21
1229.1	Solute carrier family 25, member 5 (adenine nucleotid translocator 2, fibroblast isoform)
1240.8	Highly similar to JC4871 phospholipase C
1241.5	Highly similar to 40S RIBOSOMAL PROTEIN S25
1245.1	Highly similar to 40S RIBOSOMAL PROTEIN S28
1249	thioredoxin (Txn)
1252	Low molecular mass polypeptide 2
1256.7	polyubiquitin
1258.2	Highly similar to EUKARYOTIC INITIATION FACTOR 4A-II (M.musculus)
1261	Moderately similar to RB48 MOUSE CHROMATIN ASSEMBLY FACTOR 1 P48 SUBUNIT
1265.3	Highly similar to BTF3 MOUSE TRANSCRIPTION FACTOR BTF3 (M.musculus)
1267.2	Il6st
1270.2	class I beta-tubulin
1271	Highly similar to 60S RIBOSOMAL PROTEIN L35
1274.5	ATP citrate lyase (Acly)
1279.3	NADH ubiquinone oxidoreductase subunit B13
1287.8	GPI-anchored ceruloplasmin
1288.8	Weakly similar to cold inducible RNA-binding protein (Rattus norvegicus)
1296.6	cytochrome oxidase subunit VIc (Cox6c)
1297.4	nucleoside diphosphate kinase (Nme2)
1307.3	cellular nucleic acid binding protein
1307.9	Weakly similar to ROK_HUMAN HETEROGENEOUS NUCLEAR RIBONUCLEOPROTEIN K
1312	muscle Y-box protein YB2
1312.5	Moderately similar to TBB1 RAT TUBULIN BETA CHAIN
1317.6	peroxiredoxin 1 (Prdx1)
1322.3	heterogeneous nuclear ribonucleoproteins methyltransferase-like 2 (S. cerevisiae)
1322.5	granulin
1324.9	Ferritin subunit H (Fth1)
1325.4	Best5 protein
1328.7	Weakly similar to CAG7 RAT ALPHA-N-ACETYLGALACTOSAMINIDE ALPHA-2,6-SIALYLTRANSFERASE
1334.9	ribosomal protein L22
1336.3	ribosomal protein L6 (Rpl6)
1342.3	protein L29 (Rpl29)

1344.5	ribosomal protein S10 (Rps10)
1350.6	proteasome (prosome, macropain) subunit, alpha type 6 (Psm6)
1355.4	beta-carotene 15, 15-dioxygenase
1356.3	Lysyl oxidase (Lox)
1358.7	cathepsin B (Ctsb)
1361.7	Highly similar to RADIATION-INDUCIBLE IMMEDIATE-EARLY GENE IEX-1 (M.musculus)
1362.3	ribosomal protein L18 (Rpl18)
1364.6	Highly similar to RUXF_HUMAN SMALL NUCLEAR RIBONUCLEOPROTEIN F
1371.1	Stromal cell-derived factor 1
1379	mRNA for ribosomal protein S9
1396.4	Weakly similar to ARL4 MOUSE ADP-RIBOSYLATION FACTOR-LIKE PROTEIN 4 (R.norvegicus)
1399.5	Highly similar to RL11_HUMAN 60S RIBOSOMAL PROTEIN L11
1403.3	Rat MHC class I RT1 (RT44)
1403.4	ER-60 protease (ER60)
1404.3	complement component 1, q subcomponent binding protein (C1qbp)
1408	CDK110
1425.8	peroxiredoxin 6 (Prdx6)
1426.3	secretory leukocyte protease inhibitor (Slpi)
1432.4	ribosomal protein S15 (Rps15)
1436.2	H3 histone, family 3B
1464.1	polyubiquitin
1466.5	translation elongation factor 1-delta subunit
1490.3	Aldolase A, fructose-bisphosphate (Aldoa)
1501	ribosomal protein L14
1502.8	Highly similar to 2008109A set gene
1506.4	Rat laminin receptor mRNA, 3 end
1519.5	schlafen 4
1526.9	double-stranded RNA-binding protein p74
1530.7	ribosomal protein S11
1541.1	calpactin I heavy chain
1541.7	guanine nucleotide binding protein (G protein), beta polypeptide 2-like 1 (Gnb211)
1555.3	stearyl-CoA desaturase
1571.8	R5RT18 ribosomal protein L18a, cytosolic (validated)
1581.4	thymosin, beta 10 (Tmsb10)
1598.4	ribosomal protein L24
1604	Highly similar to OAZ RAT ORNITHINE DECARBOXYLASE ANTIZYME
1609.4	Solute carrier family 11 member 2 (natural resistance-associated macrophage protein 2) (Slc11a2)
1611.5	CDK105 protein (Cdk105)
1613.7	Enolase 1, alpha (Eno1)
1619.9	Weakly similar to JC6554 probable serine proteinase
1620.4	Highly similar to B46746 glycine hydroxymethyltransferase
1620.9	Highly similar to 60S ACIDIC RIBOSOMAL PROTEIN P2
1627.1	ribosomal protein S27a
1632.2	Moderately similar to RL34 RAT 60S RIBOSOMAL PROTEIN L34
1633.3	Highly similar to ERH_HUMAN ENHANCER OF RUDIMENTARY HOMOLOG

1662.8	Highly similar to RS3 MOUSE 40S RIBOSOMAL PROTEIN S3
1667.6	PHOSPHOGLYCERATE KINASE, TESTIS SPECIFIC
1672.8	ribosomal protein L15
1676.4	Moderately similar to HS9B RAT HEAT SHOCK PROTEIN HSP 90-BETA
1679.5	RAN, member RAS oncogene family (Ran)
1685.3	Highly similar to RL8_HUMAN 60S RIBOSOMAL PROTEIN L
1693.4	ribosomal protein L21 (Rpl21)
1702.8	proliferation related acidic leucine rich protein PAL31 (PAL31)
1704.7	type AB hnRNP protein p40
1714	chondroitin sulfate proteoglycan 2
1716.9	Moderately similar to Y101_HUMAN HYPOTHETICAL PROTEIN KIAA0101
1719.4	interferon inducible protein 10 (IP-10)
1720.1	Ribosomal protein S5
1722	Nucleoplasmin-related protein (Nuclear protein B23 (Npm1)
1723.7	golgi SNAP receptor complex member 1
1738.7	ribosomal protein L10a (Rpl10a)
1739.2	hypothetical RNA binding protein RDA288
1740.1	UDP-glucose dehydrogeanse (Ugdh)
1743.4	tumor protein, translationally-controlled 1 (Tpt1)
1745.2	ribosomal protein S2
1753.2	nuclease sensitive element binding protein 1
1767.5	B-cell translocation gene 1, anti-proliferative (Btg1)
1776.4	Weakly similar to AF154572 1 ERG2 protein
1788	ribosomal protein L28 (Rpl28)
1791.6	Highly similar to SUI1 MOUSE PROTEIN TRANSLATION FACTOR SUI1 HOMOLOG
1792.5	Rps24
1807.7	HS9B RAT HEAT SHOCK PROTEIN HSP 90-BETA
1816.7	ribosomal protein S27 (Rps27)
1826.7	ribosomal protein S14 (Rps14)
1832	ribosomal protein S26 (Rps26)
1832.2	Beta-2-microglobulin (B2m)
1835.7	Glyceraldehyde-3-phosphate dehydrogenase (Gapd)
1841	protein L4 (Rpl4)
1856.8	H2A histone family, member Z (H2afz)
1857.8	Highly similar to 60S RIBOSOMAL PROTEIN L23A
1875.7	Tuba1
1884.5	Highly similar to 60S ACIDIC RIBOSOMAL PROTEIN P1
1885.3	poly(A) binding protein, cytoplasmic 1 (Pabpc1)
1890.5	Hexokinase 3 (Hk3)
1891.2	ribosomal protein S3a (Rps3a)
1899.6	Liver activating protein (LAP, also NF-IL6, nuclear factor-IL6, previously designated TCF5) (Cebpb)
1906.8	ribosomal protein S7
1915.9	heat shock 70kD protein 8 (Hspa8)
1919	ribosomal protein S23
1931.9	ribosomal protein L35a
1967.8	ribosomal protein L13

1971.7	Nucleolin (Ncl)
1977.4	ribosomal protein L37
1997.3	Highly similar to RL7A_HUMAN 60S RIBOSOMAL PROTEIN L7A
1997.5	Highly similar to EF1B_MOUSE Elongation factor 1-beta (EF-1-beta)
1998.7	Ryudocansyndecan 4 (Sdc4)
2006.4	ribosomal protein S17
2007.4	Highly similar to 40S RIBOSOMAL PROTEIN S20
2009.5	ribosomal protein L30 (Rpl30)
2013.4	laminin receptor 1 (Lamr1)
2014	CINC-2 alpha
2021.6	Highly similar to T30827 nascent polypeptide-associated complex alpha chain, non-muscle splice form - mouse
2054.2	Highly similar to RL9 RAT 60S RIBOSOMAL PROTEIN L9
2064.3	Highly similar to 40S RIBOSOMAL PROTEIN S16
2066	Highly similar to RS18_HUMAN 40S RIBOSOMAL PROTEIN S18
2068.5	ribosomal protein S6 (Rps6)
2082.9	activating transcription factor ATF-4 (Atf4)
2102.1	heat shock protein 60 (liver)
2109.6	ribosomal protein S8 (Rps8)
2114.2	unknown Glu-Pro dipeptide repeat protein
2120.4	Heat shock 10 kD protein 1 (chaperonin 10) (Hspe1)
2129.5	Highly similar to ubiquitin-like protein ribosomal protein S30
2145.4	Weakly similar to HG17 RAT NONHISTONE CHROMOSOMAL PROTEIN HMG-17
2167.6	Superoxide dismutase 2, mitochondrial
2193.6	Highly similar to RL12 RAT 60S RIBOSOMAL PROTEIN L12
2207.8	Highly similar to HS9B RAT HEAT SHOCK PROTEIN HSP 90-BETA
2210.3	ribosomal protein S2
2217.3	Highly similar to SUI1 MOUSE PROTEIN TRANSLATION FACTOR SUI1 HOMOLOG
2219.5	tropomyosin 3
2225.3	Moderately similar to MCA3_HUMAN Multisynthetase complex auxiliary component p18
2228.2	Highly similar to S22655 translation elongation factor eEF-1 gamma chain
2232.2	small inducible cytokine subfamily D, 1 (Scyd1)
2245.2	R.norvegicus ASI mRNA for mammalian equivalent of bacterial large ribosomal subunit protein L22
2277.9	lipid-binding protein
2287.1	acidic ribosomal protein P0 (Arbp)
2331.3	ral simian leukemia viral oncogene homolog A
2364.2	ribosomal protein L19
2371.7	ribosomal protein S13
2395.2	Highly similar to 60S RIBOSOMAL PROTEIN L37A
2447.3	ribosomal protein S12
2496.8	ribosomal protein L41
2521.4	ribosomal protein L29
2528.7	IKBA_RAT NF-kappaB inhibitor alpha
2586.1	Ribosomal protein S29
2588.7	serine protease

2713.8	Highly similar to RL26 RAT 60S RIBOSOMAL PROTEIN L26
2720.3	Moderately similar to A25113 tubulin beta chain 15
2742.8	Highly similar to RL3 RAT 60S RIBOSOMAL PROTEIN L3
2766.7	plasminogen activator inhibitor 2 type A (Pai2a)
2840	Weakly similar to HE47 RAT PROBABLE ATP-DEPENDENT RNA HELICASE P47
2946.4	Highly similar to 40S RIBOSOMAL PROTEIN S19
3005.8	ribosomal protein S15a
3139.5	adhesion molecule 1 (Icam1)
3220.7	ribosomal protein L31 (Rpl31)
3307.1	CINC-2 alpha
3407.5	CC chemokine ST38 precursor
3466	CINC-2 alpha
3950.6	lipocalin 2 (Lcn2)
4519.9	metallothionein-2 and metallothionein-1 genes
4725.1	RAT SMALL INDUCIBLE CYTOKINE A7 PRECURSOR
5023.5	Weakly similar to nerve growth factor
7587.8	Superoxide dismutase 2, mitochondrial
7699.1	SERUM AMYLOID A-3
8461.8	Small inducible gene JE (Scya2)
9409.1	gro

APPENDIX B

MANUSCRIPT SOURCES FOR TEXT AND FIGURES

Kang, L.-I.; Mars, W.M.; Michalopoulos, G.K. Signals and Cells Involved in Regulating Liver Regeneration. *Cells* **2012**, *1*, 1261-1292.

- Figures 1 and 2

Kang, L.I. and Mars, W.M. Fibrinolytic factors in liver fibrosis. *Curr Pharm Biotechnol.* 2011; 12(9): 1441-1446(6). [PMID: 21401519]

- Figures 3, 4, 6

Kang, L.I.; Isse, K.; Orr, A.; Bowen, W.C.; Demetris, A.J.; Muratoglu, S.C.; Strickland, D.K.; Michalopoulos, G.K; Mars, W.M. Tissue-type plasminogen activator down-regulates hepatic stellate cell activation through LDLR-related protein 1 in rats and mice. In preparation.

- Figures 8-9, 11-13

BIBLIOGRAPHY

1. Wolber, E.M., and Jelkmann, W. 2002. Thrombopoietin: the novel hepatic hormone. *News Physiol Sci* 17:6-10.
2. Michalopoulos, G.K. Liver regeneration after partial hepatectomy: critical analysis of mechanistic dilemmas. *Am J Pathol* 176:2-13.
3. Miyaoka, Y., Ebato, K., Kato, H., Arakawa, S., Shimizu, S., and Miyajima, A. Hypertrophy and unconventional cell division of hepatocytes underlie liver regeneration. *Curr Biol* 22:1166-1175.
4. Lim, Y.S., and Kim, W.R. 2008. The global impact of hepatic fibrosis and end-stage liver disease. *Clin Liver Dis* 12:733-746, vii.
5. Camani, C., and Kruithof, E.K. 1995. The role of the finger and growth factor domains in the clearance of tissue-type plasminogen activator by hepatocytes. *J Biol Chem* 270:26053-26056.
6. Parker, G.A., and Picut, C.A. Immune functioning in non lymphoid organs: the liver. *Toxicol Pathol* 40:237-247.
7. Friedman, S.L. 2008. Hepatic stellate cells: protean, multifunctional, and enigmatic cells of the liver. *Physiol Rev* 88:125-172.
8. Kang, L.-I., Mars, W.M., and Michalopoulos, G.K. 2012. Signals and Cells Involved in Regulating Liver Regeneration. *Cells* 1:1261-1292.
9. Higgins G.M., A.R.M. 1931. Experimental pathology of the liver – Restoration of the liver of the white rat following partial surgical removal. *Arch Pathol* 12:186-202.
10. Mitchell, C., and Willenbring, H. 2008. A reproducible and well-tolerated method for 2/3 partial hepatectomy in mice. *Nat Protoc* 3:1167-1170.
11. de Toranzo, E.G., Gomez, M.I., and Castro, J.A. 1978. Carbon tetrachloride activation, lipid peroxidation and liver necrosis in different strains of mice. *Res Commun Chem Pathol Pharmacol* 19:347-352.

12. DeCicco, L.A., Rikans, L.E., Tutor, C.G., and Hornbrook, K.R. 1998. Serum and liver concentrations of tumor necrosis factor alpha and interleukin-1beta following administration of carbon tetrachloride to male rats. *Toxicol Lett* 98:115-121.
13. Jaeschke, H., McGill, M.R., Williams, C.D., and Ramachandran, A. Current issues with acetaminophen hepatotoxicity--a clinically relevant model to test the efficacy of natural products. *Life Sci* 88:737-745.
14. Hinson, J.A., Roberts, D.W., and James, L.P. Mechanisms of acetaminophen-induced liver necrosis. *Handb Exp Pharmacol*:369-405.
15. David Josephy, P. 2005. The molecular toxicology of acetaminophen. *Drug Metab Rev* 37:581-594.
16. Lee, J.H., Ilic, Z., and Sell, S. 1996. Cell kinetics of repair after allyl alcohol-induced liver necrosis in mice. *Int J Exp Pathol* 77:63-72.
17. Pound, A.W., and McGuire, L.J. 1978. Repeated partial hepatectomy as a promoting stimulus for carcinogenic response of liver to nitrosamines in rats. *Br J Cancer* 37:585-594.
18. Bhave, V.S., Donthamsetty, S., Latendresse, J.R., Cunningham, M.L., and Mehendale, H.M. Secretory phospholipase A(2)-mediated progression of hepatotoxicity initiated by acetaminophen is exacerbated in the absence of hepatic COX-2. *Toxicol Appl Pharmacol* 251:173-180.
19. Bhave, V.S., Donthamsetty, S., Latendresse, J.R., Muskhelishvili, L., and Mehendale, H.M. 2008. Secretory phospholipase A2 mediates progression of acute liver injury in the absence of sufficient cyclooxygenase-2. *Toxicol Appl Pharmacol* 228:225-238.
20. Limaye, P.B., Bhave, V.S., Palkar, P.S., Apte, U.M., Sawant, S.P., Yu, S., Latendresse, J.R., Reddy, J.K., and Mehendale, H.M. 2006. Upregulation of calpastatin in regenerating and developing rat liver: role in resistance against hepatotoxicity. *Hepatology* 44:379-388.
21. Mehendale, H.M. Once initiated, how does toxic tissue injury expand? *Trends Pharmacol Sci* 33:200-206.
22. Mehendale, H.M. 2005. Tissue repair: an important determinant of final outcome of toxicant-induced injury. *Toxicol Pathol* 33:41-51.
23. Columbano, A., and Ledda-Columbano, G.M. 2003. Mitogenesis by ligands of nuclear receptors: an attractive model for the study of the molecular mechanisms implicated in liver growth. *Cell Death Differ* 10 Suppl 1:S19-21.
24. Columbano, A., Simbula, M., Pibiri, M., Perra, A., Deidda, M., Locker, J., Pisanu, A., Ucheddu, A., and Ledda-Columbano, G.M. 2008. Triiodothyronine stimulates

- hepatocyte proliferation in two models of impaired liver regeneration. *Cell Prolif* 41:521-531.
25. Malik, R., Habib, M., Tootle, R., and Hodgson, H. 2005. Exogenous thyroid hormone induces liver enlargement, whilst maintaining regenerative potential--a study relevant to donor preconditioning. *Am J Transplant* 5:1801-1807.
 26. Francavilla, A., Carr, B.I., Azzarone, A., Polimeno, L., Wang, Z., Van Thiel, D.H., Subbotin, V., Prelich, J.G., and Starzl, T.E. 1994. Hepatocyte proliferation and gene expression induced by triiodothyronine in vivo and in vitro. *Hepatology* 20:1237-1241.
 27. Pyper, S.R., Viswakarma, N., Yu, S., and Reddy, J.K. PPARalpha: energy combustion, hypolipidemia, inflammation and cancer. *Nucl Recept Signal* 8:e002.
 28. Qatanani, M., and Moore, D.D. 2005. CAR, the continuously advancing receptor, in drug metabolism and disease. *Curr Drug Metab* 6:329-339.
 29. Ledda-Columbano, G.M., Coni, P., Simbula, G., Zedda, I., and Columbano, A. 1993. Compensatory regeneration, mitogen-induced liver growth, and multistage chemical carcinogenesis. *Environ Health Perspect* 101 Suppl 5:163-168.
 30. Bursch, W., Taper, H.S., Lauer, B., and Schulte-Hermann, R. 1985. Quantitative histological and histochemical studies on the occurrence and stages of controlled cell death (apoptosis) during regression of rat liver hyperplasia. *Virchows Arch B Cell Pathol Incl Mol Pathol* 50:153-166.
 31. Columbano, A., Ledda-Columbano, G.M., Coni, P.P., Faa, G., Liguori, C., Santa Cruz, G., and Pani, P. 1985. Occurrence of cell death (apoptosis) during the involution of liver hyperplasia. *Lab Invest* 52:670-675.
 32. Columbano, A., and Shinozuka, H. 1996. Liver regeneration versus direct hyperplasia. *FASEB J* 10:1118-1128.
 33. Apte, U., Gkretsi, V., Bowen, W.C., Mars, W.M., Luo, J.H., Donthamsetty, S., Orr, A., Monga, S.P., Wu, C., and Michalopoulos, G.K. 2009. Enhanced liver regeneration following changes induced by hepatocyte-specific genetic ablation of integrin-linked kinase. *Hepatology* 50:844-851.
 34. Liu, B., Bell, A.W., Paranjpe, S., Bowen, W.C., Khillan, J.S., Luo, J.H., Mars, W.M., and Michalopoulos, G.K. Suppression of liver regeneration and hepatocyte proliferation in hepatocyte-targeted glypican 3 transgenic mice. *Hepatology* 52:1060-1067.
 35. Donthamsetty, S., Bowen, W., Mars, W., Bhave, V., Luo, J.H., Wu, C., Hurd, J., Orr, A., Bell, A., and Michalopoulos, G. Liver-specific ablation of integrin-linked kinase in mice results in enhanced and prolonged cell proliferation and hepatomegaly after phenobarbital administration. *Toxicol Sci* 113:358-366.

36. Donthamsetty, S., Bhave, V.S., Kliment, C.S., Bowen, W.C., Mars, W.M., Bell, A.W., Stewart, R.E., Orr, A., Wu, C., and Michalopoulos, G.K. Excessive hepatomegaly of mice with hepatocyte-targeted elimination of integrin linked kinase following treatment with 1,4-bis [2-(3,5-dichloropyridyloxy)] benzene. *Hepatology* 53:587-595.
37. Lin, C.W., Mars, W.M., Paranjpe, S., Donthamsetty, S., Bhave, V.S., Kang, L.I., Orr, A., Bowen, W.C., Bell, A.W., and Michalopoulos, G.K. Hepatocyte proliferation and hepatomegaly induced by phenobarbital and 1,4-bis [2-(3,5-dichloropyridyloxy)] benzene is suppressed in hepatocyte-targeted glypican 3 transgenic mice. *Hepatology* 54:620-630.
38. Kodama, S., and Negishi, M. 2006. Phenobarbital confers its diverse effects by activating the orphan nuclear receptor car. *Drug Metab Rev* 38:75-87.
39. Grisham, J.W. 1962. A morphologic study of deoxyribonucleic acid synthesis and cell proliferation in regenerating rat liver; autoradiography with thymidine-H3. *Cancer Res* 22:842-849.
40. Widmann, J.J., and Fahimi, H.D. 1975. Proliferation of mononuclear phagocytes (Kupffer cells) and endothelial cells in regenerating rat liver. A light and electron microscopic cytochemical study. *Am J Pathol* 80:349-366.
41. Tanaka, Y., Mak, K.M., and Lieber, C.S. 1990. Immunohistochemical detection of proliferating lipocytes in regenerating rat liver. *J Pathol* 160:129-134.
42. Stocker, E., and Heine, W.D. 1971. Regeneration of liver parenchyma under normal and pathological conditions. *Beitr Pathol* 144:400-408.
43. Stocker, E., and Heine, W.D. 1971. [Proliferation and regeneration in liver and kidney of juvenile rats. Autoradiographic studies after continuous infusion of 3H-thymidine (author's transl)]. *Verh Dtsch Ges Pathol* 55:483-488.
44. Stocker, E., Schultze, B., Heine, W.D., and Liebscher, H. 1972. [Growth and regeneration in parenchymatous organs of the rat. Autoradiographic investigations with 3 H-thymidin]. *Z Zellforsch Mikrosk Anat* 125:306-331.
45. Schmucker, D.L., and Sanchez, H. Liver regeneration and aging: a current perspective. *Curr Gerontol Geriatr Res* 2011:526379.
46. Stocker, E., Wullstein, H.K., and Brau, G. 1973. [Capacity of regeneration in liver epithelia of juvenile, repeated partially hepatectomized rats. Autoradiographic studies after continous infusion of 3H-thymidine (author's transl)]. *Virchows Arch B Cell Pathol* 14:93-103.
47. Overturf, K., al-Dhalimy, M., Ou, C.N., Finegold, M., and Grompe, M. 1997. Serial transplantation reveals the stem-cell-like regenerative potential of adult mouse hepatocytes. *Am J Pathol* 151:1273-1280.

48. Bhave, V.S., Paranjpe, S., Bowen, W.C., Donthamsetty, S., Bell, A.W., Khillan, J.S., and Michalopoulos, G.K. Genes inducing iPS phenotype play a role in hepatocyte survival and proliferation in vitro and liver regeneration in vivo. *Hepatology* 54:1360-1370.
49. Mead, J.E., and Fausto, N. 1989. Transforming growth factor alpha may be a physiological regulator of liver regeneration by means of an autocrine mechanism. *Proc Natl Acad Sci U S A* 86:1558-1562.
50. Kan, M., Huang, J.S., Mansson, P.E., Yasumitsu, H., Carr, B., and McKeehan, W.L. 1989. Heparin-binding growth factor type 1 (acidic fibroblast growth factor): a potential biphasic autocrine and paracrine regulator of hepatocyte regeneration. *Proc Natl Acad Sci U S A* 86:7432-7436.
51. LeCouter, J., Moritz, D.R., Li, B., Phillips, G.L., Liang, X.H., Gerber, H.P., Hillan, K.J., and Ferrara, N. 2003. Angiogenesis-independent endothelial protection of liver: role of VEGFR-1. *Science* 299:890-893.
52. Borkham-Kamphorst, E., Kovalenko, E., van Roeyen, C.R., Gassler, N., Bomble, M., Ostendorf, T., Floege, J., Gressner, A.M., and Weiskirchen, R. 2008. Platelet-derived growth factor isoform expression in carbon tetrachloride-induced chronic liver injury. *Lab Invest* 88:1090-1100.
53. Schirmacher, P., Geerts, A., Pietrangelo, A., Dienes, H.P., and Rogler, C.E. 1992. Hepatocyte growth factor/hepatopoietin A is expressed in fat-storing cells from rat liver but not myofibroblast-like cells derived from fat-storing cells. *Hepatology* 15:5-11.
54. Maher, J.J. 1993. Cell-specific expression of hepatocyte growth factor in liver. Upregulation in sinusoidal endothelial cells after carbon tetrachloride. *J Clin Invest* 91:2244-2252.
55. Ito, N., Kawata, S., Tamura, S., Kiso, S., Tsushima, H., Damm, D., Abraham, J.A., Higashiyama, S., Taniguchi, N., and Matsuzawa, Y. 1994. Heparin-binding EGF-like growth factor is a potent mitogen for rat hepatocytes. *Biochem Biophys Res Commun* 198:25-31.
56. Ross, M.A., Sander, C.M., Kleeb, T.B., Watkins, S.C., and Stolz, D.B. 2001. Spatiotemporal expression of angiogenesis growth factor receptors during the revascularization of regenerating rat liver. *Hepatology* 34:1135-1148.
57. Martinez-Hernandez, A., and Amenta, P.S. 1995. The extracellular matrix in hepatic regeneration. *FASEB J* 9:1401-1410.
58. Wack, K.E., Ross, M.A., Zegarra, V., Sysko, L.R., Watkins, S.C., and Stolz, D.B. 2001. Sinusoidal ultrastructure evaluated during the revascularization of regenerating rat liver. *Hepatology* 33:363-378.

59. Fujii, H., Hirose, T., Oe, S., Yasuchika, K., Azuma, H., Fujikawa, T., Nagao, M., and Yamaoka, Y. 2002. Contribution of bone marrow cells to liver regeneration after partial hepatectomy in mice. *J Hepatol* 36:653-659.
60. Zocco, M.A., Piscaglia, A.C., Giuliente, F., Arena, V., Novi, M., Rinninella, E., Tortora, A., Rumi, C., Nuzzo, G., Vecchio, F.M., et al. CD133+ stem cell mobilization after partial hepatectomy depends on resection extent and underlying disease. *Dig Liver Dis* 43:147-154.
61. Wang, L., Wang, X., Xie, G., Hill, C.K., and DeLeve, L.D. Liver sinusoidal endothelial cell progenitor cells promote liver regeneration in rats. *J Clin Invest* 122:1567-1573.
62. Wang, L., Wang, X., Chiu, J.D., van de Ven, G., Gaarde, W.A., and Deleve, L.D. Hepatic Vascular Endothelial Growth Factor Regulates Recruitment of Rat Liver Sinusoidal Endothelial Cell Progenitor Cells. *Gastroenterology*.
63. Lagasse, E., Connors, H., Al-Dhalimy, M., Reitsma, M., Dohse, M., Osborne, L., Wang, X., Finegold, M., Weissman, I.L., and Grompe, M. 2000. Purified hematopoietic stem cells can differentiate into hepatocytes in vivo. *Nat Med* 6:1229-1234.
64. Petersen, B.E., Bowen, W.C., Patrene, K.D., Mars, W.M., Sullivan, A.K., Murase, N., Boggs, S.S., Greenberger, J.S., and Goff, J.P. 1999. Bone marrow as a potential source of hepatic oval cells. *Science* 284:1168-1170.
65. Terada, N., Hamazaki, T., Oka, M., Hoki, M., Mastalerz, D.M., Nakano, Y., Meyer, E.M., Morel, L., Petersen, B.E., and Scott, E.W. 2002. Bone marrow cells adopt the phenotype of other cells by spontaneous cell fusion. *Nature* 416:542-545.
66. Wang, X., Willenbring, H., Akkari, Y., Torimaru, Y., Foster, M., Al-Dhalimy, M., Lagasse, E., Finegold, M., Olson, S., and Grompe, M. 2003. Cell fusion is the principal source of bone-marrow-derived hepatocytes. *Nature* 422:897-901.
67. Kuwahara, R., Kofman, A.V., Landis, C.S., Swenson, E.S., Barendswaard, E., and Theise, N.D. 2008. The hepatic stem cell niche: identification by label-retaining cell assay. *Hepatology* 47:1994-2002.
68. Dolle, L., Best, J., Mei, J., Al Battah, F., Reynaert, H., van Grunsven, L.A., and Geerts, A. The quest for liver progenitor cells: a practical point of view. *J Hepatol* 52:117-129.
69. Evarts, R.P., Nagy, P., Nakatsukasa, H., Marsden, E., and Thorgeirsson, S.S. 1989. In vivo differentiation of rat liver oval cells into hepatocytes. *Cancer Res* 49:1541-1547.
70. Trautwein, C., Will, M., Kubicka, S., Rakemann, T., Flemming, P., and Manns, M.P. 1999. 2-acetaminofluorene blocks cell cycle progression after hepatectomy by p21 induction and lack of cyclin E expression. *Oncogene* 18:6443-6453.
71. Limaye, P.B., Alarcon, G., Walls, A.L., Nalesnik, M.A., Michalopoulos, G.K., Demetris, A.J., and Ochoa, E.R. 2008. Expression of specific hepatocyte and cholangiocyte

- transcription factors in human liver disease and embryonic development. *Lab Invest* 88:865-872.
72. Petersen, B.E., Goff, J.P., Greenberger, J.S., and Michalopoulos, G.K. 1998. Hepatic oval cells express the hematopoietic stem cell marker Thy-1 in the rat. *Hepatology* 27:433-445.
 73. Evarts, R.P., Hu, Z., Fujio, K., Marsden, E.R., and Thorgeirsson, S.S. 1993. Activation of hepatic stem cell compartment in the rat: role of transforming growth factor alpha, hepatocyte growth factor, and acidic fibroblast growth factor in early proliferation. *Cell Growth Differ* 4:555-561.
 74. Darwiche, H., Oh, S.H., Steiger-Luther, N.C., Williams, J.M., Pintilie, D.G., Shupe, T.D., and Petersen, B.E. Inhibition of Notch signaling affects hepatic oval cell response in rat model of 2AAF-PH. *Hepat Med* 3:89-98.
 75. Thenappan, A., Li, Y., Kitisin, K., Rashid, A., Shetty, K., Johnson, L., and Mishra, L. Role of transforming growth factor beta signaling and expansion of progenitor cells in regenerating liver. *Hepatology* 51:1373-1382.
 76. Erker, L., and Grompe, M. 2007. Signaling networks in hepatic oval cell activation. *Stem Cell Res* 1:90-102.
 77. Jakubowski, A., Ambrose, C., Parr, M., Lincecum, J.M., Wang, M.Z., Zheng, T.S., Browning, B., Michaelson, J.S., Baetscher, M., Wang, B., et al. 2005. TWEAK induces liver progenitor cell proliferation. *J Clin Invest* 115:2330-2340.
 78. Mavier, P., Martin, N., Couchie, D., Preaux, A.M., Laperche, Y., and Zafrani, E.S. 2004. Expression of stromal cell-derived factor-1 and of its receptor CXCR4 in liver regeneration from oval cells in rat. *Am J Pathol* 165:1969-1977.
 79. Theise, N.D., Saxena, R., Portmann, B.C., Thung, S.N., Yee, H., Chiriboga, L., Kumar, A., and Crawford, J.M. 1999. The canals of Hering and hepatic stem cells in humans. *Hepatology* 30:1425-1433.
 80. Nagy, P., Bisgaard, H.C., and Thorgeirsson, S.S. 1994. Expression of hepatic transcription factors during liver development and oval cell differentiation. *J Cell Biol* 126:223-233.
 81. Petersen, B.E., Zajac, V.F., and Michalopoulos, G.K. 1997. Bile ductular damage induced by methylene dianiline inhibits oval cell activation. *Am J Pathol* 151:905-909.
 82. Demetris, A.J., Seaberg, E.C., Wennerberg, A., Ionellie, J., and Michalopoulos, G. 1996. Ductular reaction after submassive necrosis in humans. Special emphasis on analysis of ductular hepatocytes. *Am J Pathol* 149:439-448.

83. Michalopoulos, G.K., Barua, L., and Bowen, W.C. 2005. Transdifferentiation of rat hepatocytes into biliary cells after bile duct ligation and toxic biliary injury. *Hepatology* 41:535-544.
84. Kordes, C., Sawitza, I., Muller-Marbach, A., Ale-Agha, N., Keitel, V., Klonowski-Stumpe, H., and Haussinger, D. 2007. CD133+ hepatic stellate cells are progenitor cells. *Biochem Biophys Res Commun* 352:410-417.
85. Yang, L., Jung, Y., Omenetti, A., Witek, R.P., Choi, S., Vandongen, H.M., Huang, J., Alpini, G.D., and Diehl, A.M. 2008. Fate-mapping evidence that hepatic stellate cells are epithelial progenitors in adult mouse livers. *Stem Cells* 26:2104-2113.
86. Lotersztajn, S., Julien, B., Teixeira-Clerc, F., Grenard, P., and Mallat, A. 2005. Hepatic fibrosis: molecular mechanisms and drug targets. *Annu Rev Pharmacol Toxicol* 45:605-628.
87. Benyon, R.C., and Arthur, M.J. 2001. Extracellular matrix degradation and the role of hepatic stellate cells. *Semin Liver Dis* 21:373-384.
88. Ramadori, G., and Saile, B. 2004. Portal tract fibrogenesis in the liver. *Lab Invest* 84:153-159.
89. Forbes, S.J., Russo, F.P., Rey, V., Burra, P., Rugge, M., Wright, N.A., and Alison, M.R. 2004. A significant proportion of myofibroblasts are of bone marrow origin in human liver fibrosis. *Gastroenterology* 126:955-963.
90. Rygiel, K.A., Robertson, H., Marshall, H.L., Pekalski, M., Zhao, L., Booth, T.A., Jones, D.E., Burt, A.D., and Kirby, J.A. 2008. Epithelial-mesenchymal transition contributes to portal tract fibrogenesis during human chronic liver disease. *Lab Invest* 88:112-123.
91. Xia, J.L., Dai, C., Michalopoulos, G.K., and Liu, Y. 2006. Hepatocyte growth factor attenuates liver fibrosis induced by bile duct ligation. *Am J Pathol* 168:1500-1512.
92. Gressner, A.M., Weiskirchen, R., Breitkopf, K., and Dooley, S. 2002. Roles of TGF-beta in hepatic fibrosis. *Front Biosci* 7:d793-807.
93. Rachfal, A.W., and Brigstock, D.R. 2003. Connective tissue growth factor (CTGF/CCN2) in hepatic fibrosis. *Hepatol Res* 26:1-9.
94. Knittel, T., Mehde, M., Grundmann, A., Saile, B., Scharf, J.G., and Ramadori, G. 2000. Expression of matrix metalloproteinases and their inhibitors during hepatic tissue repair in the rat. *Histochemistry and Cell Biology* 113:443-453.
95. Kim, T.H., Mars, W.M., Stolz, D.B., and Michalopoulos, G.K. 2000. Expression and activation of pro-MMP-2 and pro-MMP-9 during rat liver regeneration. *Hepatology* 31:75-82.

96. Boucher, P., Li, W.P., Matz, R.L., Takayama, Y., Auwerx, J., Anderson, R.G., and Herz, J. 2007. LRP1 functions as an atheroprotective integrator of TGFbeta and PDGF signals in the vascular wall: implications for Marfan syndrome. *PLoS One* 2:e448.
97. Romero-Calvo, I., Ocon, B., Martinez-Moya, P., Suarez, M.D., Zarzuelo, A., Martinez-Augustin, O., and de Medina, F.S. 2010. Reversible Ponceau staining as a loading control alternative to actin in Western blots. *Anal Biochem* 401:318-320.
98. Varin, F., and Huet, P.M. 1985. Hepatic microcirculation in the perfused cirrhotic rat liver. *J Clin Invest* 76:1904-1912.
99. Lee, J.S., Semela, D., Iredale, J., and Shah, V.H. 2007. Sinusoidal remodeling and angiogenesis: a new function for the liver-specific pericyte? *Hepatology* 45:817-825.
100. Kang, L.I., and Mars, W.M. 2011. Fibrinolytic factors in liver fibrosis. *Curr Pharm Biotechnol* 12:1441-1446.
101. Iredale, J.P. 2001. Hepatic stellate cell behavior during resolution of liver injury. *Semin Liver Dis* 21:427-436.
102. Elsharkawy, A.M., Oakley, F., and Mann, D.A. 2005. The role and regulation of hepatic stellate cell apoptosis in reversal of liver fibrosis. *Apoptosis* 10:927-939.
103. Iredale, J.P., Benyon, R.C., Pickering, J., McCullen, M., Northrop, M., Pawley, S., Hovell, C., and Arthur, M.J.P. 1998. Mechanisms of spontaneous resolution of rat liver fibrosis - Hepatic stellate cell apoptosis and reduced hepatic expression of metalloproteinase inhibitors. *Journal of Clinical Investigation* 102:538-549.
104. Pinzani, M., and Vizzutti, F. 2008. Fibrosis and cirrhosis reversibility: clinical features and implications. *Clin Liver Dis* 12:901-913, x.
105. Shiratori, Y., Imazeki, F., Moriyama, M., Yano, M., Arakawa, Y., Yokosuka, O., Kuroki, T., Nishiguchi, S., Sata, M., Yamada, G., et al. 2000. Histologic improvement of fibrosis in patients with hepatitis C who have sustained response to interferon therapy. *Ann Intern Med* 132:517-524.
106. Rockey, D.C. 2008. Current and future anti-fibrotic therapies for chronic liver disease. *Clin Liver Dis* 12:939-962, xi.
107. Bataller, R., and Brenner, D.A. 2001. Hepatic stellate cells as a target for the treatment of liver fibrosis. *Seminars in Liver Disease* 21:437-451.
108. Thompson, A.J., and Patel, K. Antifibrotic therapies: will we ever get there? *Curr Gastroenterol Rep* 12:23-29.
109. Matsuo, O., Lijnen, H.R., Ueshima, S., Kojima, S., and Smyth, S.S. 2007. A guide to murine fibrinolytic factor structure, function, assays, and genetic alterations. *Journal of Thrombosis and Haemostasis* 5:680-689.

110. Andreasen, P.A., Sottrupjensen, L., Kjoller, L., Nykjaer, A., Moestrup, S.K., Petersen, C.M., and Gliemann, J. 1994. Receptor-Mediated Endocytosis of Plasminogen Activators and Activator/Inhibitor Complexes. *Febs Letters* 338:239-245.
111. Irigoyen, J.P., Munoz-Canoves, P., Montero, L., Koziczak, M., and Nagamine, Y. 1999. The plasminogen activator system: biology and regulation. *Cellular and Molecular Life Sciences* 56:104-132.
112. Narita, M., Bu, G., Herz, J., and Schwartz, A.L. 1995. Two receptor systems are involved in the plasma clearance of tissue-type plasminogen activator (t-PA) in vivo. *J Clin Invest* 96:1164-1168.
113. Orth, K., Willnow, T., Herz, J., Gething, M.J., and Sambrook, J. 1994. Low-Density-Lipoprotein Receptor-Related Protein Is Necessary for the Internalization of Both Tissue-Type Plasminogen Activator-Inhibitor Complexes and Free Tissue-Type Plasminogen-Activator. *Journal of Biological Chemistry* 269:21117-21122.
114. Andreasen, P.A., Kjoller, L., Christensen, L., and Duffy, M.J. 1997. The urokinase-type plasminogen activator system in cancer metastasis: a review. *Int J Cancer* 72:1-22.
115. Herz, J. 2003. LRP: a bright beacon at the blood-brain barrier. *J Clin Invest* 112:1483-1485.
116. Bezerra, J.A., Currier, A.R., Melin-Aldana, H., Sabla, G., Bugge, T.H., Kombrinck, K.W., and Degen, J.L. 2001. Plasminogen activators direct reorganization of the liver lobule after acute injury. *Am J Pathol* 158:921-929.
117. Bezerra, J.A., Bugge, T.H., Melin-Aldana, H., Sabla, G., Kombrinck, K.W., Witte, D.P., and Degen, J.L. 1999. Plasminogen deficiency leads to impaired remodeling after a toxic injury to the liver. *Proc Natl Acad Sci U S A* 96:15143-15148.
118. Currier, A.R., Sabla, G., Locaputo, S., Melin-Aldana, H., Degen, J.L., and Bezerra, J.A. 2003. Plasminogen directs the pleiotropic effects of uPA in liver injury and repair. *Am J Physiol Gastrointest Liver Physiol* 284:G508-515.
119. Pohl, J.F., Melin-Aldana, H., Sabla, G., Degen, J.L., and Bezerra, J.A. 2001. Plasminogen deficiency leads to impaired lobular reorganization and matrix accumulation after chronic liver injury. *Am J Pathol* 159:2179-2186.
120. Shanmukhappa, K., Matte, U., Degen, J.L., and Bezerra, J.A. 2009. Plasmin-mediated Proteolysis Is Required for Hepatocyte Growth Factor Activation during Liver Repair. *Journal of Biological Chemistry* 284:12917-12923.
121. Mars, W.M., Kim, T.H., Stolz, D.B., Liu, M.L., and Michalopoulos, G.K. 1996. Presence of urokinase in serum-free primary rat hepatocyte cultures and its role in activating hepatocyte growth factor. *Cancer Res* 56:2837-2843.

122. Mars, W.M., Zarnegar, R., and Michalopoulos, G.K. 1993. Activation of Hepatocyte Growth-Factor by the Plasminogen Activators Upa and Tpa. *American Journal of Pathology* 143:949-958.
123. Huh, C.G., Factor, V.M., Sanchez, A., Uchida, K., Conner, E.A., and Thorgeirsson, S.S. 2004. Hepatocyte growth factor/c-met signaling pathway is required for efficient liver regeneration and repair. *Proceedings of the National Academy of Sciences of the United States of America* 101:4477-4482.
124. Papatheodoridis, G.V., Papakonstantinou, E., Andrioti, E., Cholongitas, E., Petraki, K., Kontopoulou, I., and Hadziyannis, S.J. 2003. Thrombotic risk factors and extent of liver fibrosis in chronic viral hepatitis. *Gut* 52:404-409.
125. Schoedel, K.E., Tyner, V.Z., Kim, T., Michalopoulos, G.K., and Mars, W.M. 2003. HGF, MET, and matrix-related proteases in hepatocellular carcinoma, fibrolamellar variant, cirrhotic and normal liver. *Modern Pathology* 16:14-21.
126. Cramer, T., Schuppan, D., Bauer, M., Pfander, D., Neuhaus, P., and Herbst, H. 2004. Hepatocyte growth factor and c-Met expression in rat and human liver fibrosis. *Liver International* 24:335-344.
127. Zhang, L.P., Takahara, T., Yata, Y., Furui, K., Jin, B., Kawada, N., and Watanabe, A. 1999. Increased expression of plasminogen activator and plasminogen activator inhibitor during liver fibrogenesis of rats: role of stellate cells. *Journal of Hepatology* 31:703-711.
128. Leyland, H., Gentry, J., Arthur, M.J.P., and Benyon, R.C. 1996. The plasminogen-activating system in hepatic stellate cells. *Hepatology* 24:1172-1178.
129. Martinez-Rizo, A., Bueno-Topete, M., Gonzalez-Cuevas, J., and Armendariz-Borunda, J. Plasmin plays a key role in the regulation of profibrogenic molecules in hepatic stellate cells. *Liver Int* 30:298-310.
130. Kaibori, M., Inoue, T., Sakakura, Y., Oda, M., Nagahama, T., Kwon, A.H., Kamiyama, Y., Miyazawa, K., and Okumura, T. 2002. Impairment of activation of hepatocyte growth factor precursor into its mature form in rats with liver cirrhosis. *Journal of Surgical Research* 106:108-114.
131. Wang, H., Zhang, Y., and Heuckeroth, R.O. 2007. PAI-1 deficiency reduces liver fibrosis after bile duct ligation in mice through activation of tPA. *Febs Letters* 581:3098-3104.
132. Bauman, K.A., Wettlaufer, S.H., Okunishi, K., Vannella, K.M., Stoolman, J.S., Huang, S.K., Courey, A.J., White, E.S., Hogaboam, C.M., Simon, R.H., et al. The antifibrotic effects of plasminogen activation occur via prostaglandin E2 synthesis in humans and mice. *J Clin Invest* 120:1950-1960.
133. Asano, Y., Iimuro, Y., Son, G., Hirano, T., and Fujimoto, J. 2007. Hepatocyte growth factor promotes remodeling of murine liver fibrosis, accelerating recruitment of bone marrow-derived cells into the liver. *Hepatology Research* 37:1080-1094.

134. Salgado, S., Garcia, J., Vera, J., Siller, F., Bueno, M., Miranda, A., Segura, A., Grijalva, G., Segura, J., Orozco, H., et al. 2000. Liver cirrhosis is reverted by urokinase-type plasminogen activator gene therapy. *Molecular Therapy* 2:545-551.
135. Higazi, A.A., El-Haj, M., Melhem, A., Horani, A., Pappo, O., Alvarez, C.E., Muhanna, N., Friedman, S.L., and Safadi, R. 2008. Immunomodulatory effects of plasminogen activators on hepatic fibrogenesis. *Clin Exp Immunol* 152:163-173.
136. Hsiao, Y., Zou, T., Ling, C.C., Hu, H., Tao, X.M., and Song, H.Y. 2008. Disruption of tissue-type plasminogen activator gene in mice aggravated liver fibrosis. *J Gastroenterol Hepatol* 23:e258-264.
137. Seth, D., Hogg, P.J., Gorrell, M.D., McCaughan, G.W., and Haber, P.S. 2008. Direct effects of alcohol on hepatic fibrinolytic balance: implications for alcoholic liver disease. *J Hepatol* 48:614-627.
138. Boucher, P., and Herz, J. 2011. Signaling through LRP1: Protection from atherosclerosis and beyond. *Biochem Pharmacol* 81:1-5.
139. Lillis, A.P., Van Duyn, L.B., Murphy-Ullrich, J.E., and Strickland, D.K. 2008. LDL receptor-related protein 1: unique tissue-specific functions revealed by selective gene knockout studies. *Physiol Rev* 88:887-918.
140. Yepes, M., Sandkvist, M., Moore, E.G., Bugge, T.H., Strickland, D.K., and Lawrence, D.A. 2003. Tissue-type plasminogen activator induces opening of the blood-brain barrier via the LDL receptor-related protein. *J Clin Invest* 112:1533-1540.
141. Ulery, P.G., Beers, J., Mikhailenko, I., Tanzi, R.E., Rebeck, G.W., Hyman, B.T., and Strickland, D.K. 2000. Modulation of beta-amyloid precursor protein processing by the low density lipoprotein receptor-related protein (LRP). Evidence that LRP contributes to the pathogenesis of Alzheimer's disease. *J Biol Chem* 275:7410-7415.
142. Montel, V., Gaultier, A., Lester, R.D., Campana, W.M., and Gonias, S.L. 2007. The low-density lipoprotein receptor-related protein regulates cancer cell survival and metastasis development. *Cancer Res* 67:9817-9824.
143. Boucher, P., Gotthardt, M., Li, W.P., Anderson, R.G., and Herz, J. 2003. LRP: role in vascular wall integrity and protection from atherosclerosis. *Science* 300:329-332.
144. Herz, J., Clouthier, D.E., and Hammer, R.E. 1992. LDL receptor-related protein internalizes and degrades uPA-PAI-1 complexes and is essential for embryo implantation. *Cell* 71:411-421.
145. Herz, J., Kowal, R.C., Ho, Y.K., Brown, M.S., and Goldstein, J.L. 1990. Low density lipoprotein receptor-related protein mediates endocytosis of monoclonal antibodies in cultured cells and rabbit liver. *J Biol Chem* 265:21355-21362.

146. Betts, G.N., van der Geer, P., and Komives, E.A. 2008. Structural and functional consequences of tyrosine phosphorylation in the LRP1 cytoplasmic domain. *J Biol Chem* 283:15656-15664.
147. Ranganathan, S., Liu, C.X., Migliorini, M.M., Von Arnim, C.A., Peltan, I.D., Mikhailenko, I., Hyman, B.T., and Strickland, D.K. 2004. Serine and threonine phosphorylation of the low density lipoprotein receptor-related protein by protein kinase Calpha regulates endocytosis and association with adaptor molecules. *J Biol Chem* 279:40536-40544.
148. Gotthardt, M., Trommsdorff, M., Nevitt, M.F., Shelton, J., Richardson, J.A., Stockinger, W., Nimpf, J., and Herz, J. 2000. Interactions of the low density lipoprotein receptor gene family with cytosolic adaptor and scaffold proteins suggest diverse biological functions in cellular communication and signal transduction. *J Biol Chem* 275:25616-25624.
149. Barnes, H., Ackermann, E.J., and van der Geer, P. 2003. v-Src induces Shc binding to tyrosine 63 in the cytoplasmic domain of the LDL receptor-related protein 1. *Oncogene* 22:3589-3597.
150. Kounnas, M.Z., Argraves, W.S., and Strickland, D.K. 1992. The 39-kDa receptor-associated protein interacts with two members of the low density lipoprotein receptor family, alpha 2-macroglobulin receptor and glycoprotein 330. *J Biol Chem* 267:21162-21166.
151. Quinn, K.A., Pye, V.J., Dai, Y.P., Chesterman, C.N., and Owensby, D.A. 1999. Characterization of the soluble form of the low density lipoprotein receptor-related protein (LRP). *Exp Cell Res* 251:433-441.
152. May, P., Reddy, Y.K., and Herz, J. 2002. Proteolytic processing of low density lipoprotein receptor-related protein mediates regulated release of its intracellular domain. *J Biol Chem* 277:18736-18743.
153. Herz, J., and Strickland, D.K. 2001. LRP: a multifunctional scavenger and signaling receptor. *J Clin Invest* 108:779-784.
154. Yang, J., Shultz, R.W., Mars, W.M., Wegner, R.E., Li, Y., Dai, C., Nejak, K., and Liu, Y. 2002. Disruption of tissue-type plasminogen activator gene in mice reduces renal interstitial fibrosis in obstructive nephropathy. *J Clin Invest* 110:1525-1538.
155. Hu, K., Yang, J., Tanaka, S., Gonias, S.L., Mars, W.M., and Liu, Y. 2006. Tissue-type plasminogen activator acts as a cytokine that triggers intracellular signal transduction and induces matrix metalloproteinase-9 gene expression. *J Biol Chem* 281:2120-2127.
156. Hu, K., Wu, C., Mars, W.M., and Liu, Y. 2007. Tissue-type plasminogen activator promotes murine myofibroblast activation through LDL receptor-related protein 1-mediated integrin signaling. *J Clin Invest* 117:3821-3832.

157. Hu, K., Lin, L., Tan, X., Yang, J., Bu, G., Mars, W.M., and Liu, Y. 2008. tPA protects renal interstitial fibroblasts and myofibroblasts from apoptosis. *J Am Soc Nephrol* 19:503-514.
158. Shi, Y., Yamauchi, T., Gaultier, A., Takimoto, S., Campana, W.M., and Gonias, S.L. 2011. Regulation of cytokine expression by Schwann cells in response to alpha2-macroglobulin binding to LRP1. *J Neurosci Res* 89:544-551.
159. Misra, U.K., Chu, C.T., Rubenstein, D.S., Gawdi, G., and Pizzo, S.V. 1993. Receptor-recognized alpha 2-macroglobulin-methylamine elevates intracellular calcium, inositol phosphates and cyclic AMP in murine peritoneal macrophages. *Biochem J* 290 (Pt 3):885-891.
160. Zhang, H., Lee, J.M., Wang, Y., Dong, L., Ko, K.W., Pelletier, L., and Yao, Z. 2008. Mutational analysis of the FXNPXY motif within LDL receptor-related protein 1 (LRP1) reveals the functional importance of the tyrosine residues in cell growth regulation and signal transduction. *Biochem J* 409:53-64.
161. Chu, C.T., Howard, G.C., Misra, U.K., and Pizzo, S.V. 1994. Alpha 2-macroglobulin: a sensor for proteolysis. *Ann N Y Acad Sci* 737:291-307.
162. Raines, E.W. 2004. PDGF and cardiovascular disease. *Cytokine Growth Factor Rev* 15:237-254.
163. Loukinova, E., Ranganathan, S., Kuznetsov, S., Gorlatova, N., Migliorini, M.M., Loukinov, D., Ulery, P.G., Mikhailenko, I., Lawrence, D.A., and Strickland, D.K. 2002. Platelet-derived growth factor (PDGF)-induced tyrosine phosphorylation of the low density lipoprotein receptor-related protein (LRP). Evidence for integrated co-receptor function between LRP and the PDGF. *J Biol Chem* 277:15499-15506.
164. Boucher, P., Liu, P., Gotthardt, M., Hiesberger, T., Anderson, R.G., and Herz, J. 2002. Platelet-derived growth factor mediates tyrosine phosphorylation of the cytoplasmic domain of the low Density lipoprotein receptor-related protein in caveolae. *J Biol Chem* 277:15507-15513.
165. Cao, C., Lawrence, D.A., Li, Y., Von Arnim, C.A., Herz, J., Su, E.J., Makarova, A., Hyman, B.T., Strickland, D.K., and Zhang, L. 2006. Endocytic receptor LRP together with tPA and PAI-1 coordinates Mac-1-dependent macrophage migration. *EMBO J* 25:1860-1870.
166. Mars, W.M., Zarnegar, R., and Michalopoulos, G.K. 1993. Activation of hepatocyte growth factor by the plasminogen activators uPA and tPA. *Am J Pathol* 143:949-958.
167. Wang, H., Zhang, Y., and Heuckeroth, R.O. 2007. Tissue-type plasminogen activator deficiency exacerbates cholestatic liver injury in mice. *Hepatology* 45:1527-1537.

168. Gao, R., and Brigstock, D.R. 2003. Low density lipoprotein receptor-related protein (LRP) is a heparin-dependent adhesion receptor for connective tissue growth factor (CTGF) in rat activated hepatic stellate cells. *Hepato Res* 27:214-220.
169. Llorente-Cortes, V., Barbarigo, V., and Badimon, L. Low density lipoprotein receptor-related protein 1 modulates the proliferation and migration of human hepatic stellate cells. *J Cell Physiol* 227:3528-3533.
170. Migliorini, M.M., Behre, E.H., Brew, S., Ingham, K.C., and Strickland, D.K. 2003. Allosteric modulation of ligand binding to low density lipoprotein receptor-related protein by the receptor-associated protein requires critical lysine residues within its carboxyl-terminal domain. *J Biol Chem* 278:17986-17992.
171. Riccalton-Banks, L., Bhandari, R., Fry, J., and Shakesheff, K.M. 2003. A simple method for the simultaneous isolation of stellate cells and hepatocytes from rat liver tissue. *Mol Cell Biochem* 248:97-102.
172. Seglen, P.O. 1976. Preparation of isolated rat liver cells. *Methods Cell Biol* 13:29-83.
173. Kost, D.P., and Michalopoulos, G.K. 1991. Effect of 2% dimethyl sulfoxide on the mitogenic properties of epidermal growth factor and hepatocyte growth factor in primary hepatocyte culture. *J Cell Physiol* 147:274-280.
174. Michalopoulos, G.K., Bowen, W.C., Zajac, V.F., Beer-Stolz, D., Watkins, S., Kostrubsky, V., and Strom, S.C. 1999. Morphogenetic events in mixed cultures of rat hepatocytes and nonparenchymal cells maintained in biological matrices in the presence of hepatocyte growth factor and epidermal growth factor. *Hepatology* 29:90-100.
175. Michalopoulos, G.K., Bowen, W.C., Mule, K., and Stolz, D.B. 2001. Histological organization in hepatocyte organoid cultures. *Am J Pathol* 159:1877-1887.
176. Lagoa, C.E., Vodovotz, Y., Stolz, D.B., Lhuillier, F., McCloskey, C., Gallo, D., Yang, R., Ustinova, E., Fink, M.P., Billiar, T.R., et al. 2005. The role of hepatic type 1 plasminogen activator inhibitor (PAI-1) during murine hemorrhagic shock. *Hepatology* 42:390-399.
177. Li, Y., Spataro, B.C., Yang, J., Dai, C., and Liu, Y. 2005. 1,25-dihydroxyvitamin D inhibits renal interstitial myofibroblast activation by inducing hepatocyte growth factor expression. *Kidney Int* 68:1500-1510.
178. Kovalovich, K., DeAngelis, R.A., Li, W., Furth, E.E., Ciliberto, G., and Taub, R. 2000. Increased toxin-induced liver injury and fibrosis in interleukin-6-deficient mice. *Hepatology* 31:149-159.
179. Martin, A.M., Kuhlmann, C., Trossbach, S., Jaeger, S., Waldron, E., Roebroek, A., Luhmann, H.J., Laatsch, A., Weggen, S., Lessmann, V., et al. 2008. The functional role of the second NPXY motif of the LRP1 beta-chain in tissue-type plasminogen activator-mediated activation of N-methyl-D-aspartate receptors. *J Biol Chem* 283:12004-12013.

180. Williams, S.E., Ashcom, J.D., Argraves, W.S., and Strickland, D.K. 1992. A novel mechanism for controlling the activity of alpha 2-macroglobulin receptor/low density lipoprotein receptor-related protein. Multiple regulatory sites for 39-kDa receptor-associated protein. *J Biol Chem* 267:9035-9040.
181. Carmeliet, P., Schoonjans, L., Kieckens, L., Ream, B., Degen, J., Bronson, R., De Vos, R., van den Oord, J.J., Collen, D., and Mulligan, R.C. 1994. Physiological consequences of loss of plasminogen activator gene function in mice. *Nature* 368:419-424.
182. Herrmann, J., Arias, M., Van De Leur, E., Gressner, A.M., and Weiskirchen, R. 2004. CSRP2, TIMP-1, and SM22alpha promoter fragments direct hepatic stellate cell-specific transgene expression in vitro, but not in vivo. *Liver Int* 24:69-79.
183. Ghiassi-Nejad, Z., and Friedman, S.L. 2008. Advances in antifibrotic therapy. *Expert Rev Gastroenterol Hepatol* 2:803-816.
184. Zhang, D.Y., and Friedman, S.L. Fibrosis-dependent mechanisms of hepatocarcinogenesis. *Hepatology* 56:769-775.
185. Puche, J.E., Lee, Y.A., Jiao, J., Aloman, C., Fiel, M.I., Munoz, U., Kraus, T., Lee, T., Yee, H.F., Jr., and Friedman, S.L. A novel murine model to deplete hepatic stellate cells uncovers their role in amplifying liver damage in mice. *Hepatology* 57:339-350.
186. Orth, K., Willnow, T., Herz, J., Gething, M.J., and Sambrook, J. 1994. Low density lipoprotein receptor-related protein is necessary for the internalization of both tissue-type plasminogen activator-inhibitor complexes and free tissue-type plasminogen activator. *J Biol Chem* 269:21117-21122.
187. Newton, C.S., Loukinova, E., Mikhailenko, I., Ranganathan, S., Gao, Y., Haudenschild, C., and Strickland, D.K. 2005. Platelet-derived growth factor receptor-beta (PDGFR-beta) activation promotes its association with the low density lipoprotein receptor-related protein (LRP). Evidence for co-receptor function. *J Biol Chem* 280:27872-27878.
188. Shi, Y., Mantuano, E., Inoue, G., Campana, W.M., and Gonias, S.L. 2009. Ligand binding to LRP1 transactivates Trk receptors by a Src family kinase-dependent pathway. *Sci Signal* 2:ra18.
189. Stenger, R.J., and Johnson, E.A. 1971. Further observations upon the effects of phenobarbital pretreatment on the hepatotoxicity of carbon tetrachloride. *Exp Mol Pathol* 14:220-227.
190. Constandinou, C., Henderson, N., and Iredale, J.P. 2005. Modeling liver fibrosis in rodents. *Methods Mol Med* 117:237-250.
191. Cook, A.D., Vlahos, R., Massa, C.M., Braine, E.L., Lenzo, J.C., Turner, A.L., Way, K.J., and Hamilton, J.A. 2006. The effect of tissue type-plasminogen activator deletion and associated fibrin(ogen) deposition on macrophage localization in peritoneal inflammation. *Thromb Haemost* 95:659-667.

192. Hu, K., Mars, W.M., and Liu, Y. 2008. Novel actions of tissue-type plasminogen activator in chronic kidney disease. *Front Biosci* 13:5174-5186.
193. Wang, H., Zhang, Y., and Heuckeroth, R.O. 2007. PAI-1 deficiency reduces liver fibrosis after bile duct ligation in mice through activation of tPA. *FEBS Lett* 581:3098-3104.
194. Falsone, S.F., Gesslbauer, B., and Kungl, A.J. 2008. Coimmunoprecipitation and proteomic analyses. *Methods Mol Biol* 439:291-308.
195. Seki, T., Imai, H., Uno, S., Ariga, T., and Gelehrter, T.D. 1996. Production of tissue-type plasminogen activator (t-PA) and type-1 plasminogen activator inhibitor (PAI-1) in mildly cirrhotic rat liver. *Thromb Haemost* 75:801-807.
196. Zhang, L.P., Takahara, T., Yata, Y., Furui, K., Jin, B., Kawada, N., and Watanabe, A. 1999. Increased expression of plasminogen activator and plasminogen activator inhibitor during liver fibrogenesis of rats: role of stellate cells. *J Hepatol* 31:703-711.